Characterization of membrane lipids and. Changes therein during desiccation and rehydration of the resurrection plant *Xerophyta humilis* (Bak) Dur and Schinz.

by

Freedom Tshabuse

Thesis submitted for the Degree of
Doctor of Philosophy
in the Department of Molecular and Cell Biology,
University of Cape Town

September 2017

Declaration

I declare that "**Characterization of membrane lipids and, Changes therein during desiccation and rehydration of the resurrection plant *Xerophyta humilis* (Bak) Dur and Schinz."** is my work, that it has not been submitted for any degree or examination in any other university, and that all the sources I have used or quoted have been indicated and acknowledged by complete references.

Mr Tshabuse Freedom September 2017

Signed by candidate

Signature Removed

Dedication

To the loving memory of my Grandfather, Frank Raita Tshabuse (1925-2016).

To my grandmother Sarah Phophi Tshabuse, I will never be able to fully put into words how much you mean to me. Lets be real-bragging about you is easy.

To my parents, who has supported me in all my endeavors.

To my family, thanks for your support.

To my Plant Stress Laboratory mates, who makes life fun.

Acknowledgements

This thesis grew out of a series of dialogues with my supervisor professor Jill M. Farrant. Jill brought me closer to the reality I had initially perceived. Her comments on chapter drafts are themselves a cause in critical thought upon which I will always draw. Her capacity to combine critique with an immediate empathy and commitment towards her students will always inspire me. Amid the laughter and chapter drafts, Jill was always there to offer quite encouragement, at times embarrassed by her own extraordinary kindness. I am grateful to God for making it possible to work under her supervision.

I'm very grateful for my years at the Plants Stress Laboratory (PSL), made possible by the NRF and UCT Science Faculty support.

I would also like to gratefully acknowledge the enthusiastic supervision of my co-supervisor Dr Eric Ruelland. With his enthusiasm, his inspiration, and great efforts to explain things clearly and simply, he helped to make my study fun. Through-out my thesis-writing period, he provided encouragement, sound advice, good teaching, and lots of good ideas. I would have been lost without him.

I'm grateful to PSL group for providing a stimulating and fun environment in which to learn and grow. I'm especially grateful to Keren Cooper and Dr Suhail Rafudeen for always being within my screaming range when I needed help the most. I would also like to acknowledge Ms Hawwa E.Gabier, your contributions make it possible for me to finish writing this thesis.

Lastly I would like to thank my family, my brothers, sisters, uncles, aunties, parents for their emotional and financial support.

Abstract

Drought is the primary challenge facing agricultural productivity and food sustainability productivity in Africa and many parts of the world. Very few higher plants, including crop plants, can survive periods of extended water loss. However, a small group of angiosperms, termed resurrection plants are able to lose up to 95% of their cellular water content in vegetative tissue upon extended periods of water, remain in an air-dry for months to years and regain full metabolic activity in the same tissue upon re-watering. The aim of this study was to investigate the changes in acyl chain composition within the major glycerophospholipids (in total and chloroplast suspension) and galactolipids (chloroplast suspension) at different stages of dehydration and rehydration treatments in the resurrection plant *Xerophyta humilis* (Bak) Dur and Schniz. This was done in order to ascertain their roles during acquisition of desiccation tolerance in *X. humilis*.

The galactolipids and glycerophospholipids acyl chain compositions were determined by multiple reaction monitoring (MRM) mass spectrometry. The glycerophospholipids profiles from total leaves and roots lipid extracts showed an increased representation of unsaturated molecular species such as 18:3/18:3 (in leaves) and 18:3/18:2 (in leaves and roots) during dehydration, with a decrease in saturated and mono-saturated molecular species such as 16:0/16:0. Rehydration was associated with the opposite trend. Furthermore, increased representation of molecular species with unusual fatty acids were observed during dehydration, with the odd-numbered fatty acids such as 15:0, 17:0 and 19:0 increasing during dehydration and decreasing during re-watering. On the other hand, the 23:0 and 25:0 fatty acids decreased during dehydration and increased upon rehydration. Within the chloroplast profiles, the galactolipids (i.e. monogalactosyldiacylglycerolipids and digalactosyldiacylglycerolipids) showed maintenance of 18:3/18:3 and 18:3/18:2 molecular species during dehydration and rehydration. The phosphatidylglycerolipids profiles in the chloroplast, together with the uncommon chloroplastic glycerophospholipids such as phosphatidylethanolamine, phosphatidylcholine and phosphatidylinositol also showed an increase in the unsaturated molecular species during dehydration and decrease upon rehydration.

Taken together, our data suggest that water deficit in *X. humilis* roots and leaves induce fatty acid unsaturation, as well as production of uncommon fatty acids. These unsaturated fatty acids may aid in maintaining membrane integrity during dehydration. This study shows that changes in lipid composition are part of the desiccation tolerance strategies used by *X. humilis*.

Table of Contents

List of Tables

List of Figures

total MGDG MRM transition signal) within *X. humilis* leaves subjected to gradual dehydration and rehydration treatment.

Chapter 1:

Introduction

1.1. Desiccation tolerance and resurrection plants

Based on the critical water level for survival, two types of tolerance have been distinguished namely, drought tolerance and desiccation tolerance (Hoekstra *et al.,* 2001). Drought tolerance (as opposed to drought resistance) implies that the plant is tolerant to moderate dehydration, down to a moisture content below which there is no bulk cytoplasmic water present (~23% water on fresh weight basis, or ~ 0.3 g H_2O/g dry weight^{-1} (Hoekstra *et al*., 2001; Charuvi *et al*., 2015). Conversely, desiccation tolerance is the ability of an organism to dry to equilibrium with the air dry state, this being equivalent of ≤ 0.08 g H_20/g dry weight^{-1} and to resume full metabolic function upon rehydration (Farrant *et al*., 2007; 2009; 2017). The vegetative tissues of most species tolerate some degree of water loss, ranging from 1-71% of cellular water (Hofler et al., 1941) but few tolerate desiccation. To date, desiccation tolerance has been reported in all three domains of life, namely archaea, bacteria and eukarya (Fig.1.1; Alpert, 2006; Berjak, 2006; Ntuli, 2012). In Plantae, desiccation tolerance is common in seeds, with over 90% of angiosperms producing desiccation tolerant (orthodox) seed. Vegetative desiccation tolerance is relatively common in bryophytes, lichens and fern allies, but is rarely found in tracheophytes, with only 64 species of fern (1% of all ferns) and 135 angiosperm species (0.04% of flowering plants) exhibiting desiccation tolerance (Gaff and Oliver, 2013; Gacheve *et al.,* 2013; Farrant *et al*., 2007; 2017).

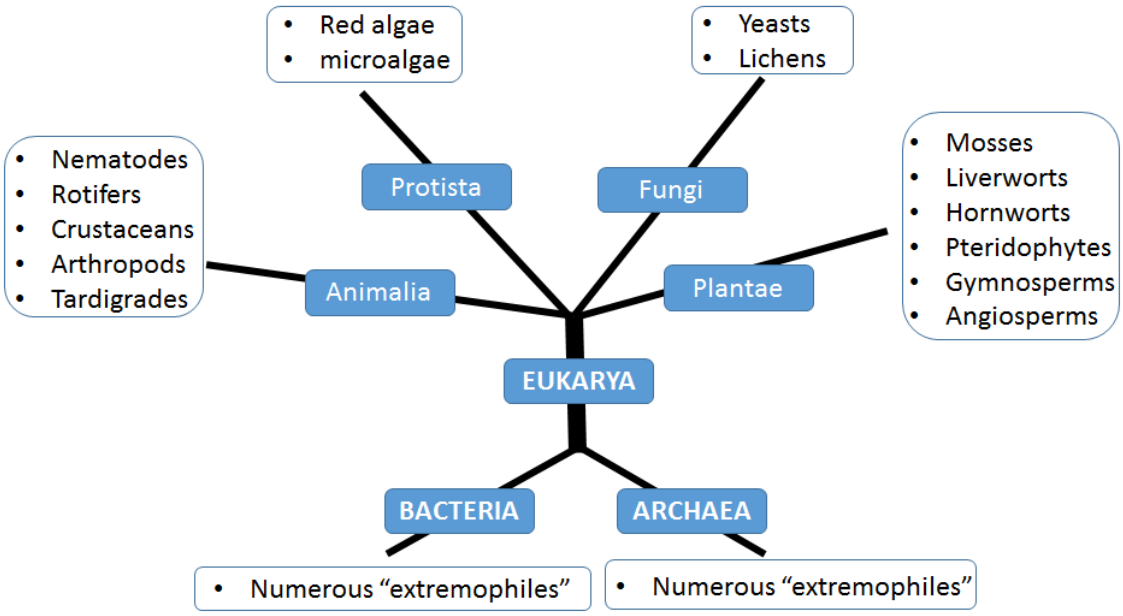

Fig 1.1: Schematic representation of desiccation tolerance among the three domains of life- archaea, bacteria, and eukarya (taken from Alpert, 2006). The transparent boxes represent desiccation tolerant organisms.

Such plants are called resurrection plants (Gaff, 1971). Several of these angiosperm resurrection plants have been studied in some detail, but to date, there have been few comprehensive systems studies done on any one species. Species such as *Boea hygrometrica* (reviewed in Mitra *et al.,* 2013; Xiao *et al.,* 2015; Zhu *et al.,* 2015), *Craterostigma plantagineum* (reviewed in Suarez-Rodrigues *et al.,* 2010; Dinakar and Bartels, 2013), *Haberlea rhodopensis* (Djilianov *et al.,* 2005; Moyankova *et al.,* 2014) *Myrothanmus flabellifolia* (Moore *et al.,* 2006; 2007a,b; 2009; Ma *et al*., 2015); *Sporobolus stapfianus (*reviewed in Le *et al.,* 2007; Gaff *et al.,* 2009; Oliver *et al.,* 2011a,b; Yobi *et al*., 2017), *Ramonda serbica, R. nathaliae* (reviewed in Rakić *et al.,* 2015), *Xerophyta humilis* and *Xerophyta viscosa* (reviewed in Collett *et al.,* 2004; Farrant, 2007; Farrant *et al.,* 2015; Costa *et al*., 2017) have been studied. In general, these species can be divided into two main types, depending on their responses to photosynthetic stress associated with desiccation, namely homoiochlorophyllous desiccation tolerant (HTD) and poikilochlorophyllous desiccation tolerant (PDT; Fig 1.2).

Fig 1.2: Plants of PDT (*X. humilis*, A-B) and HDT (*M. fabelliofolia*, C-D) at fully hydrated and dehydrated stages. At desiccated stage both plants shrink and had a withered appearance (B and D).

HDT plants which are the majority, retain most of their chlorophyll and preserve photosynthetic structures during desiccation (Farrant, 2000; Yordanov *et al*., 2003; Tuba, 2008; Toldi *et al*., 2009). These plants recover their use of photosynthetic capabilities within 24 hours following rehydration (Bernacchia *et al.,* 1996). Conversely, the PDT species breakdown their photosynthetic systems by an ordered deconstruction process during desiccation and re-synthesize by an ordered reconstruction process upon rehydration, thus taking longer (48-72 hours) to recover full metabolic competency (Sherwin and Farrant, 1996; Ingle *et al.,* 2008; Toldi *et al*., 2009). These plants are adapted to sites where drought periods are extended over weeks or months.

Water, the most abundant material in living organisms, plays a crucial role in the survival and growth of plants (Hsiao, 1973). Water acts as a solvent for mineral nutrients, a transportation agent for these nutrients to various parts of the plant and as a raw material for photosynthesis, a basic process underlying all life (Martin and Ruiz-Torres, 1992; Farrant *et al*., 2007). A period of drought stress in plants interferes with many cellular and whole plant functions (Gursoy *et al.*, 2012). The loss of water can result in subcellular stresses such as: 1). Mechanical stress associated with turgor

loss 2) Disruption of macromolecular integrity and 3). Free radical mediated damage (Vertucci and Farrant, 1995; Farrant *et al*., 2007; 2012; 2016). The molecular and physiological basis of these adaptive mechanisms in resurrection plants is very complex and varies between species (Bartels and Salamini, 2001; Mitra *et al.*, 2013; Farrant *et al*., 2016).

1.2. Mechanisms associated with desiccation tolerance in angiosperms of relevance to this study

Among the ever-changing environmental components, drought is considered one of the most lethal stresses affecting crop plants (Aslam *et al.,* 2013; Kumar *et al.,* 2013). Since plants lack mobility to move to a favourable environment, their growth, development and yield is heavily affected by drought stress. Drought stress is known to cause multiplex changes, and upon water loss below critical values (species dependent) sensitive species suffer irreversible damages (Barak and Farrant, 2016). However, resurrection plants employ a series of distinct morphological, physiological, biochemical, and genetic protective mechanisms to tolerate extreme desiccation (Farrant *et al.,* 2012; Dinakar and Bartels, 2013). Studies on the understanding of key mechanisms of drought tolerance acquisition have so far only investigated relatively few DT species (see review above). Such studies revealed common key mechanisms among desiccation tolerant species and their changes have been correlated with the acquisition of desiccation tolerance. These key mechanisms are briefly discussed below.

1.2.1 Reactive Oxygen Species scavenging

Reactive Oxygen Species (ROS) are molecules with an unpaired electron and are highly reactive. In plants, free radicals form as bi-products of metabolic processes involving electron transport and include molecules such as singlet oxygen ($^1O_2$), superoxide (O_2^-), the hydroxyl radical (.OH) and nitric oxide (NO)

(Halliwell and Gutteridge, 1999; Sharma *et al.,* 2012). Depending on their concentration in plants, ROS exert both deleterious and beneficial effects (Sharma *et al*., 2012; Caverzan *et al.,* 2016). Under hydrated conditions in plants, ROS are generally controlled in homeostasis by various antioxidants such as the water-soluble glutathione, ascorbic acid, the lipid soluble tocopherols and β-carotene, together with enzymes such as superoxide dismutase, ascorbate peroxidase, glutathione reductase and catalase (Mittler, 2002; Farrant *et al*., 2007; 2016). However, severe water loss in desiccation sensitive plants results in the disruption of electron transport, which leads to the increased generation of ROS (Bailly, 2004; Selivanov *et al*., 2011). Excessive accumulation of ROS in the cell may lead to damage in the cell structures, nucleic acids, lipids and proteins (Valko *et al.,* 2006; Dinakar and Bartels, 2013; Giarole *et al*., 2017). Oxidative stress-induced peroxidation of membrane lipids is very damaging, because it leads to an alteration in membrane fluidity, which in turn leads to increased membrane permeability, inactivation of membrane-bound enzymes, and impaired normal cellular functioning (Bailey *et al.,* 2003). This can be fatal in desiccation-sensitive plants. In the chloroplast, a major site of ROS production during dehydration, ROS damage is minimized by different strategies depending on the type of resurrection plant species. In HDT species, ROS-associated damage is minimized by leaf folding and production of ROS-scavenging antioxidants such as anthocyanins, ascorbate, and glutathione*;* whilst in PDT species, chloroplast dismantling and chlorophyll degradation are effective mechanisms for ROS minimization (see Sherwin and Farrant, 1998; Farrant, 2000; Farrant *et al*., 2007, 2016 for a deeper understanding).

1.2.2 Cellular stabilization

Cellular stability by accumulation of select carbohydrates is a common desiccation tolerant system response (reviewed in Farrant *et al*., 2012; 2016) and has been proposed to be central to the ability of resurrection plants to achieve desiccation tolerance (Hincha and Hagemann, 2004; Akinci and Losel, 2012). Soluble sugars, mostly sucrose, galactinol and raffinose family oligosaccharide (RFOs) accumulate upon dehydration and are correlated with

desiccation tolerance (Vertucci and Farrant, 1995; Ingram and Bartels, 1996; Martinelli, 2008). The non-reducing disaccharide trehalose accumulates in some (e.g. *M. flabellifolius* and *Tripogon Loifolius*) but not all resurrection plants (Moore *et al.,* 2007; Williams *et al.,* 2015). Trehalose is reported to be important for membrane protection by preventing the increase of gel-to-liquid transition temperatures (Tm) of dehydrated lipid bilayers (Bryant *et al*., 2001; Ohtake *et al*., 2006). This is thought to be achieved by replacing the water molecules that interact with polar head groups of lipids and thus maintaining sufficient spacing between lipids to keep the acyl chains in a liquid-crystalline state (Ohtake *et al*., 2006). Ultimately, carbohydrates may also preserve proteins by a process called vitrification, an amorphous metastable state in which the disordered and physical properties of the liquid state is retained. Vitrification decreases the probability of chemical reactions and is crucial for the plant to survive in the dry state (Toldi *et al*., 2009).

1.2.3 Accumulation of stress-associated proteins

Accumulation of stress-associated proteins such Late Embryogenesis Abundant (LEA) proteins and small Heat Shock Proteins (sHSP) are a common phenomenon that occurs both in desiccation tolerance and desiccation-sensitive plants (van den Dries *et al*., 2011; Gechev *et al.,* 2013; Farrant *et al.,* 2016). With respect to the former, in desiccation tolerant plants, researchers have reported higher levels of LEA transcripts during dehydration compared to sensitive plants (Ataei *et al.,* 2016). Based on their amino acids similarities, LEA proteins has been categorised into many groups (Dure *et al.,* 1989; Tunnacliffe and Wise, 2007). Although their exact functions during dehydration are unknown, LEA proteins have been proposed to be involved in desiccation acquisition in desiccation tolerant plants. This is due to the up-regulation in their gene expression in orthodox seeds during maturation (Ingram and Bartels, 1996; Farrant *et al.*, 2012), as well as in resurrection plants such as *Craterostigma plantagineum, Lindernia brevidens, X. humilis* and *X. viscosa* during dehydration (Collet *et al.,* 2004; Philips *et al.,* 2008; Costa *et al*., 2017). Their proposed roles during acquisition of desiccation tolerance includes

protection of enzymatic activities, prevention of protein-aggregate formation and potential stabilization of cellular membranes (Reyes *et al.,* 2005; Tunnacliffe and Wise, 2007; Farrant *et al.,* 2017).

1.3. Maintenance of membrane integrity and fluidity during water loss

Cell membranes are the primary targets of the many plant stresses, and maintenance of their integrity and stability under water loss is a major component contributing to water deficit tolerance in plants (Bajji *et al*., 2001; Bryant *et al*., 2001). Cell membranes are mainly composed of proteins and lipids (Fig 1.3). Lipids are the main component of cell membranes, displaying a wide diversity of functions, which include structural support, energy storage, cell signalling and membrane trafficking (Dowhan and Bogdanov, 2002). Because of their complexity, lipids are difficult to define (Dashty, 2014). According to the international lipids classification and nomenclature committee, lipids are grouped into eight categories namely fatty acyl, glycerolipids, (including glycerophospholipids), sphingolipids, sterols, prenol lipids, saccharolipids and polyketide (Table 1.1; Fahy *et al*., 2005). Lipid are comprised of over 1.68 million molecular species (Li *et al*., 2014). Glycerolipids are the most abundant class of membrane lipids and play a pivotal role in maintaining membrane integrity (Hoekstra *et al*., 2001; Dashty, 2014).

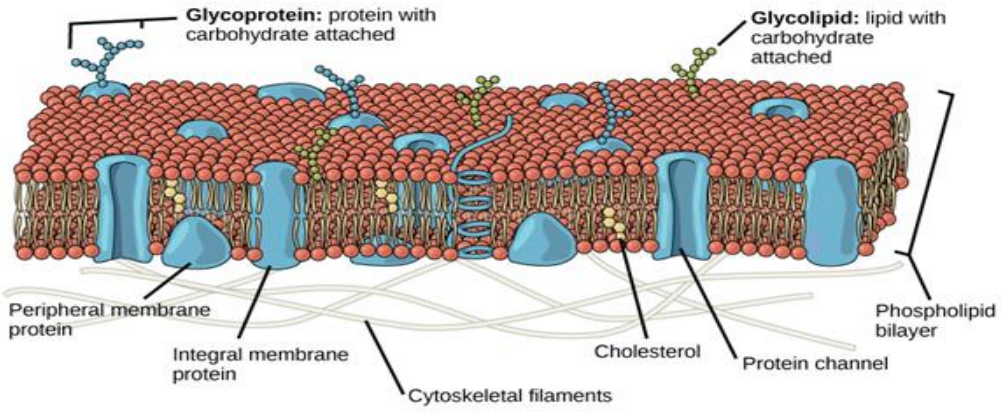

Fig 1.3: Representation of bio-membrane structure. Peripheral membrane proteins associate either with the lipid surface of with other membrane proteins. Lipids in close association with proteins appear as light grey head groups and fluid bilayer lipid appear as navy acyl chains (Boundless, 2016).

Glycerolipid are made up of a polar head group nucleated by a glycerol moiety to which two fatty acid tails are esterified at positions *sn*1 and *sn*2 (Eyster, 2007; Wolf and Quinn, 2008; Li *et al.,* 2015). In the case of phosphoglycerolipid, the polar groups consist of a phosphate esterified to the carbon-3 position of the glycerol to which a base (choline, ethanolamine), polyol (inositol, glycerol) or amino acid (serine) is attached (Wolf and Quinn, 2008). We thus obtain phosphatidylcholine (PC), phosphatidylethanolamine (PE), phosphatidylinositol (PI), phosphatidylglycerol (PG) and phosphatidylserine (DPG) Fig 1.4; Furt *et al.,*2011; van Meer and de Kroon, 2011). Others glycerolipids can be galactolipids for which the polar head is galactosyl moiety esterified to the *sn*3. One distinguish monogalactosyldiacylglycerol (MGDG) from digalactosyldiacylglycerol (DGDG), or even trigalactosyldiacylglycerol or tetragalactosyldiacylglycerol. Sphingolipids are a class of lipids containing a backbone of sphingo bases (which is made by the condensation of serine and of palmitoyl acid) with an amine alcohol linked to the long, unsaturated hydrocarbon chain by an amide bond (Hannun and Obeid, 2008).

Table 1.1: Lipid categories and their examples (Fahy *et al*., 2005)

Category	Abbreviation	Example
Fatty acyls	FA	Dodecanoic acid
Glycerolipids	GL	1-hexadecanoyl-2-(9z-octadecanyol)-*sn*-glycerol
Glycerophospholipids	GP	1-hexadecanoyl-2-(9z-octadecanyol)-*sn*-glycerol-3-phosphocholine
Sphingolipids	SP	N-(tetradecanoyl)-sphingo-4-enine
Sterol lipids		Cholest-5-en-3β-ol
Prenol lipids	PR	2*E*, 6*E*-farnesol
Saccharolipids	SL	UDP-3-O-(3*R*-hydroxy-tetradecanyol)-αD-*N*-acetlglucosamine
Polyketides	PK	Aflatoxin-B_1

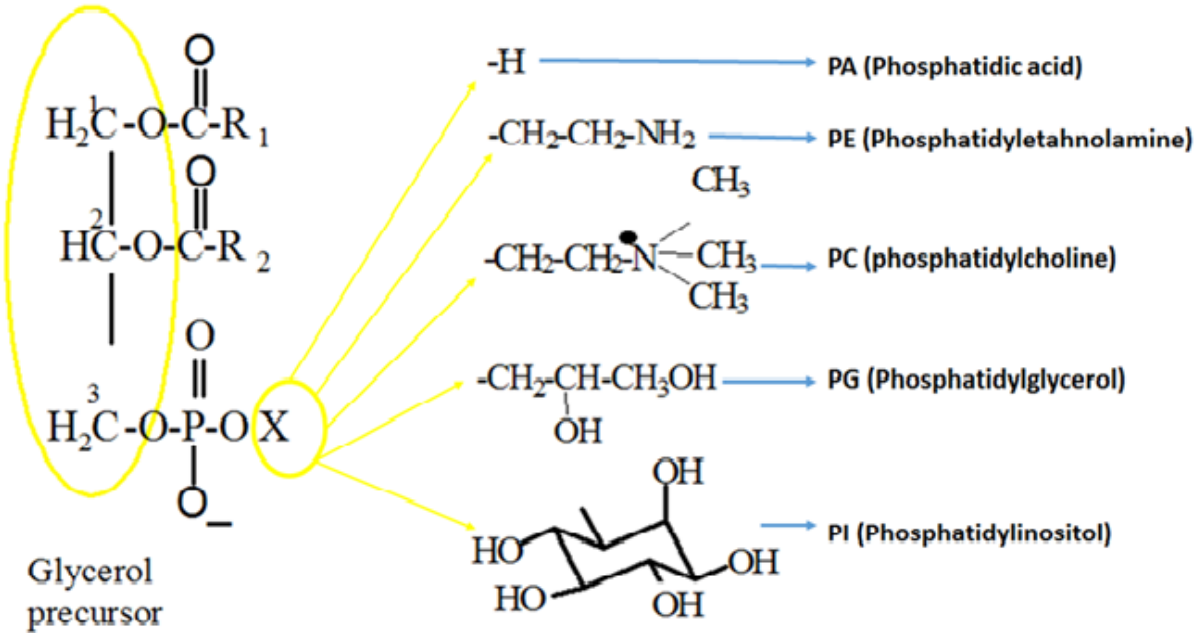

Fig 1.4: Structure of the glycerophospholipids and their classes (Bandary and Haughey, 2012).

Membranes are a matrix in which protein and lipids are in movement. The biophysical properties of biomembranes is largely determined by the polarity, acyl chain length and level of fatty acids unsaturation that comprise that membrane (Millar *et al*., 1998; Murakami *et al*., 2000). In plant cells, phospholipids contain high levels of 16-carbon and 18-carbon fatty acids. They are termed common fatty acids (Furt *et al*., 2011). These fatty acids are classified into saturated (without double bonds) and unsaturated fatty acids (with one or more double bonds) (Table 1.2; Wallis *et al.,* 2002; Bazinet and Laye, 2014).

Table 1.2: Examples of common plant lipids and their degrees of saturation (Bazinet and Laye, 2014)

Name	**Type**	**Number of carbon atom**	**Number of double bonds**	**Symbol**
Palmitic acid	Saturated	16	0	16:0
Stearic acid	Saturated	18	0	18:0
Oleic acid	Monosaturated	18	1	18:1n-9
α-linoleic acid	ω-3-polyunsaturated	18	3	18:3n-3
Eicosapentaenoic acid	ω-3-polyunsaturated	20	5	20:5n-3
Docosapentaenoic acid	ω-3-polyunsaturated	22	5	22:5n-3
Docosahexaenoic acid	ω-3-polyunsaturated	22	6	22:6n-3
Linoleic acid	ω-6-polyunsaturated	18	2	18:2n-6
Arachidonic acid	ω-6-polyunsaturated	20	4	20:4n-6

In drought-sensitive plants, severe loss of water is accompanied by irreversible structural changes such as decreased cellular volume, protein denaturation and increased membrane fusion, and ultimately loss of cell viability (Vertucci and Farrant, 1995; Yordanov *et al.*, 2003). Severe water loss in plant cells promotes the loss of the hydrophobic effect of water which is crucial for macromolecules and membrane structure maintenance. Loss of this effect ultimately leads to cellular membrane damage (Farrant *et al.,* 2007). Cellular membrane damage generally arises due to increased membrane lipid peroxidation, where free radicals facilitate the formation of double bonds between fatty acids, which are prone to ROS attack under unfavourable environmental stresses (Elstner, 1982; Smirnoff, 1993; Foyer *et al*., 1994). Resurrection plants are able to survive the loss of most of their intracellular water, by employing effective membrane defence mechanisms, such as altering their lipid composition and/or degrees of saturation. Significant changes in membrane lipids have been observed during both dehydration and rehydration in the resurrection plants, S*porobolus stapfianus, Haberlea rhodopensis, Barbacinea purpurea* and *Salaginella lepidophylla, Paraisometrum mileense* during dehydration and rehydration cycles (Oliver *et al*., 2011; Yobi *et al.,* 2013; Dinakar and Bartels, 2013; Li *et al*., 2014; Sugiyama *et al.,* 2014; Rafsanjani *et al*., 2015). The main findings of these studies suggest that desiccation tolerance was associated with the accumulation of polyunsaturated fatty acids. In the current work the nature of and changes in fatty acids associated with desiccation tolerance in the resurrection plant *X. humilis* (Bak.) and Schinz will be examined.

X. humilis is a poikilochlorophyllous monocot resurrection plant that has been studied in relation to its physiological, biochemical and molecular responses to desiccation (Dace et al., 1998; Farrant, 2000; Collett et al., 2003; 2004; Ingle et al., 2008; Beckett et al., 2012). As yet, there has been no analysis of lipid metabolism in this species and thus the aim of this study was to determine the nature of structural lipids present in the leaves and roots of *X. humilis,* and to investigate the changes to lipids during desiccation and rehydration. Several differences have been reported between this species and the HDT, *Craterostigma* species, particularly in relation to mechanisms of mechanical stabilization and protection of photosynthesis during desiccation, both of which involve membrane dynamics (reviewed above and Farrant *et al*., 1999; 2003;

Farrant, 2000; Farrant *et al*., 2007; Moore *et al*., 2012; Chavuri *et al*., 2015). Thus, a secondary aim was to ascertain if such differences extend to lipidomic responses of such species, and/or whether unifying features in fact do exist among desiccation tolerant types. We used lipidomic analyses based on electrospray ionization mass spectrometry (ESI-MS/MS) (Rainteau *et al.,* 2012) to investigate changes of membrane molecular species in response to dehydration and subsequent rehydration in *X. humilis*. Gas Chromatography- Mass Specrometry (GCMS) was used to confirm the identity of unusual lipids found in this species. Taken together, the results showed an increase in the unsaturation of fatty acids in the cell membranes of *X. humilis* leaves and roots during water deficit, and this increase in unsaturation may be important in the plant's adaptation to tolerance of desiccation. Increased fatty acid unsaturation has been reported in plants' adaptation to various other environmental stresses, including cold (Ruelland et al., 2009; Mironov *et al.,* 2012) and high temperatures stresses (Zheng *et al*., 2011); and it has been suggested to play a primary role in the proper maintenance and biophysical characteristics of cellular membranes. The potential impact of such lipid modification in *X. humilis* in relation to desiccation is discussed.

1.4. Lipidomic analysis

Apart from being structural components of bio-membranes and energy providers, lipids are also involved in cellular signalling and cell-cell interactions (Tarahovsky *et al.,* 2008; Hou *et al.,* 2016). These diverse roles of lipids have led to the emergence of the field of lipidomics (Wenk, 2005). Lipidomics is the large-scale study of structure and function of complete lipids in biological systems, as well as their interactions with other lipids, proteins and metabolites (Wenk, 2010; Merrill *et al.,* 2013; Brugger, 2014). In comparison to other "omics" fields such as proteomics, transcriptomics and genomics, lipidomics involves the comprehensive measurement of lipids in a given system (cell tissue or organism) under a given set of conditions (Brugger, 2014; Ernst *et al.,* 2014; Li *et al.,* 2014). The major drawback in lipidomic analysis is the diverse nature of lipids, with each individual lipid having its own rules of fragmentation and its

specific ionization efficiency (Kofeler *et al.,* 2012). However, improved lipidomic analytical approaches such as gas chromatography mass spectrometry (GC-MS), direct injection mass spectrometry (DIMS), thin layer chromatography (TLC), nuclear magnetic resonance (NMR), capillary electrophoresis mass spectrometry (CE-MS) and high-performance liquid chromatography (HPLC) has greatly enhanced our knowledge about lipids at the individual level (Ernst *et al.,* 2014). Major disadvantages of these techniques includes (1) low sensitivity and selectivity (TLC and HPLC), (2) the need for time-consuming derivatization methods (GC-MS), and (3) the requirement for radioisotopes with their inherent health issues, notably in regards to ^{32}P-orthorphosphate (O'Donnell *et al*., 2014). Because of its sensitivity and selectivity, mass spectrometry (MS)-based techniques have emerged as the technique of choice for quantitative and qualitative lipidomic analysis. Lipidomic analysis using mass spectrometry technique can be achieved using two separate approaches, including Shotgun lipidomics (also referred to as DIMS) or LC-MS (Serhan, 2005; Han *et al.,* 2012; Knittelfelder *et al.,* 2014).

1.4.1. Shotgun lipidomics/(DIMS)

Shotgun lipidomics is a high throughput approach, which involves the direct infusion of complex mixtures (without chromatographic separation) into a mass spectrometer, followed by scanning of a defined mass window using high-resolution instruments (Han *et al.,* 2012). The underlying principle of this approach is the constant flow of biological samples into the electrospray ionizatio (ESI) source, thus allowing for constant ratio of ion peak intensities between lipid species, as well as minimizing lipid aggregation, which is a major problem in lipidomics (Wang *et al*., 2015).This methodology allows researchers to analyse many samples in a short period. Over the years, three major shotgun lipidomic approaches have been documented in literature namely: Tandem MS-based shotgun lipidomics, high mass accuracy-based shotgun lipidomics and multidimensional MS-based shotgun lipidomics (Wang *et al.,* 2016).

1.4.1.1. Tandem MS-based shotgun lipidomics

In this approach, precursor ion scanning (PIS) and/or neutral ion scanning (NIS) is used to monitor the class-specific fragments associated with or loss of the head group to analyse individual molecular species (Yang and Han, 2011). Tandem MS-based shotgun lipidomics is very robust, and relies on the use of two internal standards for accurate lipid profiling and quantification. This approach has been widely used in the profiling and quantification of lipid species in many biological samples (Hsu et al., 2003; Nicks *et al*., 2006; Welti *et al*., 2007). However, some drawbacks include, but are not limited to, appearances of isobaric species in specific MS/MS spectrum, and limited dynamic range of quantification due to the lack of sensitive diagnostic MS/MS (Wang *et al.,* 2016).

1.4.1.2. High mass accuracy-based shotgun lipidomics

In this approach, a hybrid-type based mass spectrometry such as quadrupole-time of flight (Q-TOF) or Obitrap is used to acquire full mass spectra of lipid species after collision induced dissociation (CID; Wang et al., 2014). In this technique, the individual lipid species are quantified by comparing their intensities with that of spiked internal standards in the class (Zech *et al*., 2009; Klose *et al.,* 2010; Sampaio *et al*., 2011). This approach has been recently used to study and quantify lipids in yeasts (Klose *et al*., 2010), and animals (Sampaio *et al.,* 2011). The major drawback in this approach is the restricted dynamic range of the detector, which restricts quantification to a narrow concentration range (Kofeler *et al*., 2012).

1.4.1.3. Multidimensional MS-based shotgun lipidomics (MDMS-SL)

In this approach, individual lipid classes are identified and quantified based on their unique chemistries such as differential hydrophobicity or stability under acidic or basic conditions, after direct infusion (Han and Gross, 2005; Jiang *et al*., 2007; Han *et al.,* 2011; Yang *et al.,* 2015). MDMS-SL is a very sensitive

technique, with high efficiency, reproducible, and broad coverage, widely employed in the analysis of various classes of glycolipids, glycerophospholipids and sphingolipids (Han and Gross, 2005). The major drawback of in MDMS-SL technique is the inability to detect and quantify low abundance species (Gross and Han, 2011).

Despite the advantages associated with shotgun lipidomic approaches, the inability to remove contaminating isobaric species (due to lack of chromatographic separation) in the samples prior to ion fragment detection, as well as the failure to detect very low abundance lipid species in biological samples are the major drawbacks that makes it a lesser preferred technique over LC-MS-based approach. This is because chromatographic separation is able to remove contaminating isobaric species while simultaneously enriching the low abundant species for accurate quantification by MS (Yang and Wang, 2015).

1.4.2. Liquid chromatography (LC)-MS

LC-MS has emerged as the preferred technique for the detection and characterization of organic molecules, which combines the resolving power of liquid chromatography and the detection of specificity of mass spectrometer (Pitt, 2009). In this technique, lipids are first separated by liquid chromatography, to remove isobaric contaminating species. Depending on the nature of the lipids of interest (i.e. polar or apolar lipids), a specific chromatographic column will be used (Allwood and Goodacre, 2010). Lipids are then ionized in the electron spray ionization (ESI), before separation on the mass detector based on their mass to charge (*m/z*) (mass: charge ratio, where mass is divided by the total net charge of the molecule) ratio (Figure 1.5; Korfmacher, 2005). The use of LC-MS in plant metabolomics has increased drastically over the years (Allwood and Goodacre, 2010; t'Kindt *et al*., 2010; Jorge *et al.*, 2015; Wang, 2015).

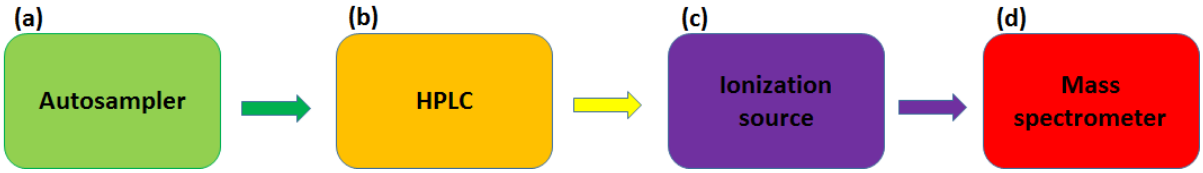

Fig 1.5: Elements of an LC-MS system. (a). Autosampler, which loads the samples onto the HPLC; (b). HPLC, which decontaminates the samples from isobaric species; (c). Ionization source which is the interface for LC to MS; (d). MS, which separates the analytes based on their mass to charge (*m/z*) ratio (Korfmacher, 2005).

Until recently, many scientists have employed the use of LC-MS in the Multiple Reaction Monitoring (MRM) mode for lipid identification and quantification in biological samples (Rainteau *et al*., 2012; Djafi *et al.,* 2013; Tsugawa *et al.,* 2014). This is because MRM exploits the capability of triple quadrupole (QQQ) MS for the quantitative analysis (Shaner *et al*., 2009; Quehenberger *et al*., 2010).

1.4.2.1. LC-MS/MS in the SRM (or MRM) mode

LC-MS/MS has emerged as an innovative technique able to analyse many molecular species in the same sample after separation by their characteristic parent *m/z* and daughter ions that form after collision-induced fragmentation (where molecules are collisionally activated using an inert gas, then broken apart into small daughter ions that are separately analysed) (Rainteau *et al*., 2012; Djafi *et al*., 2013). Since the introduction of the triple quadrupole (QQQ) mass spectrometer in 1979, the LC-MS/MS approach is mostly performed in the selected reaction-monitoring mode (SRM). The plural form is multiple reaction-monitoring mode, (MRM) (Mani *et al*., 2012). In the MRM mode, the samples are ionized by electrospray ionization and then enter the first quadrupole (Q1). The first quadrupole is set to allow only the predefined *m/z* value of the precursor ion to pass into the second quadrupole (Q2), also known as the collision cell. In the second quadrupole, the selected ions enter a higher-pressure region with an inert gas (argon gas), resulting in the fragmentation of the selected precursor ion into many product ions. Only the preselected product ions with

specific *m/z* values are allowed pass through the third quadrupole (Q3) onto the detector (Fig 1.6; Djafi *et al*., 2013; Rainteau *et al*., 2012).

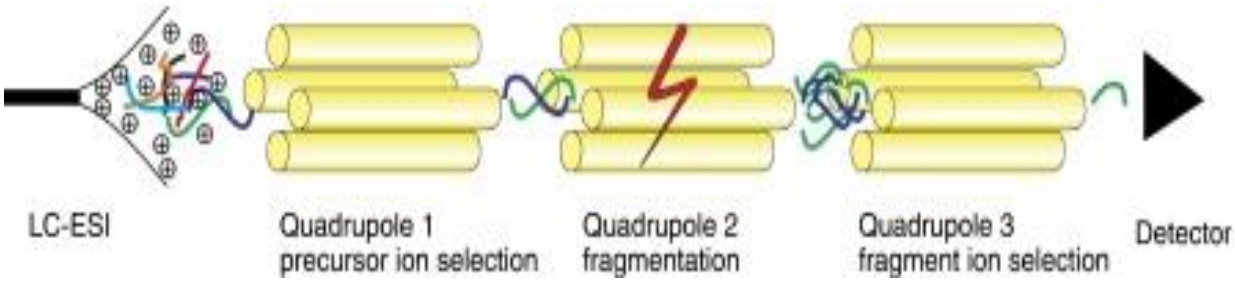

Fig 1.6: Multiple reaction monitoring technique. Molecular ions of a specific analytes are selected in Q1 and fragmented in Q2 (Lange *et al*., 2008). ESI, electrospray ionization. Molecular ions of one or several contaminants are isolated and fragmented together. A fragment ion of interest is selected in Q3 and its intensity measured no the detector.

LC-MS/MS has many advantages including high analytical sensitivity and specificity, wide dynamic range, ability to analyse multiple samples simultaneously, as well as minimum sample preparations (Chace, 2001; Shackleton, 2010; Kusknir *et al*. 2011; Zhou *et al.,* 2014). Because of these advantages, LC-MS/MS has been intensively employed in clinical laboratories (Chace, 2001; Shackleton, 2010), and is gaining popularity in the profiling and quantification of lipid classes and their species in plant research (Rainteau *et al*., 2012; Djafi *et al*., 2013; Okazaki *et al.,* 2013; Zhou *et al.,* 2014).

1.5. Significance of this study

Because of their sessile nature, plants encounter a plethora of biotic and abiotic stressors in their natural environments. In order to survive and flourish, these plants must be able to withstand these stressors. Biotic stressors include microorganisms, insects and herbivores, while abiotic stressors include temperature, soil water availability, salt, light and metal ions (Hammond-Kosack and Jones, 2000). Soil water stress comprises of both low water stress (e.g. drought stress) and high water stress (e.g. flooding; Farooq et al., 2009). Drought is a meteorological condition brought about by periods of insufficient rain, which severely limits the amounts of soil water available (Gimbel *et al.,* 2015). In plants, drought can be experienced when either water supply to the roots becomes limited or water is lost during increased accelerated transpirational rates (Anjum *et al.,* 2011). South Africa has a broad and well-developed agricultural sector that largely maintains sufficient food supply both for animal and human consumption. Unfortunately, this agricultural sector has suffered from cyclical drought which adversely impacts food security since the country relies heavily on rain-fed agriculture (Cambers *et al*., 2009; Hardy *et al.,* 2011). Furthermore, increased periods of severe drought due to global warming is to be expected. By the year 2050 it is predicted that, an additional 30 million African people will be affected by famine (Clover, 2003). Additionally, other environmental factors such as poor soil quality, raising temperatures and limited arable land exacerbate the problem. The challenge for future generations is to ensure increased agricultural production and to develop mechanisms for improving drought tolerant or resistant crops. This can be done in many ways, including the use of resurrection plants, which are native to the country and offer a good source for novel gene mining that can be further engineered into crop plants (Toldi *et al.,* 2009). In this study, a resurrection plant *X. humilis* has been used as a study model, to complement previous physiological and “omics” studies performed on this species. *X. humilis* is a monocotyledonous resurrection plant belonging to the family *Velloziaceae* (Mello-Silva, 2005; Myers and Farrant, 2010, Mello-Silva *et al.,* 2011). The *Velloziaceae* family has approximately 250 tropical species distributed across the world, with one species occurring in China, another one in Yemen and Saudi Arabia, and approximately 30 species in Africa and Madagascar, and the rest in South America (Mello-Silva *et al*., 2011).

Thus, the overall aim of this study is to establish the nature of and changes in membrane lipids composition in *X. humilis* during the dehydration and rehydration treatments. Specific fragmentation was used to scan the masses of the main glycerophospholipids present in the roots and leaves of *X. humilis*. Subsequently, LC-MS/MS in the MRM mode was used to study changes in membrane lipids composition during the dehydration and subsequent rehydration. Since *X. humilis* is a PDT resurrection plant, the nature of and changes in chloroplast lipids during desiccation and recovery therefrom was also examined.

Chapter 2:

Materials and methods

2.1. Plant Collection and Relative Water Content (RWC) Determination

Xerophyta humilis (Bak.) and Schniz plants were collected from Borakalalo National Park (North West Province, South Africa) and maintained in trays in a glasshouse as described by Sherwin and Farrant (1996). For the experiments described below, plants were removed to controlled growth chambers (ADAPTIS A350) where they were maintained under conditions of: 10ºC /25ºC, 16h/8h day/night, 325 μmol s^{-1} m^{-2}, and allowed to acclimate for 2 weeks before dehydration. Plants were desiccated over a period of 3 weeks by withholding water and then rehydrated by thorough watering of the soil. At regular intervals during the dehydration and rehydration cycles, whole plants (n=5) were removed and leaves and roots separated. Adhering soil particles were removed from roots by gentle brushing. Water content was determined for three leaves and roots, taken from different plants, and the remainder of the tissues were flashed frozen in liquid nitrogen and stored at -80ºC until required. Drying and rehydration cycles were repeated twice for all experiments outlined below.

Absolute and normalized relative water content (RWC) was determined as described by Sherwin and Farrant *et al.* (1998). Absolute water contents were determined gravimetrically by oven drying for 48h at 72ºC and water content calculated according to the formula: 100 X [(FW-DW)/DW], where FW= fresh weight, DW= dry weight (48 hours after incubation at 72ºC). RWC was calculated as normalized to the absolute water content of fully turgid plants immediately prior to the commencement of dehydration (Farrant *et al.,* 2017). Leaf and root samples from *X. humilis* harvested at four dehydration points were selected for further analyses. These were: Fully hydrated tissues (RWC=100%), moderate stress (RWC=60%), severe stress (RWC=40%) and the air dry state (RWC=10%). Plants were sampled after 9, 12, 24, 36 and 48 hours of rehydration.

2.2. Extraction of Total Lipids

The total lipids from each sample at different stages of dehydration-rehydration were extracted according to a modified Bligh and Dyer method (Bligh and Dyer, 1959). One gram of lyophilised plant material (leaves or roots) was ground into powder in liquid nitrogen into a powder using a pestle and mortar and then placed into 10 ml of boiling isopropanol in pyrex tubes, to stop the chemical reactions. The tubes were shaken vigorously followed by the addition of 10 ml of chloroform, and further shaking. Ten milliliters (10 ml) of NaCl (0.98%) was added into the tubes. The tubes were placed on ice overnight to allow the samples to separate into the two phases (the polar phase on top and the apolar phase at the bottom). The apolar phase was carefully recovered by using a one litre pipette and dried under a gentle stream of nitrogen gas and then resuspended in 400 µl of chloroform supplemented with 0.02% (v/v) butylated hydroxytoluene to prevent poly-unsaturated fatty acids (PUFA) degradation. The polar phase was discarded. Samples were kept at -20ºC for downstream experiments.

2.3. Lipid separation by TLC

Lipids extracted from leaves or roots were spotted on silica gel and separated by thin layer chromatography (TLC) in the acidic solvent system composed of chloroform/methanol/acetone/acetic acid/water (100/20/40/20/10; v/v/v/v) (Lepage, 1967). Separated molecules corresponding to the different lipid standards were visualized after staining the plate with iodine vapour and heating the plate at 140ºC for 10 min. Using this stain most compounds are charred to give grey or black spots (Jork *et al.,* 1990). Images of the plates were acquired by a ChemicDoc Imaging System (BioRad) and analysed by ImageLab (BioRad).

2.4. Mass Spectrometry

The High Performance Liquid Chromatography (HPLC) separation of plant extracts was performed using an Agilent 1100 HPLC system using a 250 mm X 4 mm (length

x internal diameter) 5 µm Lichrospher silica column, at 65ºC (Rainteau *et al*., 2012). The mobile phases consisted of hexane/isopropanol/water (628:248:24, v/v/v) supplemented with 10 mg/L ammonium formiate (A) and isopropanol/water (850:146, v/v) supplemented with 10 mg/L ammonium formiate (B). The injection volume was 5 µL. The percentage of B was increased linearly from 0% to 40% in 45 minutes and then to 100% in 3 minutes. This elution sequence was followed by an equilibrium period for 2 minutes with 100% B before returning to 100% A. Finally, the column was equilibrated for 8 minutes, leading to a total runtime of 60 minutes. The flow of the mobile phase was 3005 µL/min. The distinct glycerophospholipid classes were eluted successively as a function of the polar head group. Phospholipids were detected and the structure ascertained by collision induced dissociation (CID) in a tandem mass spectrometer (QTrap2000, ABSciex) used in the negative (capillary voltage -4500V) or positive mode (capillary voltage +5000V) depending on the nature of the fragmentation of the glycerophospholipid head group. Precursor ion and natural loss was used as detection mode depending on the particular glycerophospholipid. The elution of phospholipids triggered an Enhanced Resolution (ER) mass spectrum of the parent phospholipid ions. The triggering was piloted by a pre-set Informative Dependent Acquisition (IDA) software module of Analyst 1.4.2 software. The quantification of identified phospholipid molecular species was performed in the Multiple Reaction Monitoring (MRM) mode.

2.5. Deisotopization

The isotopic distribution of the Carbon (C) within phospholipid molecules was calculated according to Rainteau *et a.l* (2012) as follows: Carbon-13 (^{13}C) was considered to occur at 1.1% of the frequency of carbon-12 (^{12}C). For the MRM transition, a correction coefficient was calculated considering that the monitored transition is in part due to an isotopic overlap. Using PC as an example, the lipid molecular species *m/z* 798.2 (16:1/18:3-PC) is monitored as 798.5→277.2 and 798.5→253.2. These ^{13}C atoms can be incorporated either in the fatty acid tail or in the glycerophosphocholine head group, and monitored as *m/z* 800.5. Incorporation of

^{13}C atoms in the fatty acids 16:1 is monitored as *m/z* 255.2, and in 18:3 is monitored as 279.2 (overlapping with the signal due to 16:0/18:2-PC and 16:1/18:2-PC, respectively). The incorporation of ^{13}C atoms in the glycerophosphocholine head group is monitored as *m/z* 277.2 and *m/z* 253.2 (overlapping with the signal due to 16:0/18:3-PC and 16:1/18:3-PC, respectively). Therefore, the resulting signal intensities arising from *m/z* 800.5 which is attributed to 16:0/18:2-PC, 16:1/18:2-PC, 16:0/18:3-PC and 16:1/18:3-PC, was corrected for isotopic overlap with 16:1/18:3-PC. The correction factor for each transition was calculated using the formula $Z=1-(I_{M-2}/I_M)$ $0.011^2m(m-1)/2$; where m is the carbon number of the part of molecule where the two ^{13}C atoms are incorporated in the molecule at the lowest molecular weight to lead to an isotopic contamination of the signal at M molecular weight, and I_{M-2} and I_M are the peak intensities of MRM transitions at molecular weight (M-2) and M, respectively (Han, 2001). These corrections were performed for all the glycerophospholipids from all weights for all MRM transition when necessary.

2.6. Fatty acid analysis

200 mg of plant material (leaves or roots) were ground into a powder and 100 mg was further homogenized twice for 30s at 6000 rpm, using a Precellys 24-Dual homogenizer in the presence of glass beads (0.5 mm) and 2 ml of chloroform:methanol (2:1: v/v). After centrifugation (5000 rpm, 2min), the supernatant was collected and 2 ml of KCL (2M):methanol (4:1; v/v) added. The lipid phase was transferred into a nitrogen evaporator system. One hundred microliters (100 µl) of lipid were incubated with 200 µl of 10% (v/v) KOH in MeOH at 80ºC for 1h after which 200 µl of H_2SO_4 solution (10N) was added to stop chemical reactions. Saponified material was extracted twice with 1.5 ml of chloroform:methanol (2:1; v/v). Chloroform (500 µl) was added, mixed and centrifuged at 1500 rpm for 5 min. After solvent evaporation, 750 µl of methanol:HCl (5N) (9:1; v/v) was added and incubated for 1h at 80ºC, following which 2 ml of heptane was added with mixing. The heptane phase was collected and the sample was placed in a nitrogen evaporation system. Fatty acid methyl esters (FAMEs) were kept at -20ºC for downstream GCMS analysis, using a Triphus autosampler (Thermo-Fisher Q exactive GC). MS control and spectral

processing was carried out using Xcalibur software. For samples from leaves, A BPX70 capillary column (SGE; 60 m x 0.25 mm; porosity 0.25 µm) was used for the separation of fatty acid methyl esters. The GC oven temperature was set to 120ºC and held for 2 min, then increased to 250ºC at 3ºC/min, maintained at 250ºC for 5 min. The injection volume was 1 µl and was set at 250ºC with a splitless mode. The helium carrier gas flow was 1.2 ml/min. For MS in electronic impact mode, the ion source and interface temperatures were set at 250ºC. Detection was in full scan mode between *m/z* 50 and 500. Analysis was performed in scan mode with resolution at 60000, AGT target at 1E6 ion and a maximum injection time of 200 ms. Identification of the different fatty acid methyl esters present in the lipid extracts was performed usinga standard solution comprised of 37 fatty acid methyl esters (Sigma; 47885-U Supelco), and comparison to the National Institute of Standards and Technology database (NIST data bank, 2014) and confirmed by high accuracy mass of molecular ion and their fragments. The relative percentage of each fatty acid was calculated as the ratio of the surface area of the considered peak to the total area of all peaks.

2.7. Chloroplast Isolation

Eight grams (8g) of *X. humilis* leaves was homogenized with 35 ml of cold grinding solution (0.33 M sorbitol, 10 mM sodium pyrophosphate, 4 mM magnesium chloride, 2 mM ascorbic acid, pH 6.5). The homogenized tissues were filtered through four layers of cheesecloth into a 50 mL centrifuge tube and centrifuged for 1 minute at 1350 Xg at 4°C to pellet cellular debris. The supernatant was transferred into a clean 50 mL centrifuge tube and centrifuged for 7 minutes at 6535 Xg at 4°C to pellet the chloroplasts. The supernatant was decanted and the chloroplast pellet re-suspended into 3 mL of suspension buffer. The tubes containing the chloroplast suspensions were covered with foil and stored at -20°C for subsequent use. In order to test for chloroplast purity in the above extractions chlorophyll content of isolated chloroplast was measured and western blot analyses was performed.

2.8. Chlorophyll content

In order to test the efficacy of the isolation protocol, the chlorophyll content of isolated chloroplast extracted from hydrated *X. humilis* leaves was determined. This was not done on samples from desiccated leaves, as being a poikilochlorophyllous resurrection plant, chlorophyll is no longer present in these tissues. Ten microliters (10 µl) of chloroplast suspension were added to 0.1 mL of 80% acetone solution and thoroughly mixed. The mixture was centrifuged at 3000 X g for 2 min. The supernatant was retained and its absorbance measured at 652nm using 80% acetone as the reference blank. Estimation of chlorophyll concentration was calculated using the following relationship from the Sigma Chloroplast isolation kit (CPISO); mg/ml of chl = (Absorbance x dilution factor)/extinction coefficient. Chlorophyll content was expressed on a unit of chlorophyll basis (mg/chl).

2.9. Protein Isolation and Western Blotting

In order to determine the purity of chloroplast isolations, western blotting was performed on chloroplast suspensions extracted from leaves at various stages of dehydration and rehydration. The presence of chloroplast was confirmed by use of cyanobacteria homolog of plat CHL27 cyclase (CRD1) antibody which is a thylakoid marker (Cannife *et al.,* 2014). Five hundred microliters (500 µl) of chloroplast suspension was added into 1.5 mL of extraction buffer 1 (0.5M Tris-HCL pH 7.5, 10mM EDTA, 1% Triton, 2% β-mercaptoethanol, 40% PVPP, 1mM PMSF, and 1mM benzomidine) and vortexed for 3 minutes. The mixture was centrifuged at maximum speed for 15 minutes, and the resulting supernatant was split into two clean separate tubes (approx. 600 µL in each tube). Twice the volume of extraction buffer 2 (10% TCA in acetone, 0.7% β-mercaptoethanol 1mM PMSF, and 1mM benzomidine) was added to the tubes and incubated at -20 ^{O}C overnight. The tubes were centrifuged at maximum speed for 15 minutes and the pellet was washed with 1 mL of cold ammonium acetate followed by incubation at -20 ^{O}C for 20 minutes (this was repeated to ensure a clean white pellet). The pellet was dried for 3 minutes at room temperature to remove excess ammonium acetate and re-suspended in 2% SDS solution. The

extracted proteins were quantified using a modified Bradford assay. Extracted proteins (24 µl per sample) were separated using 1 dimensional SDS PAGE (12% acrylamide) and electrophoresed at 100V until the dye front completely reached the end of the gel. The gels were subjected to electro-blotting for probing with antibodies.

Following electrophoresis, proteins were transferred onto a nitrocellulose membrane at 100V for 1 hour by electroblotting, after which the membrane was briefly stained with Ponceau S for 30 seconds and destained by briefly washing with 1 x TBST for a minute. The membrane was blocked with a 1X TBST containing 10% (w/v) fat-free milk powder for 1 hour at room temperature with gentle shaking. The membrane was probed with a 1:10000 (1uL in 10mL) anti-CRD1 (cyanobacterial homolog of plant CHL27 cyclase) as a primary antibody and incubated at 4 ^{O}C overnight with gently shaking. After the primary antibody incubation, the membrane was washed thrice for 5 minutes in 1X TBST. This was followed by incubation for one hour with a 1:20000 (1uL in 20mL) goat anti-rabbit secondary antibody at room temperature. The membrane was washed thrice for 5 minutes with a 1X TBST. Proteins were detected using a chemiluminescent substrate (WesternBright) and visualized on the gel doc system.

2.10. Transmission Electron Microscopy (TEM)

Leaves were cut into 2 mm segments which were placed in Eppendorf tubes containing 500 µL of fixative 1 (2.5% glutaraldehyde in 0.1 M phosphate buffer with 0.5% caffeine) and left at 4ºC overnight. After the incubation period, the samples were fixed for an hour in an equal volume of 250 µl of 2% Osmium tetraoxide (OsO_4) and 0.2 M phosphate buffer. This was followed with three washes of 0.1 M phosphate buffer. The samples were dehydrated by a serial ethanol gradient as follows: 5 minutes in 30% (v/v) ethanol, 5 minutes in 50% (v/v) ethanol, 5 minutes in 70% ethanol, 5 minutes in 85% (v/v) ethanol, 5 minutes in 95% (v/v) ethanol, and 10 minutes in 100% (v/v) acetone. Each dehydration step was repeated twice. The samples were infiltrated with Spurr resins 1: 1 acetone (100%): resin for 18 h., 3:1 (resin: 100% acetone) for 4 h, 50% resin for 4 h, 50% resin overnight. The samples were polymerised for 16 h at

80°C, followed by sectioning at a gold interference (95 nm) with a Reichert Ultracut-S microtome. Sections were stained in 2% (w/v) uranyl acetate and 1 % (w/v) lead citrate and viewed with a Jeol 200 ex transmission electron microscope.

2.11. Statistical analyses

Data obtained in the study was analysed using XLStat implemented in Excel Principal component analysis and factor analysis was performed as exploratory multivariate analysis tools that allow for the reduction of the dimensionality of large datasets were generated by MRM mass spectrometry. The factor analysis was performed using the principal factor method as the extraction method applied iteratively. The correlations were calculated as the Pearson coefficients. As for principal component analysis, the matrix was built with Pearson's.

Chapter 3:

Nature of phosphoglycerolipids in leaves and roots of *X. humilis* during dehydration and rehydration stress treatment

3.1. Results

3.1.1. Relative water content of *Xerophyta humilis* during the drought stress treatment

Withholding water resulted in an apparent similar rate of decline in RWC of both leaves and roots after 9 days, reaching 9% on day 13 (Supplementary Figure 3.16; page 165). Repetition of dehydration and rehydration kinetic studies showed that this was consistent . Other studies have demonstrated that roots initiate dehydration earlier than leaves, and sampling in this study might have precluded picking up these initial discrepancies. However, the similar rate of decline in RWC in root and leaf tissues over the majority of the dehydration and rehydration process is most likely due to the small stature of this plant. Dehydration was associated with visible phenotypical changes such as leaf de-greening, and decrease in leaf size, which intensified with water deficit (Figure 3.2). In the fully dehydrated state, the leaves appeared completely shrunken with yellowish discoloration (Figure 3.2 D). Leaf de-greening has been reported as one of the unique mechanisms which allows *X. humilis* (Farrant, 2000) and other PDT plants to tolerate water deficit (Farrant, 2000; Farrant *et al.,* 2003). This mechanism is initiated upon drought induced senescence in desiccation sensitive plants, and in PDT plants as a protective strategy to prevent excess production of photosynthetically produced ROS and senescence among other things (Farrant, 2000; Williams et al. 2015). These appear to be common strategies which occur during dehydration, and are associated with a decrease in water potential (Scoffoni *et al.,* 2014; Essaghi *et al*., 2016). After re-watering, the plants regained their hydrated state relatively quickly reaching a RWC of 96% after 48 hours (Figure 3.2 I).

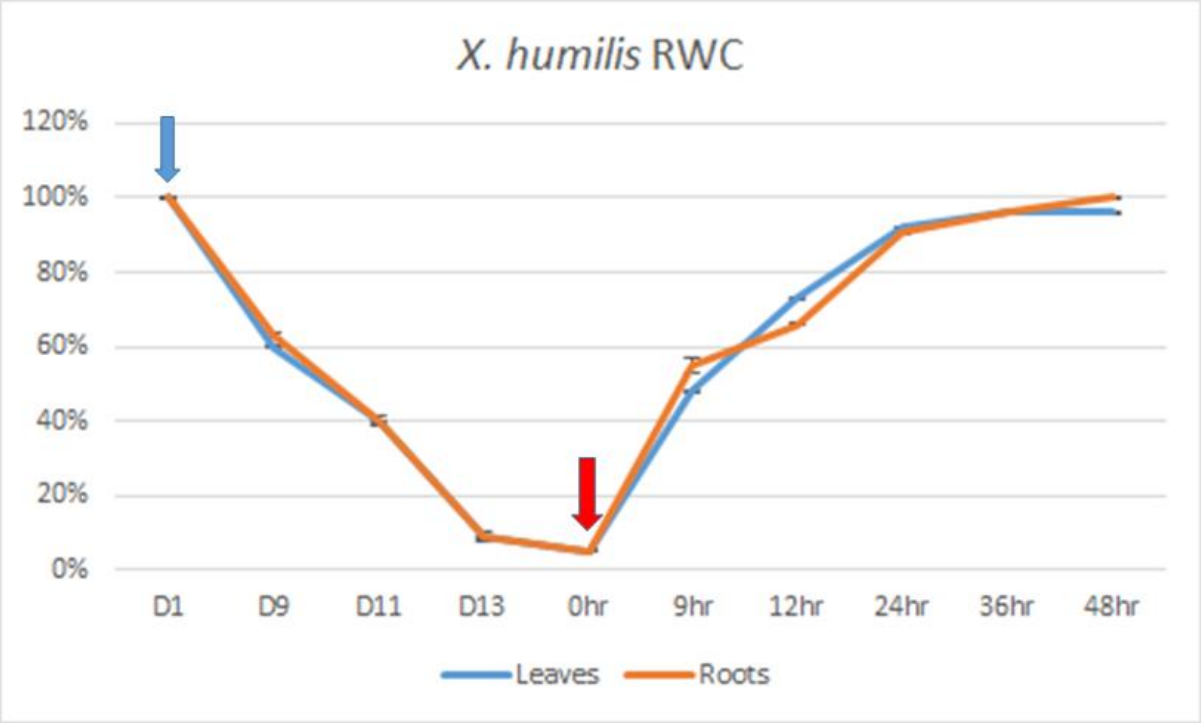

Figure 3.1: Relative water content (RWC in %) of *X. humilis* plants over the course of drought treatment. The blue arrow on D1 indicates the suspension of watering, the red arrow on 0hr corresponds to the rehydration. The dehydration and rehydration experiments were carried out under a 16 hr light, 325 μmol s^{-1} m^{-2}, 25ºC and 8 hr dark, 10ºC regime.

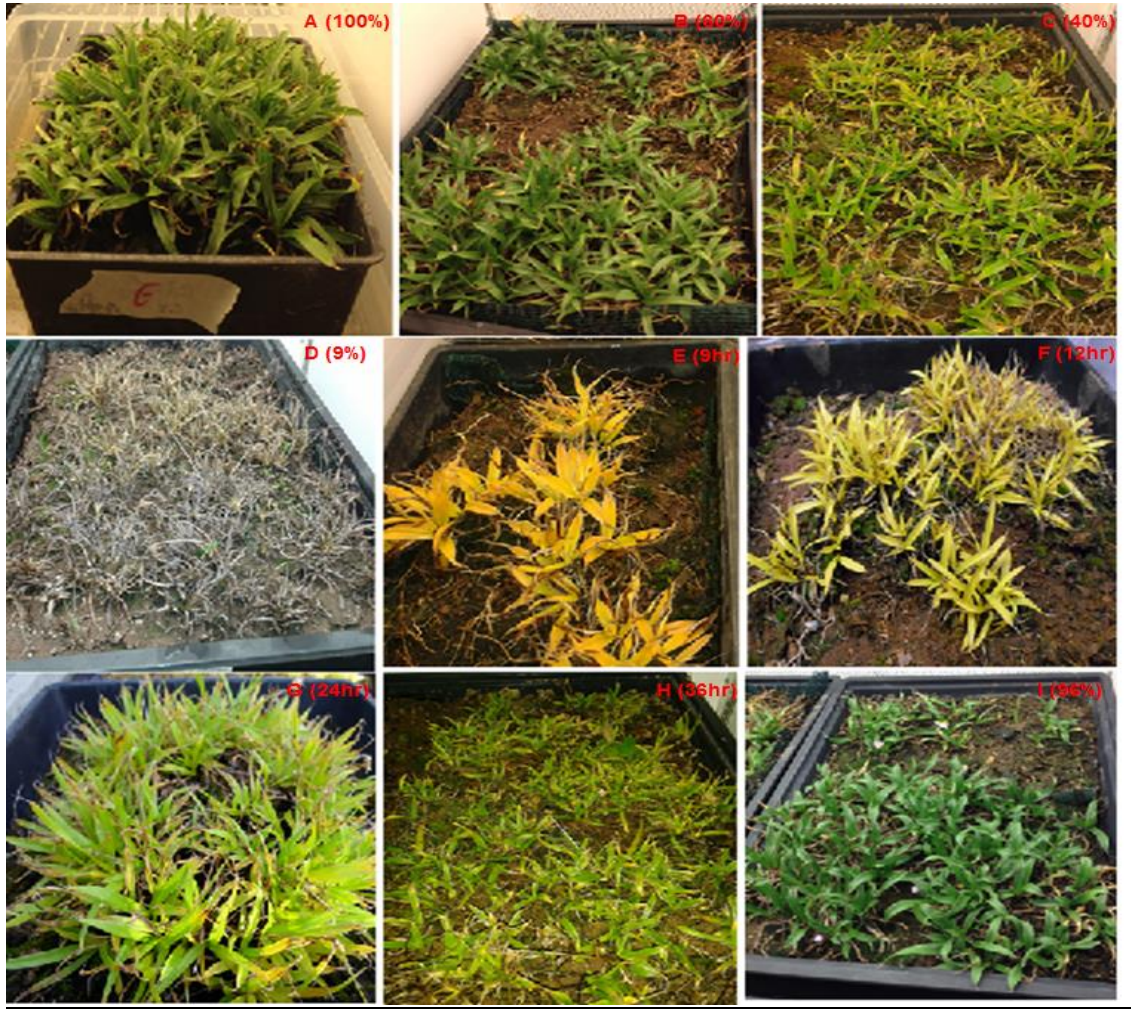

Figure 3.2: Images of *X. humilis* plant during the dehydration (A-D) and rehydration treatment in the Conviron (E-I). The dehydration and rehydration experiments were carried out under a 16 hr light, 325 μmol s^{-1} m^{-2}, 25ºC and 8 hr dark, 10ºC regime.

3.1.2. Thin Layer Chromatography (TLC) analysis

In this study, TLC technique was used to analyse total lipids from fully hydrated (100% RWC) dehydrated and rehydrated leaves and roots of *X. humilis* plant (Figure 3.3). TLC is a quick and inexpensive technique that has been routinely used to analysis lipids from various sources (Skipski *et al.,* 1965; Touchstone, 1995). In this technique, separation is based on the adsorption affinity of the molecule to a stationary phase (e.g silica gel), where the molecules with higher affinity to the stationary phase travels slower and those with lower affinity to the stationary phase travel faster (Touchstone, 1995). The results confirmed the presence of phospholipids from all major classes in both root and leaf tissue. The amount of lipids was found to change upon dehydration and rehydration. Therefore, further composition analysis was undertaken.

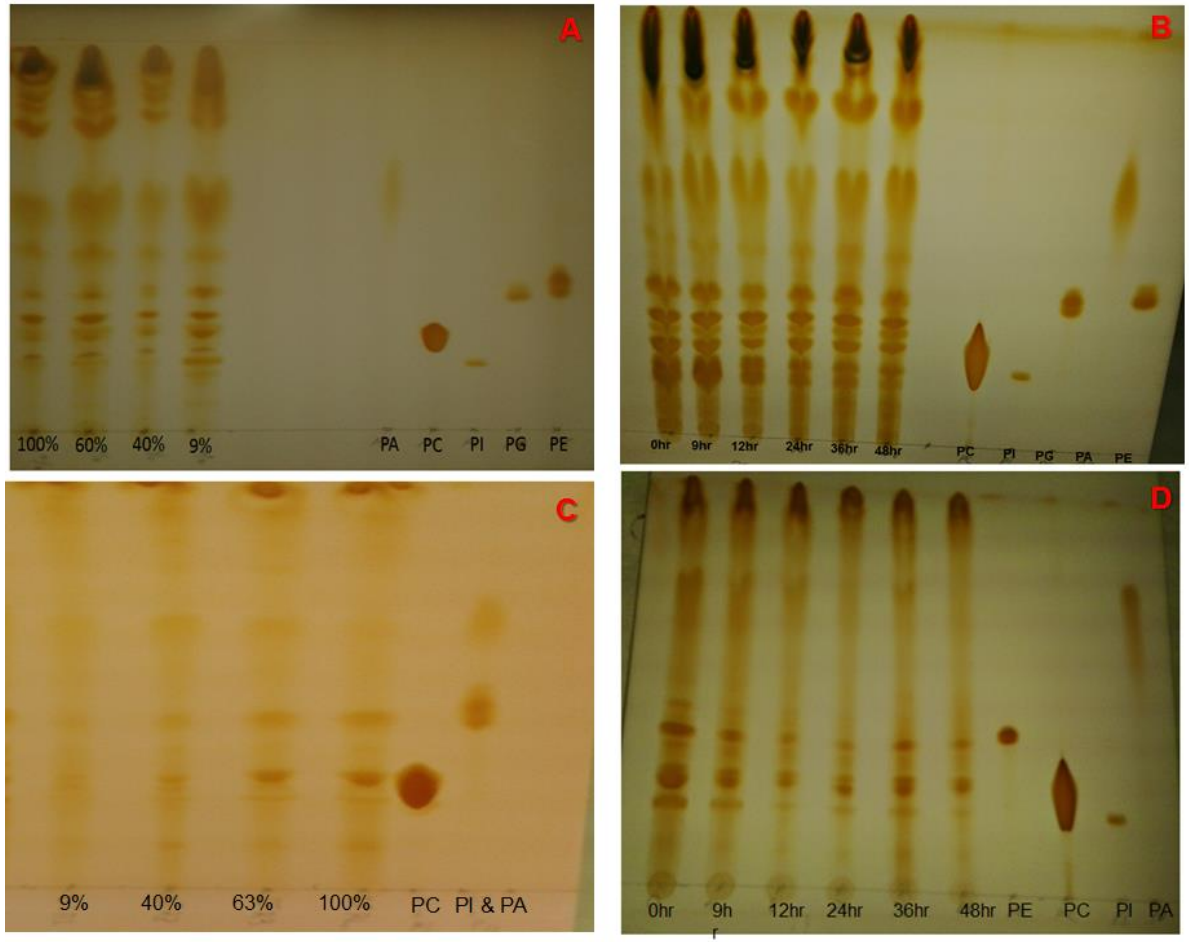

Figure 3.3: Images of 1d-dimensional TLC separation of total lipids extracted from *X. humilis* leaves (A,B) and roots (C,D) respectively. PA, PC, PI, PG, and PE are standards used tp confirm the location of specific lipids class on the silica gel plates.

3.1.3. Mass scan analysis of the main phosphoglycerolipids in the leaves and roots of *X. humilis*

The masses of phosphoglycerolipids from fully hydrated (100% RWC), and desiccated (9% RWC) leaves and roots of *X. humilis* plants were analysed by Tandem mass spectrometry (MS) implemented with collision-induced dissociation (CID) (Larsen *et al*., 2001; Hopfgartner *et al.*, 2004; Rainteau *et al*., 2012). In this technique, the parent glycerophospholipid is detected in the first quadrupole (Q1) of the tandem MS, the second quadrupole (Q2) is the intermediary stage filled with inert gas where CID of the parent ion occurs, and the resultant ion-fragments are detected in the third quadrupole (Q3).

In the present study, mass scan spectrum of phosphatidylinositol (PI) was obtained by precursor ion scanning at *m/z* 241 (negative mode); the ion with m/z 241, was detected in Q3, which corresponds to the inositol phosphate ion. The mass scan spectrum of phosphatidylcholine (PC) was obtained by neutral loss scan of 60 *amu* (negative mode; release of methyl formate). Phosphatidylethanolamine (PE) was obtained by neutral loss scan of 141 *amu* (positive mode; release of ethanolaminephosphate), whilst that of phosphatidylglycerol (PG) was obtained by precursor ion scanning at *m/z* 227 (negative mode; release of a glycerophosphoglycerol ion -H_2O). The obtained masses for PE and PC correspond to the $[M+H]^+$ ions and the $[M+HCOO]^-$ ions, respectively. For PI and PG they corresponded to the $[M-H]^-$ ions (Figure 3.4). Table 3.1 shows the molecular ion masses (*m/z*) and corresponding theoretical number of Carbon (C) in the fatty acids obtained. Using the enhanced product ion (EPI) mode, we were able to obtain fragment ions of most of molecular ions corresponding to those masses.

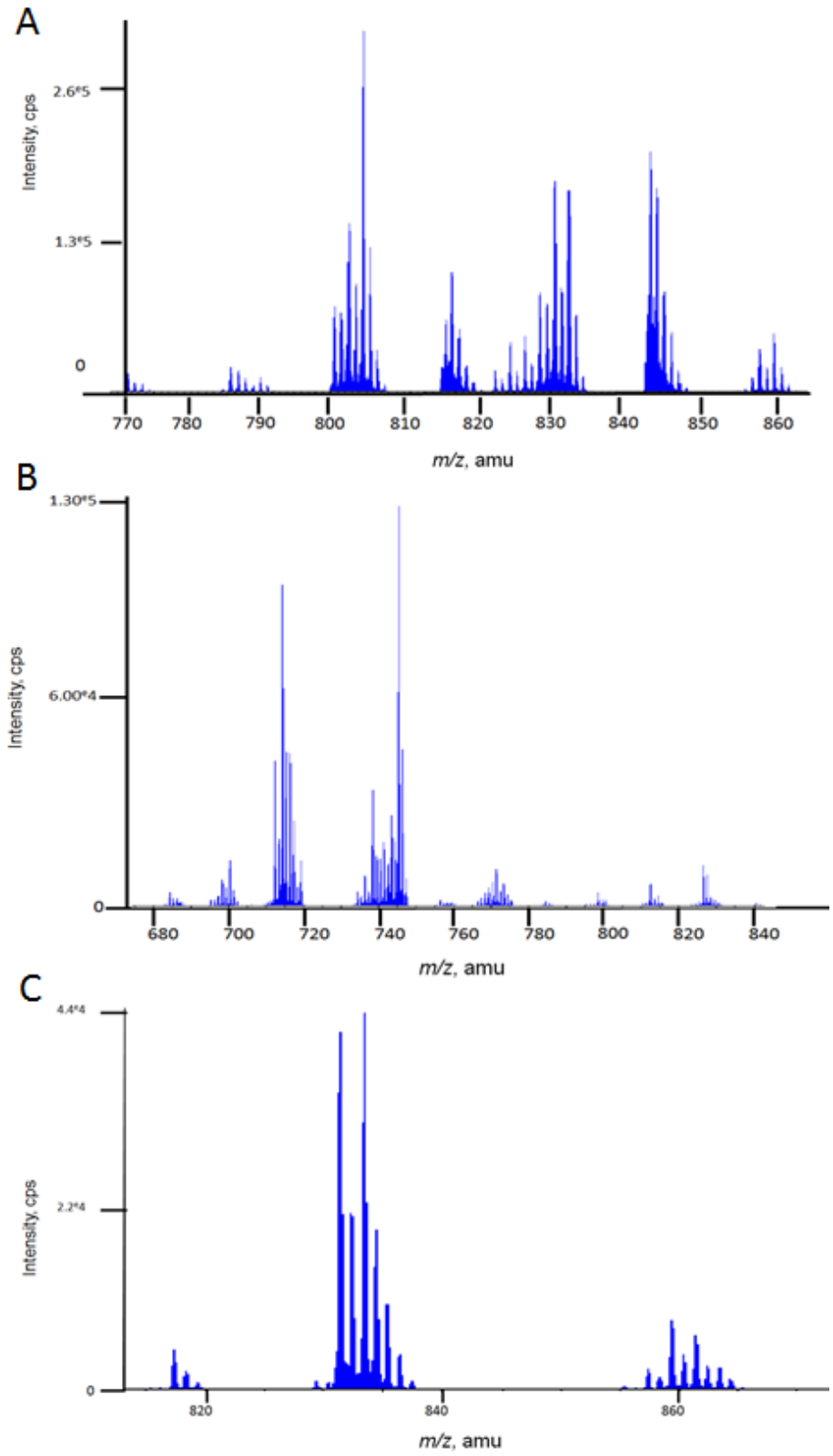

Figure 3.4: Mass scan of the main glycerophospholipids from fully hydrated leaves of *X. humilis*. Mass of parents ions of phosphatidylcholine (A), phosphatidylethanolamine (B), and phosphatidylinositol (C) were recorded by the neutral loss of fragment 60 *amu* (from negative ions), the neutral loss of fragment 141 *amu* (from positive ions), and precursor ion of fragment *m/z* 241(from negative ions), respectively. Mass spectra correspond to the $[M+HCOO]^-$ ions for PC, $[M+H]^+$ ions for PE, and for PI $[M-H]^-$ ions.

Table 3.1: List of all the molecular species detected by MRM. The list was established from PC, PI, PG and PE enhanced resolution mass spectra. From the spectra the molecular species can be deduced as "carbon number:double bond. The detailed fatty acid composition of the molecular species consistent with carbon number:double-bond formula can be assayed by transitions parent →product ions after CID of the ester bonds. In bold: m/z detected for PE, PI, PC and PG by enhanced-resolution mass scanning. In green coloured are the unusual fatty acids. For PE and PI the parent ions *m/z* correspond to the $[M-H]^-$ and for PC it corresponds to $[M+HCOO]^-$. In agreement with formula a difference of 2 amu is noted between *m/z* of PE MRM (negative ionization mode M-H) and neutral loss of *m/z* 141 (positive ionization, M+H).

Molecular ion mass	number of carbon : number of insaturation	**Composition according to EPI fragmentation**
PC		
764.5	C31:0	**15:0/16:0**
772.5	C32:3	**14:0/18:3**
774.5	C32:2	**14:0/18:2**
		16:1/16:1
776.5	C32:1	**14:0/18:1**
		16:0/16:1
778.5	C32:0	**16:0/16:0**
786.5	C33:3	15:0/18:3
788.5	C33:2	**15:0/18:2**
		15:0/18:1
792.5	C33:0	
798.5	C34:4	
800.5	C34:3	**16:0/18:3**
802.5	C34:2	**16:0/18:2**
804.5	C34:1	**16:0/18:1**
806.5	C34:0	
814.5	C35:3	**17:0/18:3**
816.5	C35:2	
818.5	C35:1	**17:0/18:1**
822.5	C36:6	**18:3/18:3**
824.5	C36:5	**18:3/18:2**
826.5	C36:4	**18:2/18:2**
		18:1/18:3
828.5	C36:3	**18:2/18:1**
		18:0/18:3
830.6	C36:2	**18:1/18:1**
		18:0/18:2
832.6	C36:1	**18:0/18:1**
		16:0/20:1
834.5	C36:0	**18:0/18:0**
844.5	C37:2	**19:0/18:2**
		19:1/18:1
846.5	C37:1	**19:0/18:1**
858.5	C38:2	**20:1/18:1**
860.5	C38:1	**20:0/18:1**
886.6	C40:1	**18:2/22:0**
888.6	C40:1	**18:1/22:0**
900.5	C41:2	**18:2/23:0**
914.6	C42:2	**18:2/24:0**
PE		

684.5	C32:3	14:0/18:3
684.5	C32:2	14:0/18:2
698.5	C33:3	15:0/18:3
700.5	C33:2	15:0/18:2
710.5	C34:4	
712.5	C34:3	**16:0/18:3**
714.5	C34:2	**16:0/18:2**
716.5	C34:1	**16:0/18:1**
718.5	C34:0	
734.5	C36:6	**18:3/18:3**
736.5	C36:5	**18:3/18:2**
738.5	C36:4	**18:2/18:2**
		18:1/18:3
740.5	C36:3	**18:2/18:1**
		18:0/18:3
742.6	C36:2	**18:1/18:1**
		18:0/18:2
		16:0/20:2
744.6	C36:1	**18:0/18:1**
		16:0/20:1
746.5	C36:0	
768.5	C38:3	**20:1/18:2**
770.5	C38:2	20:1/18:1
		18:2/20:0
772.5	C38:1	
772.5	C40:2	18:2/22:0
812.7	C41:2	**23:0/18:2**
814.7	C41:1	**23:0/18:1**
824.7	C42:3	**24:0/18:3**
826.7	C42:2	**24:0/18:2**
828.7	C42:1	**24:0/18:1**
840.7	C43:2	**25:0/18:2**
854.7	C44:2	**26:0/18:2**
PI		
795.5	C31:0	**15:0/16:0**
809.5	C32:0	**16:0/16:0**
817.5	C33:3	**15:0/18:3**
819.5	C33:2	**15:0/18:2**
829.5	C34:4	
831.5	C34:3	**16:0/18:3**
833.5	C34:2	**16:0/18:2**
835.5	C34:1	**16:0/18:1**
837.5	C34:0	
853.5	C36:6	**18:3/18:3**
855.5	C36:5	
857.5	C36:4	18:2/18:2
		18:1/18:3
859.5	C36:3	**18:2/18:1**
		18:0/18:3
861.6	C36:2	**18:1/18:1**
		18:0/18:2
863.6	C36:1	**18:0/18:1**

865.5	C36:0	
PG		
749.6	C34:0	16:0/18:0
747.6	C34:1	16:0/18:1
		16:1/18:0
745.6	C34:2	16:1/18:1
741.6	C42:4	16:1/18:3
721.6	C32:0	16:0/16:0
719.6	C32:1	16:1/16:0

In addition to the expected masses of even numbered fatty acids, masses that could only correspond to odd-numbered fatty acids was detected in all classes (highlighted in green in Table 3.1) except for PG. Figure 3.5 illustrates the fragmentation pattern of the PC *m/z* 788 ion, which fragments to an ion of *m/z* 279, which corresponds to 18:2-fatty acid. It also leads to a fragment ion of *m/z* 241.

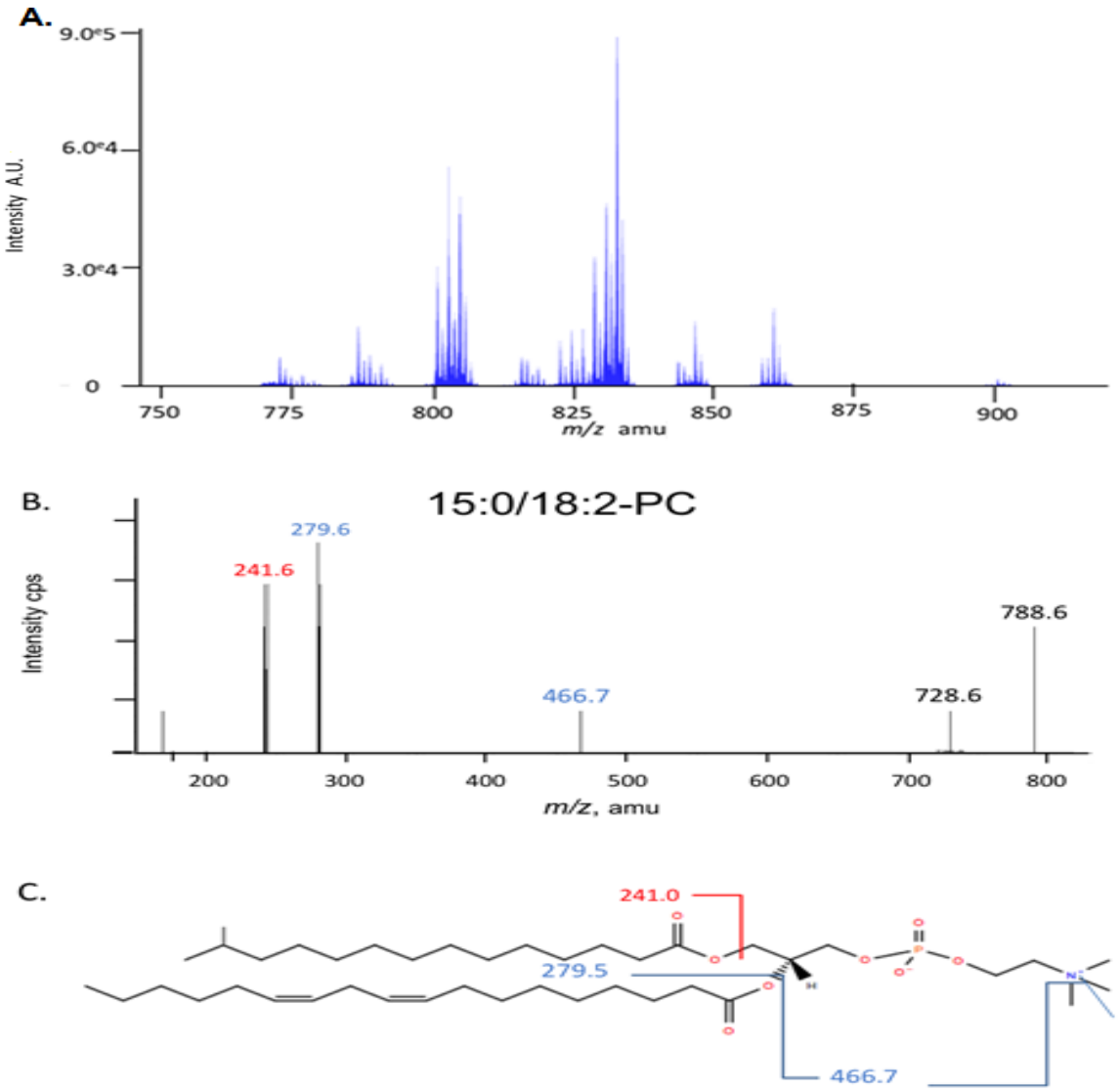

Figure 3.5: EPI fragmentation spectra of a PC of *m/z* 788.6. A: triple quadrupole mass spectra of lipids extracted from hydrated leaves for the neutral loss of 60 amu scan. B: the product ion spectrum of *m/z* 788.6. C: the parent ion spectrum is compatible with a 15:0/18:2-PC, the precursor ion is detected in the first quadrupole (Q1) of the Tandem MS, the second quadrupole (Q2) is the intermediary stage filled with inert gas where collision induced dissociation of the precursor ion occurs, and the resultant ion-fragments are detected in the third quadrupole (Q3). It should also be noted that a m/z 466.7 is another indication of fatty acid at *m/z* 241 bound to the glycerol.

A fragment ion with a *m/z* of 241 is expected for PI, because it corresponds to the inositol phosphate ion released during fragmentation. In order to confirm that an ion with m/z of 241 is not released only by PI, a precursor of 241 *amu* mass scan was performed. Most of the parent ions leading to a fragment ion of m/z 241 eluted in a

peak at retention time 39'. But some parent ions elute in peaks at 20' and 34'. The peak at 39' corresponded to PI molecules, as confirmed by the masses of the parent ions in this peak, and by the fragments. The masses and the fragmentations of the parent ions in the peaks at 20' and 34' undoubtedly establish that some parent ions of *m/z* 241 ions co-elute with PE and PC, respectively (Figure 3.6).

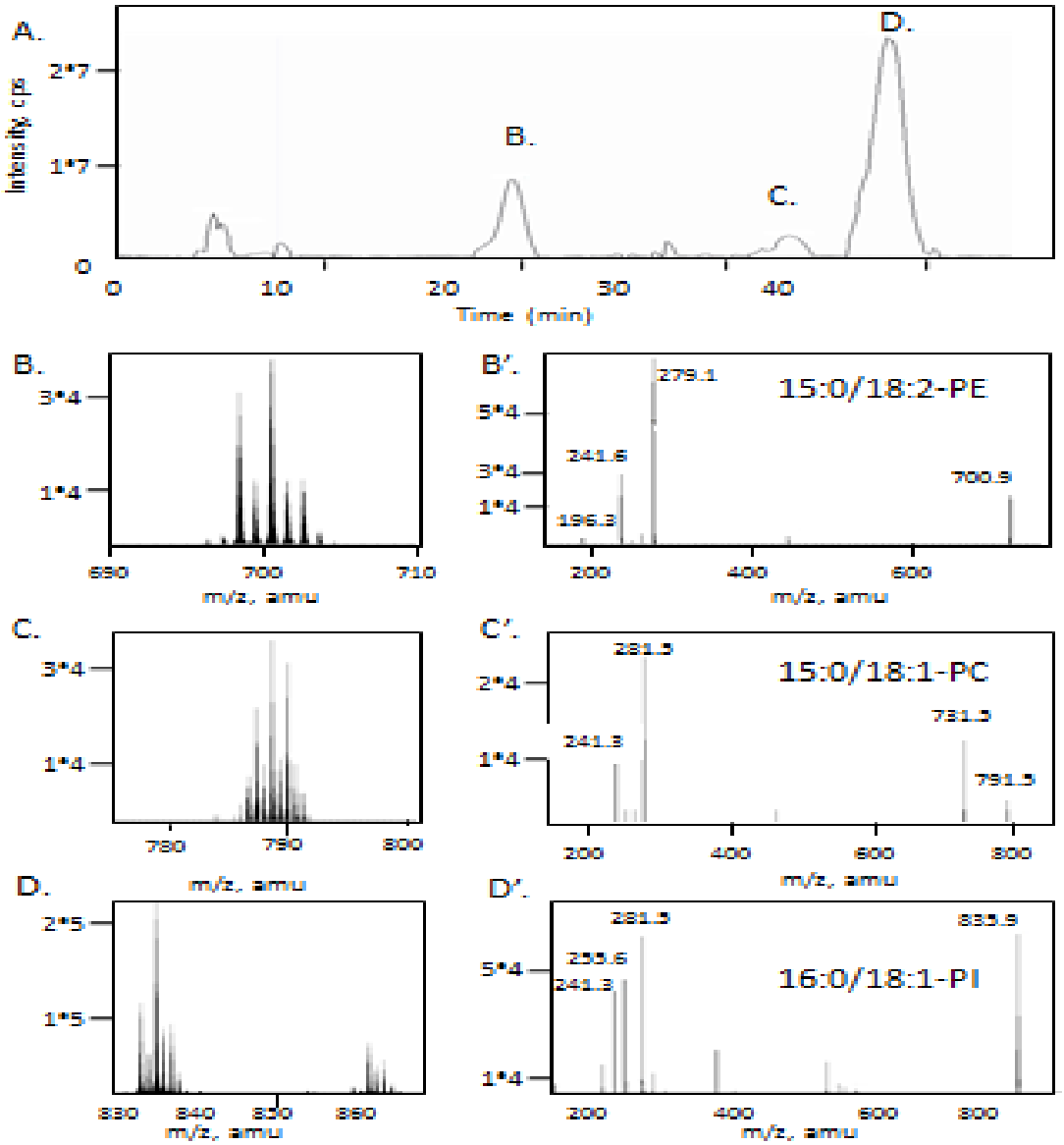

Figure 3.6: Total-ion-current (TIC) of precursor 241 scan of *X. humilis*. leaves at fully dehydrated and hydrated. The peak eluting at 39' correspond to PI molecular species. An ER analysis in this time window corresponding to this peak leads to masses typical of PI (D), which is confirmed by EPI analysis. The peak at 20' and 34' correspond to PE and PC molecular species respectively.

For example, the phospholipid with a *m/z* 788.6 that was analysed is a PC. It elutes from the liquid chromatography column upstream of the mass quadrupoles together with the other PC molecules. Furthermore, it generates a fragment ion with a *m/z* 728.6; which is a neutral loss of 60, typical of PCs, and represents the loss of a methyl and formiate from the formiate adduct precursor ion.

In order to confirm the existence of the unusual fatty acids, a different technique, namely gas chromatography was used. In this technique, total lipids were first submitted to methylation, so that the formed methyl esters of fatty acids could be separated in the column. This analyses confirmed that the fragment ion with a *m/z* 241 was identified by gas chromatography as 255 (mass of 16:0-alkyl ion; Figure 3.7) minus 14, the mass for CH_2. Therefore, an ion of m/z 241 could be a 15:0-alkyl.

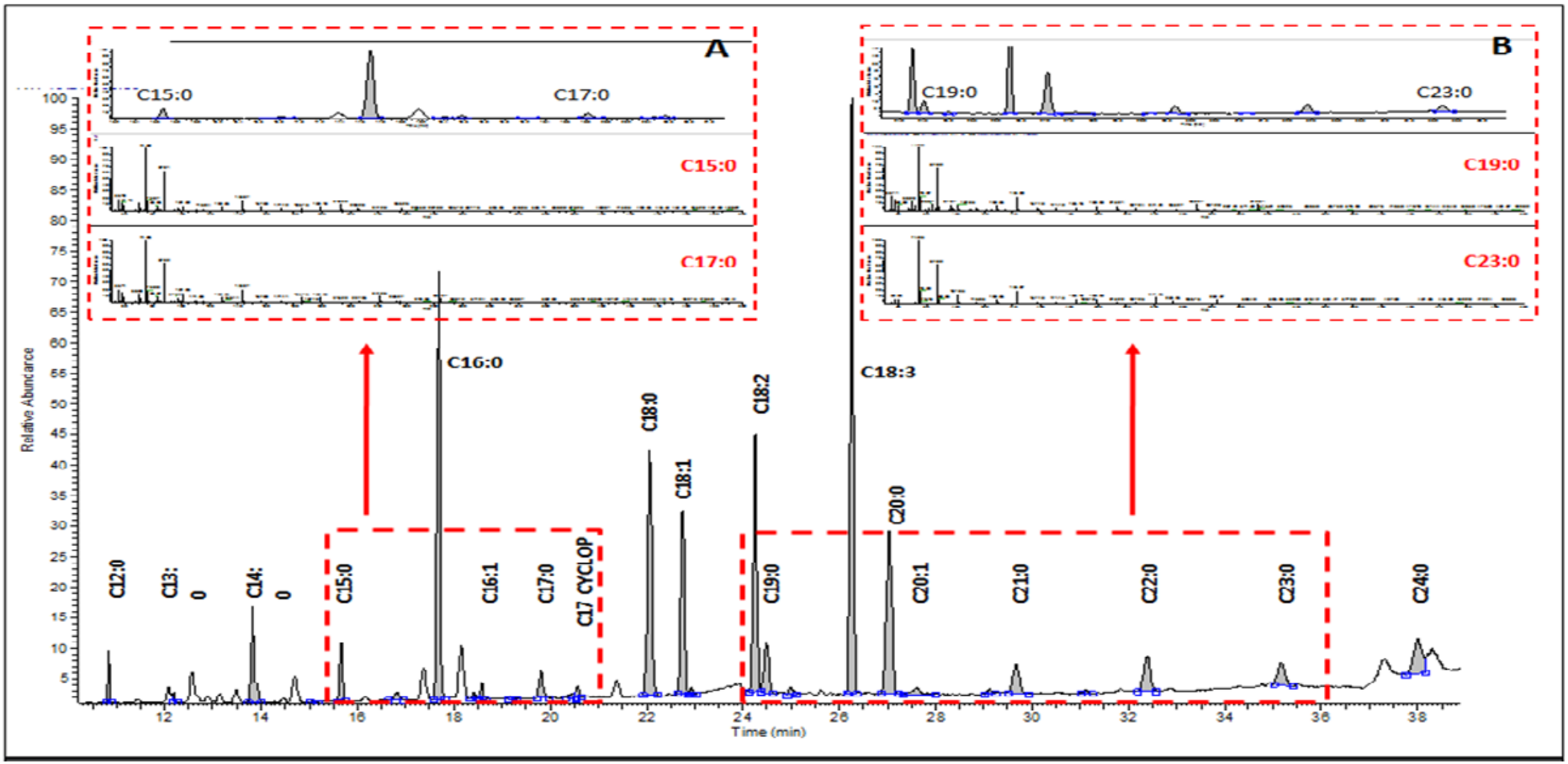

Figure 3.7: Identification of unusual fatty acids by GC in hydrated *X. humilis* leaves. A and B: section of total ion chromatogram showing unusual fatty acids and their corresponding spectra. Metabolites are identified from exact retention time and comparison of the corresponding mass spectrum with those in the National Institute of Standards and Technology database and those of FAME standard mixtures. The GC showed the presence of common fatty acids including palmitic (C16:0), palmitoleic (C16:1), stearic (C18:0), oleic (C18:1) linoleic (C18:2) and linolenic acid (C18:3). The unusual fatty acids were also present and includes myristic (C14:0), pentadecanoic (C15:0), margaric (C17:0), nonadecanoic (C19:0), arachidic (C20:0), paullinic (C20:1), heneicosylic (C21:0), behenic (C22:0), tricosylic (C23:0) and lignoleic acid (C24:0) were also confirmed by GC.

It is possible to assign to the different fragment ions the fatty acid to which they correspond (Table 3.2). Using the fragmentation spectra, it was possible to assign to the different masses of molecular ions their composition (see third column of Table 3.1)

Table 3.2: List of the fatty acids and their corresponding *m/z.* Results are expressed as % of total peak (n=3).

m/z of fragment ions	Fatty acyls
227	14:0
241	15:0
255	16:0
269	17:0
277	18:3
279	18:2
281	18:1
283	18:0
295	19:1
297	19:0
309	20:1
311	20:0
339	22:0
353	23:0
367	24:0
381	25:0
396	26:0

3.1.4. Nature of and changes in molecular species of lipids during dehydration and recovery of roots and leaves of *X. humilis*

Tandem mass spectrometry in the multiple reaction monitoring (MRM) mode was then utilized to analyse the changes in lipid molecular species of *X. humilis* leaves and roots during dehydration and rehydration. In this method, the ion *m/z* that are detected in Q1 and Q3 have to be pre-set as this is an *a priori* technique in which only transitions (couples of masses) of expected molecular species are quantified. The table of MRM transitions was designed based on the mass scan and fragmentation scan data outlined above. The composition of PI, PC, PE and PG in hydrated tissues and during dehydration and rehydration are given in section 3.5 and 3.6 below. The factor analysis was performed using the principle factor method as the extraction method was applied iterartively.

3.1.5. 3.1.5. Analysis of changes in membrane lipids of leaves and roots of *X. humilis* using LC-MS/MS in the MRM mode

3.1.5.1. Lipid molecular species and fatty acid composition within PC

The MRM method does not allow for the quantification of the total amount of lipid in each class, which therefore limits comparison among them. For instance, we cannot evaluate the amount of PC and compare it to the amount of PE. However, it is possible to detect and analyse changes within any class with respect to the fatty acids esterified on the glycerol backbone. By way of illustration, the changes in PC composition during dehydration and rehydration are given below. In fully hydrated leaves, there was a higher amount of more prevalent PC species such as 16:0/18:1-PC, 16:0/18:2-PC, 16:0/18:3–PC and 18:0/18:1-PC, accounting for 23%, 11%, 11%, and 9% of total PC molecular species respectively (as quantified by corresponding MRM transition; Table 3.3; Supplementary Figure 3.8). A trace amount of PC molecular species with unusual fatty acids such as 14:0/18:2-PC, 14:0/18:3-PC, 20:1/18:2-, 20:1/18:1-PC, 18:2/20:0-PC, 17:0/18:2-PC,14:0/18:1-PC, accounted for 0,4%, 0,3% 0,2%, 0,2%, 0,2%, and 0,1% of total molecular species respectively (Table 3.3). Dehydration below 40% RWC resulted in an increases in poly-unsaturated lipid molecular species 18:2/18:3-PC, 18:1/18:3-PC, and 18:3/18:3-PC decreases in the more saturated molecular species 18:1/18:1-PC, 18:0/18:0-PC, 16:0/18:2-PC, 16:0/18:1-PC and 15:0/18:1-PC. On rehydration, there was an increase in 16:0/18:3-PC, 16:0/18:2-PC and 16:0/18:1-PC, and a decrease in 18:3/18:3-PC, 18:1/18:3-PC, 18:1/18:1-PC, 18:2/18:1-PC and 18:2/18:2-PC between 24 (92% RWC) and 48 hours (96% RWC; Supplementary Figure 3.8).

In the roots, the molecular species 16:0/18:2-PC, 16:0/18:1-PC, 18:2/18:2-PC and 18:2/18:1 were the highest in fully hydrated plants, accounting for 38%, 16%, 12% and 10% of the total molecular species, respectively (Table 3.4). Upon dehydration, the relative percentage of 16:0/18:2-PC decreased sharply; whereas the 16:0/18:1-PC had an initial increase, and started decreasing when the root RWC had dropped to below 63%. The 18:2/18:2-PC had an initial decrease upon dehydration, followed by

a massive increase when the root RWC had dropped to below 63% (Supplementary Figure 3.9). Rehydration had reverse patterns on these molecular species, and most achieved the highest values after 12 h of rehydration. As it would be expected, the unusual molecular species such as 20:1/18:2-PC, 20:1/18:1-PC, 18:2/20:0-PC and 18:1/20:0-PC were present at low concentrations, accounting for 0.18%, 0.13%, 0.29% and 0.13% of the total molecular species, respectively (Table 3.4). Their values had a sharp increase with dehydration intensity, and continued to increase even when the plant was left in a fully dehydrated state for 3 weeks. On rehydration, these unusual molecular species containing PC lipids decreased.

Table 3.3: PC lipid molecular species (in % of total MRM transition signal) analysis of the *X. humilis* leaves during dehydration and rehydration. The values highlighted in blue represent the plant during dehydration and the ones in red represent the plant during rehydration. Water content values are given as RWC in percentages at different sampling points.

PC (Leaves)	100%	60%	40%	9%	0h (5%)	9h (48%)	12h (73%)	24h (92%)	36h (96%)	48h (96%)
15:0/16:0	0,21	0,56	0,3	0,05	0,04	0,08	0,06	0,37	0,44	0,56
14:0/18:3	0,32	0,5	0,42	0,36	0,33	0,25	0,24	0,65	0,85	0,64
14:0/18:2	0,42	0,71	0,69	0,37	0,24	0,19	0,23	0,62	0,67	0,75
14:0/18:1	0,06	1,96	1,64	0,5	0,29	0,24	0,31	0,72	0,76	0,66
16:0/16:0	0,52	0,56	0,2	0,1	0,08	0,18	0,1	0,26	0,26	0,35
15:0/18:3	1,84	1,4	1,25	1,31	1,37	0,91	1,44	2,33	2,64	2,19
15:0/18:2	1,89	1,99	2	1,36	0,75	0,83	1,36	2,26	1,96	2,79
15:0/18:1	3,22	4,27	3,56	1,27	1,1	0,86	1,04	1,74	1,66	1,71
16:0/18:3	10,81	6,21	5,65	6,84	6,86	6,03	7,3	10,99	12,82	11,42
16:0/18:2	11,04	10,5	10,83	7,53	6,36	6,26	6,94	10,01	9,6	13,94
16:0/18:1	22,74	26,55	22,11	8,75	7,76	8,67	8,34	12,12	11,11	13,04
17:0/18:2	0,86	0,8	0,87	0,78	0,8	0,82	0,72	0,89	0,72	1,08
17:0/18:1	1,87	2,25	1,78	0,92	0,79	0,89	0,88	0,95	0,88	1,11
18:3/18:3	1,41	0,91	1,11	6,26	8,8	6,57	6,8	3,4	4,34	2,45
18:3/18:2	2,39	1,97	2,4	9,65	8,72	9,49	8,65	5,95	6,22	5,13
18:2/18:2	2,68	2,84	3,86	7,7	7,02	5,07	4,96	3,88	3,83	4,35
18:1/18:3	3,11	3,65	3,2	7,57	7	7,67	8,45	5,89	5,56	3,53
18:2/18:1	5,22	8,22	8,48	11,07	11,58	9,6	10,21	8,26	6,83	6,31
18:0/18:3	6,03	2,6	3,92	6,07	8,09	8,8	7,49	8	10,51	9,85
18:1/18:1	5,18	8,2	6,82	6,45	7,08	6,17	7,19	4,61	3,97	2,63
18:0/18:2	3,49	2,42	3,96	5,18	4,67	7,55	5,41	4,93	5,91	6,28
18:0/18:1	9,31	8,39	10,93	7,69	6,2	8,41	8,15	7,56	6,11	6,65
19:0/18:1	1,8	0,82	1,17	0,86	0,78	0,75	0,76	0,75	0,53	0,61
20:1/18:2	0,24	0,45	0,59	0,6	0,78	1,08	0,64	0,48	0,45	0,43
20:1/18:1	0,22	0,55	0,79	0,54	0,98	0,97	0,65	0,43	0,44	0,29

18:2/20:0	0,66	0,3	0,49	0,57	0,79	0,77	0,73	0,58	0,7	0,73
18:1/20:0	1,46	0,42	0,98	0,63	0,71	0,92	0,86	0,75	0,82	0,57

Table 3.4: PC lipid molecular species (%) analysis of the *X. humilis* roots during dehydration and rehydration. The values highlighted in blue represent the plant during dehydration and the ones in red represent the plant during rehydration. The % of fatty acid were calculated from the % of the molecular species (i.e. % of total MRM transition signal). Water content values are given as RWC in percentages at different sampling points.

PC (Roots)	100%	63%	40%	9%	0hr (4%)	9hr (55%)	12hr (66%)	24hr (91%)	36hr (96%)	48hr (100%)
15:0/16:0	1,07	2,22	0,21	0,21	0,46	0,38	0,61	2,81	2,81	2,48
14:0/18:3	0,04	0,05	0,05	0,03	0,07	0,02	0,03	0,09	0,03	0,06
14:0/18:2	0,55	0,73	0,8	0,64	1,35	0,38	0,57	0,42	0,63	0,53
14:0/18:1	0,21	0,48	0,44	0,21	0,23	0,17	0,37	0,47	0,5	0,42
16:0/16:0	1,14	1,63	0,21	0,28	0,36	0,78	1,06	2,04	1,56	1,67
15:0/18:3	0,25	0,21	0,28	0,32	0,51	0,18	0,23	0,31	0,24	0,17
15:0/18:2	4,17	4,63	4,85	4	6,31	3,31	3,67	3,01	4,29	3,49
15:0/18:1	1,35	2,12	1,65	0,93	0,79	1,12	1,75	1,42	1,65	1,89
16:0/18:3	1,93	1,08	1,69	2,16	2,08	1,44	1,41	1,03	1,32	0,89
16:0/18:2	38,26	30,36	26,53	26,62	22,24	28,31	31,86	25,73	31,1	28,39
16:0/18:1	16,27	19,07	16,23	12,04	6,91	16,99	20,08	24,54	20,29	24,42
17:0/18:2	1,39	1,02	1,01	0,93	1,32	1,17	1,05	0,8	1,08	0,79
17:0/18:1	0,73	0,8	0,75	0,45	0,58	0,67	0,7	0,88	0,89	0,96
18:3/18:3	0,04	0,04	0,12	0,19	0,36	0,1	0,06	0,03	0,09	0,03
18:3/18:2	1,13	0,83	2,12	3,2	4,71	1,7	0,98	0,67	0,87	0,46
18:2/18:2	12,41	10,39	13,38	17,96	21,05	13,42	9,81	7,62	9,21	8,76
18:1/18:3	0,41	0,46	0,71	0,89	0,73	0,72	0,53	0,45	0,39	0,36
18:2/18:1	10,17	12	15,45	17,94	15,8	14,75	12,19	11,42	11,01	11,05
18:0/18:3	0,13	0,12	0,11	0,11	0,14	0,17	0,15	0,18	0,26	0,27
18:1/18:1	3,83	6,67	6,44	5,44	3,55	5,08	5,47	8,31	5,15	5,17
18:0/18:2	2,14	1,47	2,13	1,93	3,53	2,55	2,23	2,41	2,29	2,75
18:0/18:1	1,45	1,83	2,12	1,41	1,8	2,06	2,23	3,07	2,21	2,88
19:0/18:1	0,2	0,27	0,33	0,28	0,45	0,94	0,71	0,66	0,43	0,46

20:1/18:2	0,18	0,42	0,6	0,48	1,21	0,64	0,38	0,17	0,26	0,29
20:1/18:1	0,13	0,26	0,52	0,26	0,46	0,4	0,23	0,2	0,19	0,3
18:2/20:0	0,29	0,45	0,75	0,73	2,03	1,59	0,95	0,66	0,65	0,62
18:1/20:0	0,13	0,42	0,52	0,36	0,68	0,96	0,71	0,6	0,59	0,53

The fully hydrated leaves were composed of high level of common fatty acids such as C18:1, C16:0, C18:2, C18:3 and C18:0, accounting of 30%, 23%, 16%, 14%, and 9% of the total fatty acids, respectively (Table 3.5). Unusual fatty acids are present in small amounts, with C14:0 and C19:0 making up only 0.9% each of the total fatty acids. Dehydration was associated with differential patterns in the changes of these fatty acids. C18:1 and C15:0 contents showed a tendency to increase in leaves when drying from the fully hydrated condition to above 60%, decreasing with intensification of water deficit in RWC of below 60%. However, a sharp decrease was noted for C16:0 fatty acid during dehydration. The content of C18:2 and C18:3 fatty acids increased significantly throughout desiccation. Rehydration was associated with an increase in the fatty acids that decreased during dehydration and vice versa. It is also important to note that the fatty acids with the C18-backbone did not change notably during rehydration. Furthermore, a very small turnover was observed for the unusual fatty acids during the dehydration and rehydration treatments. From the results, it can be concluded that dehydration of *X. humilis* leaves is associated with an increase in the content of polyunsaturated fatty acids, and a slight decrease in monosaturated fatty acids.

In the roots (Table 3.6), C18:2, C16:0, and C18:1 were the most predominant fatty acids accounting for 42%, 30%, and 19% of the total PC fatty acids at 100% RWC respectively. The minor fatty acids were C14:0, C19:0, and C20:1 which accounted for 0.9%, 0.9% and 0.4% of total PC fatty acids respectively. During dehydration, the content of 18:1 fatty acids increased initially during the first stages of dehydration from 100% - 60% RWC, and then decreased with treatment (Table 3.6). However, the content of C16:0 decreased gradually with dehydration. The content of C18:2 in PC decreased initially during the first stages of dehydration from 100% - 60% RWC, and then increased with the intensification of the dehydration treatment. Furthermore, the relative amount in PC of the unusual fatty acids C14:0 and C19:0 remained stable during dehydration, and increased over time in the air dry root, while the C20:1 levels increased with increased water deficit. Rehydration was associated with a reversal in the changes of fatty acids.

Table 3.5: PC fatty acids (%) analysis of leaves of *X. humilis* during dehydration and rehydration. The values highlighted in blue represent tissues during dehydration and those in red represent tissues during rehydration. The % of fatty acid were calculated from the % of the molecular species (i.e. % of total MRM transition signal). Water content values are given as RWC in percentages at different sampling points.

PC (Leaves)	100%	60%	40%	9%	0hr (5%)	9hr (48%)	12hr (73%)	24hr (92%)	36hr (96%)	48hr (96%)
14:0	0.9	1.6	1.4	0.6	0.4	0.3	1	0.4	1.1	1.1
15:0	3.6	4.1	3.6	2	1.6	1.3	3.4	1.9	3.4.3.4	3.6
16:0	23	22.5	19.7	11.7	10.6	10.7	17	11.4	17.2	19.8
17:0	1.4	1.5	1.3	0.9	0.8	0.8	0.9	0.8	0.8	1.1
18:0	9.4	6.7	9.4	9.5	9.5	12.4	10.2	10.5	11	11.4
18:1	30.2	36.7	34.1	26.4	25.7	25.6	24.3	27	21.3	19.9
18:2	15.8	16.5	19	25.4	24.4	23.4	20.9	22.4	20	23.1
18:3	13.7	9.1	9.5	22.2	25	23.1	20.9	23.6	23.7	18.8
19:0	0.9	0.4	0.6	0.4	0.4	0.4	0.4	0.4	0.3	0.3
20:0	1.1	0.4	0.7	0.6	0.8	0.8	0.7	0.8	0.8	0.7
20:1	0.2	0.5	0.7	0.6	0.9	1	0.5	0.6	0.5	0.4

Table 3.6: PC fatty acids (in weight %) analysis of the *X. humilis* roots during dehydration and rehydration. The values highlighted in blue represent tissues during dehydration and the those in red represent tissues plant during rehydration. The % of fatty acid were calculated from the % of the molecular species (i.e. % of total MRM transition signal). Water content values are given as RWC in percentages at different sampling points.

PC (Roots)	100%	63%	40%	9%	0hr (4%)	9hr (55%)	12hr (66%)	24hr (91%)	36hr (96%)	48hr (100%)
14:0	0.4	0.6	0.6	0.4	0.8	0.3	0.5	0.5	0.6	0.5
15:0	3.4	4.6	3.5	2.7	4	2.5	3.1	3.8	4.5	4
16:0	29.9	28	22.5	20.8	24.3	24.3	28	29.1	29.3	29.7
17:0	1.1	1	0.9	0.7	0.9	0.9	0.9	0.8	1	0.9
18:0	1.9	1.7	2.2	1.7	2.7	2.4	2.3	2.8	2.4	2.9
18:1	19.4	25.5	25.8	22.8	17.8	24.5	25.2	30.2	24.2	26.8
18:2	41.5	36.3	40.5	46.2	50.4	40.6	36.7	30.3	35.3	32.9
18:3	2	1.4	2.6	3.5	4.5	2.2	1.7	1.4	1.6	1.1
19:0	0.1	0.1	0.2	0.1	0.2	0.5	0.4	0.3	0.2	0.2
20:0	0.2	0.4	0.6	0.5	1.5	1.3	0.8	0.6	0.6	0.6
20:1	0.2	0.3	0.6	0.4	0.8	0.5	0.2	0.2	0.2	0.3

3.1.5.2. Lipid molecular species and fatty acid composition within PI

Previous studies which investigated both desiccation sensitive (tobacco; Zhai *et al.,* 2012) and tolerant species (Craterostigma plantagineum; Gasulla *et al*., 2013) found that there is accumulation of PI when plants were exposed to water deficit. It has been proposed that this fatty acid species assists in stabilizing biomembranes as well as functions as a precursor for the biosynthesis of the secondary messenger glycosyl inositol phosphorylceramides (GIPC), which in turn might prevent precipitation of macromolecules in the tightly packed cytoplasm of a desiccated cell by establishing hydrogen with them. Changes in the molecular species within the PI of *X. humilis* is presented in Table 3.7. The most abundant molecular species within PI in the fully hydrated leaves of *X. humilis* are 16:0/18:3-PI, 16:0/18:2-PI, 16:0/18:1-PI, which make up 27%, 25% and 12% of total PI, respectively. However, upon dehydration the 16:0/18:2-PI, 16:0/18:3-PI molecular species, together with 15:0/16:0-PI, 16:0/16:0-PI, and 16:0/18:1-PI decreased significantly. The molecular species 16:0/18:3-PI, 18:0/18:2-PI and 18:3/18:3-PI are the only species that had a significant increase during dehydration (supplementary figure 3.10). It should be noted that the trends observed during dehydration are not recovered fully after rehydration for 48hrs. It is possible that full recovery would occur during a more extended rehydration period. In the roots, the predominant molecular species in the fully hydrated state were 16:0/18:2-PI and 16:0/18:1-PI (Table 3.8)**,** accounting for 53% and 19% of total molecular species, respectively. During dehydration, molecular 16:0/18:2-PI decreased slightly from 53% to 49%, followed by a gradual increase with intensification of water loss. This molecular species further decreased on initial rehydration. The 16:0/18:1-PI molecular species increased from 19% at 100% RWC to 23% at 63% RWC, and then decreased slightly to 17% in fully dehydrated tissues (9% RWC; supplementary figure 3.11). Maintenance of plants in the desiccated state for 3 weeks did bring about a further reduction in average tissue RWC to 4%, and the molecular species 16:0/18:1-PI continued to decrease to a minimum level of 14%. Upon rehydration, the molecular species 16:0/18:1-PI increased to 24% of total PI after 48hrs of rehydration. The saturated molecular species 15:0/16:0-PI and 16:0/16:0-PI had an overall decrease during dehydration, and increased upon rehydration (Supplementary Figure 3.11). It is possible that full reversion to the situation typical of

plants at full turgor prior to dehydration did occur after 48hrs, but such data was not determined during this study.

Table 3.7: PI lipid molecular species analysis of *X. humilis* leaves (% of total MRM transition signal) during dehydration and rehydration. The values highlighted in blue represent tissues during dehydration and those in red represent plant tissues during rehydration. Water content values are given as RWC in percentages at different sampling points.

PI (leaves)	100%	60%	40%	9%	0h (5%)	9h (48%)	12h (73%)	24h (92%)	36h (96%)	48h (96%)
15:0/16:0	3,83	4,47	1,99	0,91	1,52	0,96	1,34	2,12	1,29	2,14
16:0/16:1	0,91	0,93	0,46	0,43	0,57	0,45	0,55	0,52	0,55	0,69
16:0/16:0	2,85	4,74	1,4	0,59	1,12	0,6	0,34	0,72	0,71	1,22
15:0/18:3	2,99	2,76	3,66	4,53	5,41	4,76	6,96	5,66	5,07	5,14
15:0/18:2	1,81	1,85	2,19	2	1,53	1,95	2,03	2,05	1,69	1,99
15:0/18:1	0,62	0,79	0,47	0,55	0,64	0,52	0,45	0,51	0,39	0,38
16:0/18:3	27,2	20,28	23,01	27,37	34,99	28,8	27,86	31,84	35,8	34
16:0/18:2	25,64	25,09	23,65	18,34	15,64	18,42	14,88	17,28	15,99	18,13
16:0/18:1	11,99	16,24	8,91	7,73	7,55	7,59	5,71	6,36	6,83	6
16:0/18:0	0,75	1,23	0,65	0,52	0,66	0,32	0,27	0,38	0,45	0,65
17:0/18:3	2,19	2,34	3,02	2,94	3,25	3,1	2,89	3,35	3,08	3,05
17:0/18:2	1,66	1,93	2,23	1,58	1,32	1,56	1,15	1,55	1,26	1,35
17:0/18:1	1,01	1,53	1,01	0,5	0,69	0,48	0,51	0,65	0,54	0,67
18:3/18:3	0,38	0,41	1,71	4,11	3,45	4,33	5,2	2,09	2,53	1,46
18:3/18:2	0,59	0,48	1,19	2,92	2,11	2,81	3,08	1,49	1,54	1,36
18:2/18:2	0,63	0,54	0,77	1,3	1,38	1,29	1,72	0,74	0,63	0,86
18:1/18:3	1,03	1,05	1,59	2,45	1,58	2,49	3,24	1,77	1,84	1,56
18:2/18:1	1,38	1,31	1,5	1,86	1,47	1,8	4,34	1,52	1,53	1,85
18:0/18:3	6,71	5,64	11,91	12,15	11,12	12,7	8,88	11,94	12,46	9,3
18:1/18:1	0,63	0,55	0,41	0,33	0,3	0,28	2,54	0,9	0,82	1,16
18:0/18:2	3,11	3,23	5,94	4,25	2,89	4,02	3,2	4,07	3,39	4,03
18:0/18:1	2,07	2,57	2,33	0,86	0,78	0,76	2,86	2,51	1,81	2,99

Table 3.8: PI lipid molecular species analysis in roots of *X. humilis* (% of total MRM transition signal) during dehydration and rehydration. The values highlighted in blue represent tissues during dehydration and those in red represent tissues during dehydration. Water content values are given as RWC in percentages at different sampling points.

PI (Roots)	100%	63%	40%	9%	0hr (4%)	9hr (55%)	12hr (66%)	24hr (91%)	36hr (96%)	48hr (100%)
15:0/16:0	5,26	1,49	3,39	3,01	4,76	7,15	7,97	10,88	12,11	6,88
16:0/16:1	1,37	1,49	0,96	1,18	0,57	1,65	1,52	1,67	1,65	1,27
16:0/16:0	6,1	6,27	3,31	3,32	5,1	5,89	5,47	9,03	8,88	7,82
15:0/18:3	0,35	0,21	0,43	0,35	0,37	0,78	0,61	0,37	0,53	0,13
15:0/18:2	3,17	3,45	4,25	3,57	4,47	5,77	4,97	3,77	4,48	3,02
15:0/18:1	0,64	0,66	0,76	0,43	0,43	0,66	0,93	0,73	0,39	0,38
16:0/18:3	3,69	2,13	4,11	4,93	4,18	4,16	3,96	2,2	3,2	1,7
16:0/18:2	53,07	49,16	51,23	57,03	57,22	49,39	44,15	39,78	39,3	43,91
16:0/18:1	19,47	23,24	20,95	17,1	13,93	13,59	14,97	19,03	18,02	23,71
16:0/18:0	0,54	0,55	0,49	0,39	0,4	0,77	1,23	1,12	1,08	1,17
17:0/18:3	0,16	0,1	0,15	0,14	0,12	0,21	0,19	0,17	0,13	0,08
17:0/18:2	1,4	1,55	1,82	1,69	1,49	1,15	1,12	0,97	1,37	1,53
17:0/18:1	0,63	0,9	0,99	0,55	0,54	0,43	0,98	1,01	1,37	1,09
18:3/18:3	0,01	0	0,03	0,01	0,02	0,04	0,08	0,02	0,05	0,03
18:3/18:2	0,17	0,1	0,24	0,26	0,37	0,53	0,53	0,39	0,21	0,2
18:2/18:2	0,78	0,67	1,47	1,57	2,57	2,23	1,94	1,12	0,99	0,89
18:1/18:3	0,11	0,12	0,16	0,16	0,09	0,36	0,51	0,24	0,13	0,19
18:2/18:1	1,34	1,67	2,26	2,58	1,61	2,71	3,44	2,66	1,93	1,73
18:0/18:3	0,1	0,1	0,17	0,13	0,11	0,17	0,17	0,21	0,15	0,19
18:1/18:1	0,39	0,45	0,62	0,52	0,21	0,92	1,37	1,2	0,9	0,59
18:0/18:2	0,91	0,88	1,58	1,3	1,15	0,97	2,16	1,72	1,61	2,33
18:0/18:1	0,34	0,47	0,59	0,3	0,29	0,47	1,61	1,72	1,51	1,15

As for PC (see above), the relative amount of each fatty acid percent was extracted from the data obtained for each molecular species. PI from fully hydrated leaves had a high amount of 18:3, 18:2, and 18:1-fatty acids, accounting for 21%, 18% and 10% of total PI fatty acids, respectively (Table 3.9). A considerable increase in the 18:3-fatty acid, and a slight decrease in 18:2 and 18:1-fatty acids were observed during dehydration. The content of the remaining fatty acids seemed to be unaffected by dehydration. Furthermore, rehydration was associated with very subtle changes in the fatty acid profiles. PI in the roots (Table 3.10) was predominated with the high amount of 16:0-, 18:2 and 18:1-fatty acids, accounting for 48%, 31% and 11% of the total PI fatty acids, respectively. Slight alterations in PI fatty acids in the roots were observed during dehydration and rehydration treatment.

Table 3.9: Fatty acids composition (%) of PI in leaves of *X. humilis* subjected to gradual dehydration and rehydration treatment. The values highlighted in blue represent the tissues during dehydration and those in red represent tissues during rehydration. The % of fatty acid were calculated from the % of the molecular species (i.e. the % of total MRM transition signal). Water content values are given as RWC in percentages at different sampling points.

PI (leaves)	100%	60%	40%	9%	0hr (5%)	9hr (48%)	12hr (73%)	24hr (92%)	36hr (96%)	48hr (96%)
15:0	4.6	4.9	4.2	4	4.5	4.1	5.4	5.2	5.4	5.3
16:0	38	38.9	31	28.2	31.6	28.9	25.6	30	33	34
16:1	0.5	0.5	0.2	0.2	0.3	0.2	0.3	0.3	0.5	0.5
17:0	2.4	2.9	3.1	2.5	2.6	2.6	2.3	2.8	3.1	2.9
18:0	6.3	6.3	10.4	8.9	7.7	8.9	7.6	9.4	9,7	9,8
18:1	9.7	12.3	8.3	7.3	6.7	7.1	11.1	7.6	7,7	7,6
18:2	17.7	17.5	19.1	16.8	13.9	16.6	16.1	14.7	15	15.3
18:3	20.7	16.7	24	30.3	33	31.7	32	30.1	30.4	30.5

Table 3.10: Changes in PI fatty acid composition (in %) of *X. humilis* roots subjected to gradual dehydration and rehydration treatment. The values highlighted in blue represent the tissues during dehydration and those in red represent tissues during dehydration. The % of fatty acid were calculated from the % of the molecular species (i.e. the % of total MRM transition signal). Water content values are given as RWC in percentages at different sampling points.

PI (roots)	100%	63%	40%	9%	0hr (4%)	9hr (55%	12hr (66%)	24hr (91%)	36hr (96%)	48hr (100%)
15:0	4.7	5.1	4.4	3.7	5	7.2	7.2	7.9	8.1	8
16:0	47.8	47.5	43.9	44.9	45.6	44.2	42.3	46.4	46.8	46.5
16:1	0.7	0.7	0.5	0.6	0.3	0.8	0.8	0.8	0.9	0.8
17:0	1.1	1.3	1.5	1.2	1.1	0.9	1.1	1.1	1.1	1.1
18:0	1	1	1.4	1.1	1	1.2	2.6	2.4	2.6	2.5
18:1	11.7	14	13.5	11.1	8.7	10	12.6	13.9	13.4	13.9
18:2	30.8	29.1	32.2	34.8	35.7	32.5	30.1	25.8	24.3	24.1
18:3	2.3	1.4	2.7	2.7	2.6	3.2	3.1	1.8	1.7	1.8

3.1.5.3. Lipid molecular species and fatty acid composition within PE

Phosphatidylethanolamine (PE) is the only non-bilayer forming glycerophospholipid assessed in this study. Previous studies have shown that in response to desiccation, non-bilayer forming lipids such as PE and MGDG can undergo phase transition from lamellar to cubic phase (Williams *et al.,* 1997; Tenchov and Koynovo, 2012; Jouhet, 2013; Tenchov *et al*., 2013). This may allow them to participate in the membrane protection mechanisms during desiccation. In this study, the changes that occur in the molecular species within PE during dehydration and rehydration treatment was thus monitored. Looking at the data of fully hydrated leaves revealed a wide distribution of molecular species in the leaves of *X. humilis* (Table 3.11). The molecular species 16:0/18:2-PE, 16:0/18:1-PE, 16:0/18:3-PE were the most abundant PE species from fully hydrated leaves making up 13%, 10% and 9% of the total molecular species, respectively. The least abundant PE molecular species were the very long chained 24:0/18:1-PE, 25:0/18:2-PE, 18:1/23:0-PE and 15:0/16:0-PE making up composition of 0.24%, 0,3%, 0,32% and 0,5% respectively. Upon dehydration (supplementary figure 3.12) all the major species, including 16:0/18:2-PE, 16:0/18:1-PE, and 16:0/18:3-PE decreased slightly when tissues were dehydrated from 100% to 9% RWC, but a considerable decrease was apparent after 3 weeks maintenance in the air dried state (depicted as 0hr). All very long chained molecular species decreased during dehydration, and increased upon rehydration (Table 3.11). It is also important to note that all the polyunsaturated 18-carbon containing molecular species increased during dehydration but decreased on rehydration. Because of their non-linear nature due to the presence of double bonds, this 18-carbon fatty acid may help with preventing membrane fusion during dehydration.

The PE in fully hydrated roots was predominated with high levels of the molecular species 16:0/18:2-PE (accounting for 21% of total PE) and to a lesser extent 18:0/18:2-PE, 19:0/18:2-PE, 16:0/18:1-PE, 18:2/18:2-PE, 18:2/18:1-PE, 18:0/18:1-PE molecular species which accounted for 10%, 7%, 8%, 6%, 6% and 5% respectively (Table 3.12). The very long chained molecular species, including 18:2/22:0-PE, 18:2/23:0-PE, 18:1/23:0-PE, 24:0/18:2-PE, 24:0/18:1-PE, and 25:0/18:2-PE were

minor molecular species within this class in the roots of the fully hydrated plants. Dehydration was associated with an increase in 16:0/18:2-PE, 18:2/18:1-PE, 16:0/18:1-PE, and 18:2/18:2-PE in the PE molecular species, and an overall decrease in the 18:0/18:2-PE,18:0/18:1-PE, 19:0/18:2-PE, and 15:0/18:2-PE molecular species (Supplementary Figure 3.13). Species with long chained fatty acids, even saturated ones, increased during dehydration and decreased during rehydration. Yet this decrease was preceded by a first stage increase during the first 12 hrs (66% RWC) of rehydration.

Table 3.11: Fatty acid composition of PE (% of total MRM transition signal) of leaves of *X. humilis* subjected to gradual dehydration and rehydration treatment. The values highlighted in blue represent tissues during dehydration and those in red represent the plant during rehydration. Water content values are given as RWC in percentages at different sampling points.

PE (Leaves)	100%	60%	40%	9%	0hr (5%)	9hr (48%)	12h (73%)	24h (92%)	36h (96%)	48h (96%)
15:0/16:0	0,46	0,46	0,08	0,04	0,01	0,01	0,2	0,06	0,23	0,56
14:0/18:3	0,99	0,68	0,62	0,49	0,22	0,07	0,05	0,54	0,64	0,45
14:0/18:2	1,5	2,03	1,62	0,27	0,2	0,13	0,14	0,91	1,03	1,41
16:0/16:0	0,43	0,37	0,08	0,09	0,02	0,02	0,03	0,24	0,17	0,63
15:0/18:3	5,18	4,35	2,91	2,43	0,92	0,63	0,84	4,03	2,13	2,32
15:0/18:2	6,72	8,25	6,05	4,32	1	1,08	1,43	5,17	3,59	5,35
15:0/18:1	3,52	7,44	2,72	1,37	0,37	0,5	0,77	2,38	1,56	2,08
16:1/18:2	1,11	1,05	0,46	0,71	0,16	0,17	0,21	0,4	0,57	1,91
16:0/18:3	9,23	6,47	7,29	7,51	8,12	5,63	5,22	9,75	8,13	5,86
16:0/18:2	12,76	11,79	18,37	14,7	8,1	8,17	9,06	14,06	12,91	12,95
16:0/18:1	10,02	11,71	11,55	8,31	4,43	5,97	5,55	9,05	9,85	10,58
17:0/18:2	1,92	1,87	1,77	1,43	1	0,98	1,12	1,42	1,21	1,56
17:0/18:1	1,36	1,34	1,09	0,73	0,48	0,63	0,58	0,78	0,67	0,77
18:3/18:3	0,8	0,79	0,87	2,91	7,4	4,18	3,02	2,26	1,39	0,65
18:3/18:2	2,46	2,33	2,74	6,94	10,38	8,07	8,04	5,83	4,67	2,74
18:2/18:2	2,79	3,54	5,08	7,89	9,84	7,4	8,61	6,27	4,59	4,56
18:1/18:3	1,53	1,78	1,32	3,14	4,55	4,2	3,62	2,78	4,11	1,43
18:2/18:1	3,87	5,2	4,68	7,41	8,88	8,27	8,44	6,1	7,19	7,24
18:0/18:3	4,24	2,54	3,79	4,45	7,6	6,89	6,18	5,41	6,89	4,16
18:1/18:1	1,34	1,73	1,05	1,75	2,59	2,41	2,26	1,87	2,8	3,46
18:0/18:2	4,07	3,48	5,32	6,12	5,07	8,01	6,14	6,46	8,39	9,08
18:0/18:1	8,1	6,62	3,67	3,43	2,54	5,04	4,24	4,58	7,32	7,32
16:0/20:1	3,21	3,29	1,5	0,54	0,46	0,57	1,2	1,5	0,96	1,37
19:0/18:2	1,82	1,24	1,45	1,24	1,13	1	1,06	0,9	1,06	2,11

20:1/18:2	1,03	1,33	1,4	1,03	1,84	1,9	1,8	0,72	0,68	1,62
18:2/20:0	3,07	1,72	2,94	2,57	1,81	2,65	2,59	1,8	1,97	3,54
18:1/20:0	2,44	2,02	1,68	1,1	1	1,34	1,98	0,85	0,89	1,38
18:2/22:0	1,67	1,67	1,93	1,42	1,39	1,75	2,28	0,79	0,65	0,57
18:2/23:0	0,94	1,25	1,99	1,53	1,98	2,35	2,85	0,84	0,95	0,58
18:1/23:0	0,32	0,46	0,97	0,54	0,88	1,1	1,27	0,29	0,48	0,28
24:0/18:2	0,55	0,79	2	1,68	3,04	1,74	4,54	1,33	1,12	0,73
24:0/18:1	0,24	0,24	0,6	0,38	1,27	1,97	1,98	0,34	0,58	0,37
25:0/18:2	0,3	0,19	0,4	0,41	1,33	2,07	1,9	0,3	0,45	0,38

Table 3.12: Fatty acid composition of PE (% of total MRM transition signal) of roots of *X. humilis* subjected to gradual dehydration and rehydration treatment. The values highlighted in blue represent tissues during dehydration and those in red represent tissues during rehydration. Water content values are given as RWC in percentages at different sampling points.

PE (Roots)	100%	63%	40%	9%	0h (4%)	9h (55%)	12h (66%)	24h (91%)	36h (96%)	48h (100%)
15:0/16:0	0,51	1,55	0,04	0,03	0,01	0,04	0,07	1,18	0,93	0,99
14:0/18:3	0,21	0,11	0,06	0,03	0	0	0	0,15	0,29	0,29
14:0/18:2	1,88	3,31	1,23	0,73	0,21	0,05	0,21	0,89	1,47	0,91
16:0/16:0	0,51	0,87	0,07	0,08	0,13	0,03	0,42	1,07	1,67	0,81
15:0/18:3	0,31	0,29	0,37	0,28	0,09	0,02	0,22	0,18	0,14	1,57
15:0/18:2	6,26	8,54	7,12	5,39	2,2	1,4	3,73	2,74	4,31	3,15
15:0/18:1	1,6	2,84	1,12	0,58	0,28	0,33	1,55	2,98	3,01	2,37
16:1/18:2	1,35	1,7	0,45	0,6	0,18	0,22	0,6	2,8	1,65	2,82
16:0/18:3	1,5	1,04	1,74	2,01	0,86	0,63	0,95	0,58	0,89	3,72
16:0/18:2	21,25	17,6	31,76	32,2	18,08	19,02	23,14	3,63	13,18	10,55
16:0/18:1	8,47	9,39	12,29	10,17	6,45	10,55	12,68	11,57	14,09	12,31
17:0/18:2	2,81	2,22	1,43	1,83	1,27	1,37	2,11	1,25	1,64	1,31
17:0/18:1	1,1	1,29	0,64	0,63	0,5	0,73	1,22	0,8	1,56	1,02
18:3/18:3	0,06	0,01	0,05	0,67	0,1	0,01	0,03	0,07	0,02	0,63
18:3/18:2	0,61	0,58	1,29	1,97	2,48	0,8	0,65	0,29	0,47	2,14
18:2/18:2	6,13	8,49	14,95	19,89	25,14	12,3	8,02	1,62	2,93	3,62
18:1/18:3	0,32	0,38	0,31	0,36	0,37	0,29	0,31	0,74	0,51	1,56
18:2/18:1	6	8,54	9,72	10,93	14,96	10,78	7,52	11,7	7,91	9,84
18:0/18:3	0,85	0,25	0,1	0,13	0,11	0,21	0,37	0,72	0,37	3,38
18:1/18:1	1,92	2,47	1,73	1,54	2,16	2,27	3,95	10,73	5,66	4,81
18:0/18:2	10	4,4	1,5	1,64	3,35	3,89	5,25	14,51	8,99	10,91
18:0/18:1	5	3,9	0,8	0,76	1,25	2,39	4,48	13,16	8,38	9,5
16:0/20:1	3,2	4	0,5	0,48	0,59	3,14	3,92	1,74	1,51	1,41
19:0/18:2	6,5	5	1,1	1,46	1,67	3,16	3,18	1,98	3,52	1,52
20:1/18:2	2,5	2,7	0,6	0,72	1,47	3,23	2,38	1,79	2,52	1,29

18:2/20:0	3,2	4	0,7	0,67	1,74	2,56	2,91	3,21	3,76	3,08
18:1/20:0	1,9	1,8	0,2	0,19	0,38	2,42	2,91	1,92	2,11	1,32
18:2/22:0	1,4	0,8	1,6	0,98	2,02	2,95	1,91	0,8	1,27	0,3
18:2/23:0	1	0,6	1,9	1,1	3,51	3,71	1,33	0,92	1,25	0,71
18:1/23:0	0,3	0,3	0,5	0,2	0,64	1,09	0,37	0,55	0,55	0,4
24:0/18:2	0,7	0,5	2,4	1,48	4,73	6,64	2,26	0,49	0,76	0,48
24:0/18:1	0,4	0,3	0,7	0,28	0,96	1,61	0,58	2,52	1,74	0,74
25:0/18:2	0,7	0,4	1,1	0,59	2,22	2,04	0,75	0,71	0,96	0,57

Sixteen PE fatty acids, including C14:0, C15:0, C16:0, C16:1, C17:0, C18:0, C18:1, C18:2, C18:3, C19:0, C20:0, C20:1, C22:0, C23:0, C24:0, and C25:0 were detected in leaves and roots of *X. humilis* (Table 3.13 and 3.14, respectively). The C18:2 fatty acids accounted for 36% of the total fatty acids from PE in the fully hydrated leaves, followed by C18:1 and C18:3 fatty acids, accounting for 25% and 20% in the leaves, respectively. The fatty acids C18:2 increased during dehydration and during the first 12hr (73% RWC) of rehydration, and then declined as the plant became fully rehydrated. The C18:1 fatty acids increased during the initial stage of dehydration, and then decreased with further water loss. Levels of this fatty acid remained unchanged upon rehydration. The C18:3 fatty acids decreased in leaves during the first stages of dehydration (i.e. from 100% to 40% RWC), and increased within the desiccated plant. Minor fatty acids in hydrated leaves were C25:0 (0.1%), C24:0 (0.2%), C23:0 (0.2%), C14:0 (0.3%), and C17:0 (0.3%; Table 3.13). These fatty acids increased slightly during dehydration, but increased more substantially during the first 12 hours of rehydration after which levels declined.

In the roots of *X. humilis*, the C18:2, C18:1, and C16:0 fatty acids accounted for 62%, 17%, and 13% of the total PE fatty acids, respectively. The fatty acids C18:2 and C18:1 showed minor changes during the water deficit treatment. The C16:0 fatty acids decreased during dehydration and increased upon rehydration (Table 3.14). The levels of unusual fatty acids such as C20:0, C22:0, C23:0, C24:0, and C25:0 were the very low, accounting for 0.3%, 0,2%, 0,3%, 0,4%, and 0,1% of PE fatty acids in the fresh roots of *X. humilis*, respectively (Table 3.14). Dehydration was associated with an overall increase in the levels of these unusual fatty acids. With the exception of C23:0 and C24:0 which increased during the initial stages (up to 48% RWC) of rehydration, there was an overall decrease in the levels of the unusual fatty acids during rehydration.

Table 3.13: Fatty acid composition (%) of PE in leaves of *X. humilis* subjected to gradual dehydration and rehydration treatment. The values highlighted in blue represent the tissues during dehydration and those in red represent tissues during rehydration. The % of fatty acid were calculated from the % of the molecular species (i.e. the % of total MRM transition signal). Water content values are given as RWC in percentages at different sampling points.

PE (Leaves)	100%	60%	40%	9%	0hr (5%)	9hr (48%)	12hr (73%)	24hr (92%)	36hr (96%)	48hr (96%)
14:0	0,3	0,3	0,4	0,3	0,1	0	0	0,1	0,4	0,3
15:0	1,4	1,3	1,7	1,4	0,5	0,4	0,4	1,6	2,3	2,3
16:0	12,3	11	9,6	7,5	5,4	5,2	6,1	10	12,7	12,7
16:1	0,2	0,2	0,1	0,2	0,1	0,1	0,1	0,1	0,3	1,3
17:0	0,3	0,3	0,5	0,4	0,3	0,3	0,4	0,5	0,6	0,5
18:0	2,3	1,6	2,8	3,2	3,7	5	4	4,2	6,8	4
18:1	24,7	30,7	21,8	19,2	17,7	21,4	21,2	19,2	16,8	18,5
18:2	36,2	37,6	45	46,7	40,8	42,3	44,7	39,3	35,2	43,3
18:3	19,5	14,6	14,4	19,4	27,8	20,3	18,2	22,9	22	13,5
19:0	0,2	0,2	0,2	0,3	0,1	0,2	0,1	0,2	0,2	0,4
20:0	1	0,7	0,9	0,7	0,4	0,7	0,8	0,5	0,9	1,6
20:1	0,5	0,6	0,6	0,2	0,5	0,6	0,3	0,2	0,2	0,4
22:0	0,4	0,4	0,5	0,3	0,3	0,4	0,5	0,2	0,2	0,1
23:0	0,3	0,4	0,8	0,6	0,8	0,9	1	0,3	0,4	0,3
24:0	0,2	0,2	0,7	0,6	1,2	1,8	1,7	0,5	0,8	0,7
25:0	0,1	0,1	0,1	0,1	0,3	0,5	0,5	0,1	0,2	0,2

Table 3.14: Changes in PE fatty acid composition (in %) of roots of *X. humilis* subjected to gradual dehydration and rehydration treatment. The values highlighted in blue represent the tissues during dehydration and those in red represent tissues during rehydration. The % of fatty acid were calculated from the % of the molecular species (i.e. the % of total MRM transition signal). Water content values are given as RWC in percentages at different sampling points.

PE (Roots)	100%	63%	40%	9%	0hr (4%)	9hr (55%)	12hr (66%)	24hr (91%)	36hr (96%)	48hr (100%)
14:0	0,2	0,1	0,2	0,1	0,05	0,01	0,02	0,1	0,1	0,24
15:0	1,4	1,6	1,8	1,3	0,5	0,3	0,8	3	2,4	2,9
16:0	13	14,3	10,8	10,5	6,5	10	13	14,7	15	15
16:1	0,1	0,1	0,2	0,2	0,1	0,1	0,2	2,3	0,9	2,5
16:2	0,4	0,3	0,3	0,3	0,4	0,3	0,3	0,3	0,4	0,6
18:0	0,7	0,4	0,4	0,4	1	0,6	0,9	2,5	2,2	4,8
18:1	17	20,6	19,9	17,4	17,7	23	27	28	25,5	20
18:2	62	60	61,3	65,1	67	59	53	39,9	46	39
18:3	2,6	1,3	2,6	3,2	2,3	1,2	1,5	1,5	1,6	10,3
19:0	0,2	0,2	0,1	0,1	0,1	0,07	0,1	0,6	1	0,4
20:0	0,3	0,3	0,2	0,1	0,4	0,3	0,3	2,3	1,7	1,8
22:0	0,2	0,1	0,4	0,2	0,5	0,5	0,3	0,3	0,3	0,1
23:0	0,3	0,2	0,6	0,3	1,1	1,1	0,3	0,6	0,5	0,3
24:0	0,4	0,1	0,9	0,5	1,6	2,2	0,8	2,3	1,7	0,9
25:0	0,1	0,1	3	0,1	0,6	0,5	0,2	0,4	0,4	0,2

3.1.5.4. Lipid molecular species and fatty acid composition within PG

Within the phospholipids, which predominate the bilayer membranes, changes in PG have been observed during dehydration in the resurrection plants *Sporobolus stapfianus* and *Ramonda serbica* (Quartacci *et al.*, 1997; Quartacci *et al.*, 2002). In the fully hydrated leaves of *X. humilis* the 16:0/16:0-PG and 16:0/18:0-PG molecular species predominated, accounting for 40% and 27% of the total molecular species, respectively (Table 3.15). The unsaturated molecular species, including 18:3/18:3-PG were the minor molecular species. During dehydration (supplementary figure 3.14), the molecular species 16:0/16:0-PG initially increased from 40% within fully hydrated leaves, to 49% at 60% RWC, followed by a further marked decrease at lower RWC's. However, the molecular species 16:0/18:0-PG showed a gradual decrease upon dehydration. Both the 16:0/16:0-PG and 16:0/18:0-PG molecular species increased upon rehydration. The 15:0/16:0-PG, 16:0/16:1-PG, and 16:1/18:0-PG molecular species decreased upon dehydration and increased during rehydration. The molecular species 16:0/18:3-PG, 16:0/18:2-PG, 18:3/18:3-PG, 18:3/18:2-PG, 18:2/18:2-PG, 18:2/18;1-PG, 18:0/18:3-PG, and 18:1/18:1-PG decreased during dehydration (Supplementary Figure 3.14). However, rehydration was associated with slight changes in these molecular species. In the roots (Table 3.16), the molecular species 16:0/16:0-PG and 16:0/18:2-PG dominated, accounting for 48% and 16% of the total PG molecular species in fully hydrated plants, respectively. During dehydration (Figure 3.15), the molecular species 16:0/16:0-PG increased slightly from 48% at fully hydrated state to 52% at 63% RWC, followed by a considerable decline to 32% in air dry roots. These species increased again upon dehydration. The 16:0/18:2-PG molecular species increased gradually during dehydration and decreased upon rehydration. The minor molecular species including, 15:0/16:0; 16:0/16:1-PG; 16:0/16:0-PG; 16:1/18:0-PG; 16:0/18:0-PG; 18:1/18:1-PG, and 19:1/18:1-PG decreased during dehydration, while the 15:0/18:2-PG; 16:0/18:2-PG, 18:3/18:2-PG, and 18:0/18:2-PG increased (Supplementary Figure 3.15). It can thus be concluded that dehydration was associated with a decrease in saturated PG molecular species and an increase in unsaturated molecular species, and rehydration was associated with the reversal of these patterns.

Table 3.15: PG lipid molecular species of leaves of *X. humilis* (% of total MRM transition signal) subjected to gradual dehydration and rehydration treatment. The values highlighted in blue represent tissues during dehydration and those in red represent tissues during rehydration. Water content values are given as RWC in percentages at different sampling points.

PG (leaves)	100%	60%	40%	9%	0hr (5%)	9h (48%)	12h (73%)	24h (92%)	36h (96%)	48h (96%)
15:0/16:0	4,59	5,57	4,06	2,08	2,74	1,35	1,47	3,1	2,8	4,37
14:0/18:1	0,97	1,07	5	1,13	0,55	0,69	1,87	1,03	1,08	1,14
16:0/16:1	9,55	12,9	6,02	1,27	1,85	1,81	3,69	4,21	6,69	12,91
16:0/16:0	40,17	48,51	37,87	11,05	13,76	8,11	10,21	26,22	26,49	32,19
15:0/18:2	0,2	0,19	0,55	1,53	1,6	1,69	1,41	0,53	0,32	0,33
16:0/18:3	3,54	3,69	11,04	13,27	15,27	13,27	9,95	7,93	7,31	5,45
16:0/18:2	3,17	4,9	12,55	19,16	20,01	16,09	10,98	5,82	4,24	4,46
16:1/18:0	5,17	3,49	1,97	1,15	0,86	2,22	5,24	4,56	7,23	7,59
16:0/18:0	27,52	15,43	18,33	10,78	5,27	6,55	12,83	31,04	33,33	22,9
17:0/18:2	1,14	0,16	0,63	1,39	1,27	1,28	0,97	0,39	0,22	0,25
18:3/18:3	0,27	0,14	0,48	5,17	7,77	5,41	3,3	1	0,66	0,77
18:3/18:2	0,71	0,57	0,76	6,48	7,71	7,25	5,53	2,2	1,49	1,58
18:2/18:2	0,94	1,16	0,76	4,24	3,86	5,37	5,49	2,15	1,66	1,15
18:1/18:3	0,54	0,4	0,56	3,28	3,36	5,04	4,84	1,74	1,1	1,1
18:2/18:1	0,8	0,88	1	4,65	4,39	7,14	6,71	2,28	1,76	1,32
18:0/18:3	0,49	0,18	0,85	5	3,35	6,81	5,63	1,64	1,21	0,82
18:1/18:1	0,34	0,2	0,29	1,86	2,28	2,23	2,4	0,99	0,69	0,42
18:0/18:2	0,35	0,18	0,94	3,72	2,05	4,08	3,21	1,21	0,67	0,61
18:0/18:1	0,4	0,25	0,72	2,26	1,18	3,31	3,71	1,73	0,87	0,54
19:1/18:1	0,12	0,12	0,12	0,51	0,64	0,31	0,56	0,23	0,19	0,11

Table 3.16: PG Lipid molecular species in roots of *X. humilis* (% of total MRM transition signal) subjected to gradual dehydration and rehydration treatment. The values highlighted in blue represent tissues during dehydration and those in red represent tissues during rehydration. Water content values are given as RWC in percentages at different sampling points.

PG (roots)	100%	63%	40%	9%	0hr (5%)	9hr (48%)	12hr (73%)	24hr (92%)	36hr (96%)	48hr (96%)
15:0/16:0	6,74	7,52	4,42	2,67	8,26	4,56	4,73	5,47	6,46	7,33
14:0/18:1	0,37	0,26	0,19	0,24	0,56	3,1	3,6	4,79	3,33	2,82
16:0/16:1	2,65	2,21	0,97	0,83	0,61	7,51	8,97	12,64	8,48	7,47
16:0/16:0	47,83	52,48	27,89	16,45	31,54	17,61	19,62	23,68	28,38	25,84
15:0/18:2	0,78	1,04	2,19	2,46	3,16	2,63	2,69	2,01	1,39	1,53
16:0/18:3	2,62	1,07	4,21	4,65	2,75	2,03	1,87	1,31	1,45	2,01
16:0/18:2	15,64	16,85	45,22	48,86	33,62	24,03	21,52	10,35	9,81	10,85
16:1/18:0	1,02	0,61	0,29	0,27	0,21	1,82	2,27	3,1	3,5	2,94
16:0/18:0	4,58	3,35	3,03	2,49	1,91	7,07	8,08	10,02	10,26	8,08
17:0/18:2	0,49	0,47	1,3	1,12	1,21	1,27	0,89	0,64	0,63	0,64
18:3/18:3	0,07	0,02	0,1	0,27	0,16	0,09	0,08	0,07	0,1	0,11
18:3/18:2	1,81	0,69	2,7	5,73	4,1	2,09	1,92	1,54	1,72	3,14
18:2/18:2	3,64	5,06	1,77	4,79	6,18	7,36	6,39	5,51	4,89	4,15
18:1/18:3	0,46	0,23	0,8	1,3	0,77	1,14	0,98	1,1	0,87	1,63
18:2/18:1	1,73	2,53	1,69	4,08	2,41	4,5	3,33	2,81	2,6	2,56
18:0/18:3	0,09	0,04	0,14	0,15	0,12	0,43	0,39	0,31	0,3	0,34
18:1/18:1	4,96	2,75	1,05	1,39	0,78	4,45	4,64	5,67	6,54	8,78
18:0/18:2	0,56	0,39	1,17	1,27	0,92	3,15	3,08	2,72	2,18	1,87
18:0/18:1	1,04	0,8	0,41	0,48	0,33	2,01	2,14	2,82	2,98	2,73
19:1/18:1	2,93	1,63	0,48	0,5	0,38	3,13	2,8	3,44	4,11	5,19

Ten fatty acids were detected within the PG in the leaves and roots of *X. humilis*, including C14:0, C15:0, C16:0, C16:1, C17:0, C18:0, C18:2, C18:3, and C19:0 (Table 3.17 and 3.18) respectively. The C16:0 fatty acid accounted for 64% of total PG fatty acids, followed by C18:0 acid accounting for 17% of total fatty acids in fully hydrated leaves (Table 3.17). The C14:0, C17:0 and C19:1 were minor fatty acids in leaves, accounting for 0.5%, 0.1%, and 0.1% of total fatty acids, respectively. Dehydration was associated with an overall decrease in C16:0, C16:1, and C18:0 fatty acids; and increased levels of C18:1, C18:2, and 18:3 fatty acids. Rehydration was associated with the mirror-like changes. The C16:0, C18:2, and C18:1 fatty acids in roots accounted for 64% 14%, and 8% of the total PG fatty acids in fully hydrated plant (Table 3.18), respectively. The C14:0 and C17:0 fatty acids were the minor fatty acids in roots, accounting for 0.2% each, of total fatty acids in fully hydrated plants. Dehydration was associated with an overall decrease in C15:0, C16:0, C16:1, C18:0, and C18:1; and an increased in the C17:0, C18:2, C18:3, and C19:1 had an overall increase upon dehydration. Rehydration was associated with mirror-like changes.

Table 3.17: PG fatty acids (%) analysis of leaves of *X. humilis* subjected to gradual dehydration and rehydration treatment. The values highlighted in blue represent the tissues during dehydration and those in red represent tissues during rehydration. The % of fatty acid were calculated from the % of the molecular species (i.e. the % of total MRM transition signal). Water content values are given as RWC in percentages at different sampling points.

PG (Leaves)	100%	60%	40%	9%	0hr (5%)	9hr (48%)	12hr (73%)	24hr (92%)	36hr (96%)	48hr (96%)
14:0	0.5	0.5	0.3	0.6	0.3	0.3	0.9	0.5	0.5	0.6
15:0	2.4	2.9	2.3	1.8	2.2	1.5	1.4	1.8	1.6	2.3
16:0	64.5	69.8	63.9	34.3	36.4	27.6	29.7	52.3	53.7	57.2
16:1	7.4	8.2	4	1.2	1.4	2	4.5	4.4	7	10.3
17:0	0.1	0.1	0.3	0.7	0.6	0.6	0.5	0.2	0.1	0.1
18:0	17	9.8	0.3	11.5	6.4	11.5	5.3	20.1	21.2	16.2
18:1	1.8	1.6	11.4	7.8	7.4	10.5	11.2	4.5	3.2	2.5
18:2	3.6	4.6	1.7	22.7	22.4	24.1	19.9	8.4	6	5.4
18:3	2.9	2.6	9	19.2	22.7	16.3	16.3	7.7	6.2	5.2
19:1	0.1	0.1	0.1	0.3	0.3	0.3	0.3	0.1	0.1	0.1

Table 3.18: PG fatty acids (in weight %) analysis of roots of *X. humilis* subjected to gradual dehydration and rehydration treatment. The values highlighted in blue represent the tissues during dehydration and those in red represent tissues during rehydration. The % of fatty acid were calculated from the % of the molecular species (i.e. the % of total MRM transition signal). Water content values are given as RWC in percentages at different sampling points.

PG (Roots)	100%	60%	40%	9%	0hr (4%)	9hr (55%)	12hr (66%)	24hr (91%)	36hr (96%)	48hr (100%)
14:0	0.2	0.1	0.1	0.1	0.3	1.6	1.8	2.4	1.7	1.4
15:0	3.8	4.3	3.3	2.6	5.7	3.6	3.7	3.7	3.9	4.4
16:0	63.9	68	56.8	46.2	55.1	40.2	42.2	43.6	46.6	43.7
16:1	1.8	1.4	0.6	0.6	0.4	4.7	5.6	7.9	6	5.2
17:0	0.2	0.2	0.6	0.6	0.6	0.6	0.4	0.3	0.3	0.3
18:0	3.6	2.6	2.5	2.3	1.7	7.2	8	9.5	9.6	8
18:1	8.2	5.5	2.8	4.7	3	11.4	11.1	13.1	13.5	16.2
18:2	14.1	16	29	36.6	28.9	26.2	23.1	15.5	14.1	14.4
18:3	2.6	1	4	6.2	4	2.9	2.7	2.2	2.3	3.7
19:1	1.5	0.8	0.2	0.3	0.2	1.6	1.4	1.7	2.1	2.6

3.1.6. Leaves and roots differ in the levels of 18:3- and 18:2-fatty acids

In this study, the MRM analysis revealed higher levels of 18:3 fatty acids in the leaves of *X. humilis* than in the roots, and a higher level of 18:2 fatty acid in the roots than in the leaves. The levels of 18:3 fatty acids accounted for 19%, 21%, 14% and 3% of the total fatty acids within the PE, PI, PC and PG, respectively (Figure 3.16). Within *X. humilis* leaves, dehydration resulted in an overall increase in the levels of 18:3 fatty acids. Upon rehydration, there was a decrease in the levels of 18:3 within the PE, PI and PC, and a decrease within PG. In the roots, only a slight increase in the levels of 18:3 fatty acids within PG was observed during drying, but further increases occurred on rehydration. The levels of 18:2 fatty acid accounted for 4%, 36%, 18% and 16% within the PG, PE, PI and PC in the fully hydrated state, respectively (Figure 3.17). Dehydration had an overall increase in the levels of 18:2 fatty acid within PG, PE and PC, and a decrease during dehydration. Within PI the level of 18:2 remained unchanged during both dehydration and rehydration treatment. In the roots, the level of 18:2 fatty acid accounted for 16%, 62%, 31% and 42% of the total fatty acid within PG, PE PI and PC in the fully hydrated roots, respectively. Upon dehydration, the level of 18:2 fatty acid had a slight increase with a massive decrease upon rehydration.

Figure 3.18 gives the factorial analysis for PC as an illustration. In this analysis closer the points are to each other, the more closely correlated they are to each other, and the further apart the two points are to each other, the less correlation there is between them. Leaf samples group together on the left side of the plane and the root samples group together on the right side on the plane. This correlation in leaf samples is likely due to the high proportion of 18:3-fatty acids whereas in roots there is a high proportion of 18:2-fatty acid (Figure 3.18). Furthermore, the figure also revealed a negative correlation between the leaf and root samples.

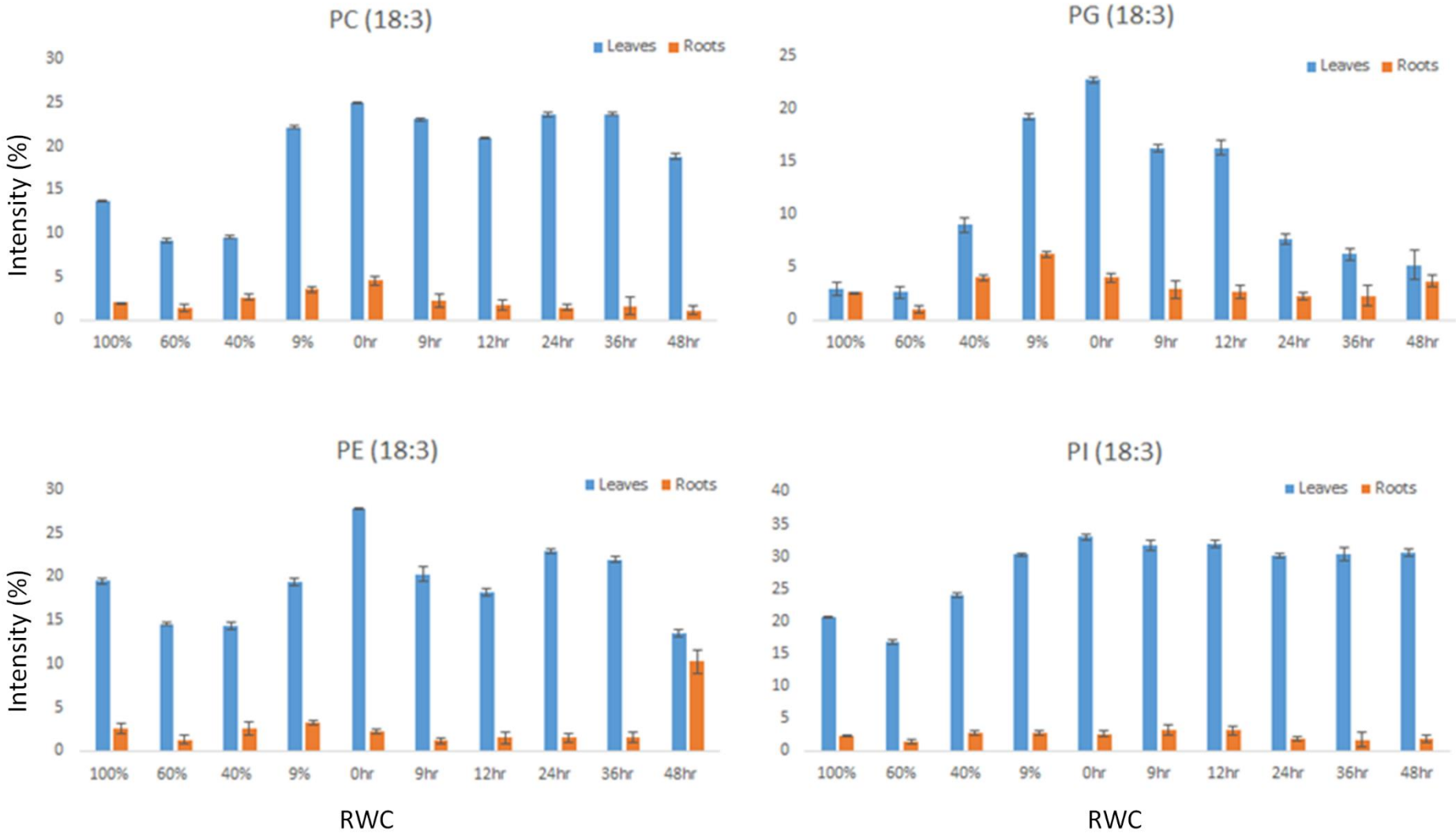

Figure 3.16: Levels of linolenic acid (18:3) within the glycerophospholipids classes in roots and leaves during desiccation and rehydration of *X. humilis*.

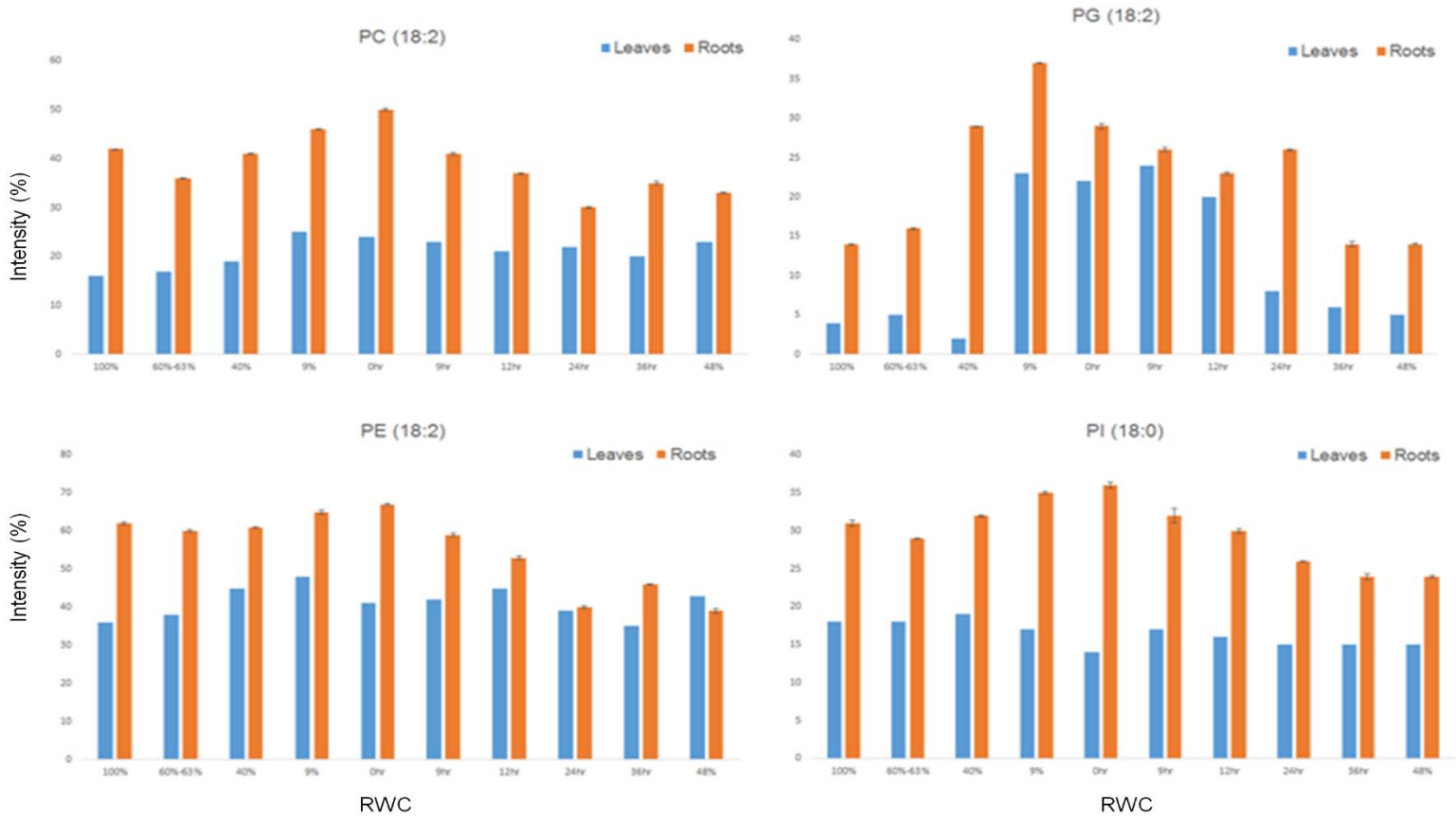

Figure 3.17: Levels of linoleic acid (18:2) within the glycerophospholipids classes in roots and leaves during dehydration and rehydration of *X. humilis*.

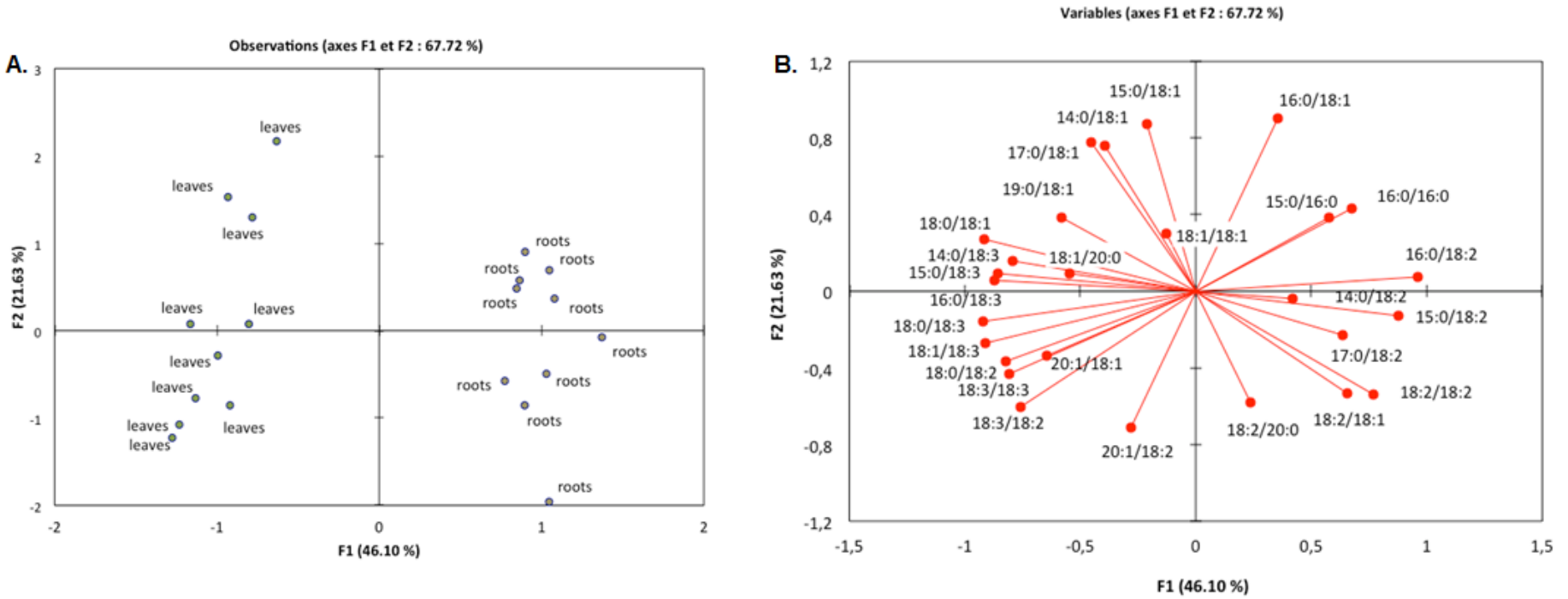

Figure 3.18: Positions of the observations on the two principal factors. A: Each observation corresponds to the PC composition at a particular RWC (not indicated here) in root and leaf tissues. B: Relation between the first two principal factors and the measured variables. In the analysis, the molecular species were used as variables. The factor analysis was performed with XLSTAT, using the principal factor method as the extraction method applied iteratively. The correlations were calculated as the Pearson coefficients.

3.1.7. Dehydration is associated with unsaturation and rehydration is associated with saturation of glycerophospholipids

To monitor the changes in saturation levels of the molecular species during dehydration and rehydration in *X. humilis* vegetation tissues, 102 different molecular species corresponding to four glycerophospholipids were analysed by principal component analysis (PCA). PCA, a multivariate technique that represents spatial relationship of variables as data points in high-dimensional Euclidean space, is popular in scientific data analyses (Abdi and Williams, 2010). In this study it was found that the RWC points during hydration and rehydration were well separated on the PCA map (Figure 3.19; 3.20). In fully dehydrated leaves (Figure 3.19), the point termed “100% RWC” was associated with the clustering of saturated molecular species including 16:0/16:0-PE, 15:0/16:0-PE, 16:0/18:0-PG; and mono-unsaturated molecular species such as 18:0/18:1-PE, 16:1/18:0-PG, 16:0/16:1-PI, and 15:0/18:1-PI. Within the air dried leaf (point 9% RWC), there was a shift from saturated molecular species to poly-unsaturated molecular species such as 18:2/183-PC, 18:2/18:2-PC, 18:3/18:3-PE, 18:2/18:3-PE, 18:2/18;3-PG, 18:3/18;3-PG, and 18:3/18:3-PI (Figure 3.19). The association of these poly-unsaturated molecular species continued throughout a 3-week period when plants were maintained in the air dried state (point 0 hr), with 18:3/18:3-PC, 18:2/18:2, 18:3/18:3-PE, 18:1/18:3-PE, and 18:2/18:3-PE found to cluster together. Rehydration was associated with saturation in the levels of molecular species, with clustering appearing more prominent at point 48 hr, associated with 16:0/18;2-PC, 16:0/18:1-PC, 16;0/16:0-PC, 15:0/18:2-PE, 14:0/18:2-PE and 16:0/18:1-PE (Figure 3.20).

The same trend, i.e. the unsaturation of molecular species during dehydration and saturation upon rehydration was also observed in the root tissue (Figure 3.21; 3.22), but it was less prominent. In the roots the point 100% RWC was associated with clustering of 18:0/18:3-PC, 18:0/18:2-PE, 17:0/18:2-PE, 18:0/18:1-PE, 16:0/16:1-PG, 18:0/18:1-PG, and 16:0/16:1-PG (Figure 3.21); while point 9% RWC was associated with poly-unsaturated molecular species such as 18:2/18:3-PC, 18:3/18:3-PC, 18:2/18:3-PE, 18:2/18:3-PG, 18:3/18:3-PG, and 18:2/18:3-PI. Upon

rehydration, clustering of molecular species with decreased unsaturated levels including 18:0/18:3-PC, 18:0/18:3-PE, 15:0/18:3-PE, 16:0/18:3-PE, and 16:0/18:1-PI was observed (Figure 3.22)

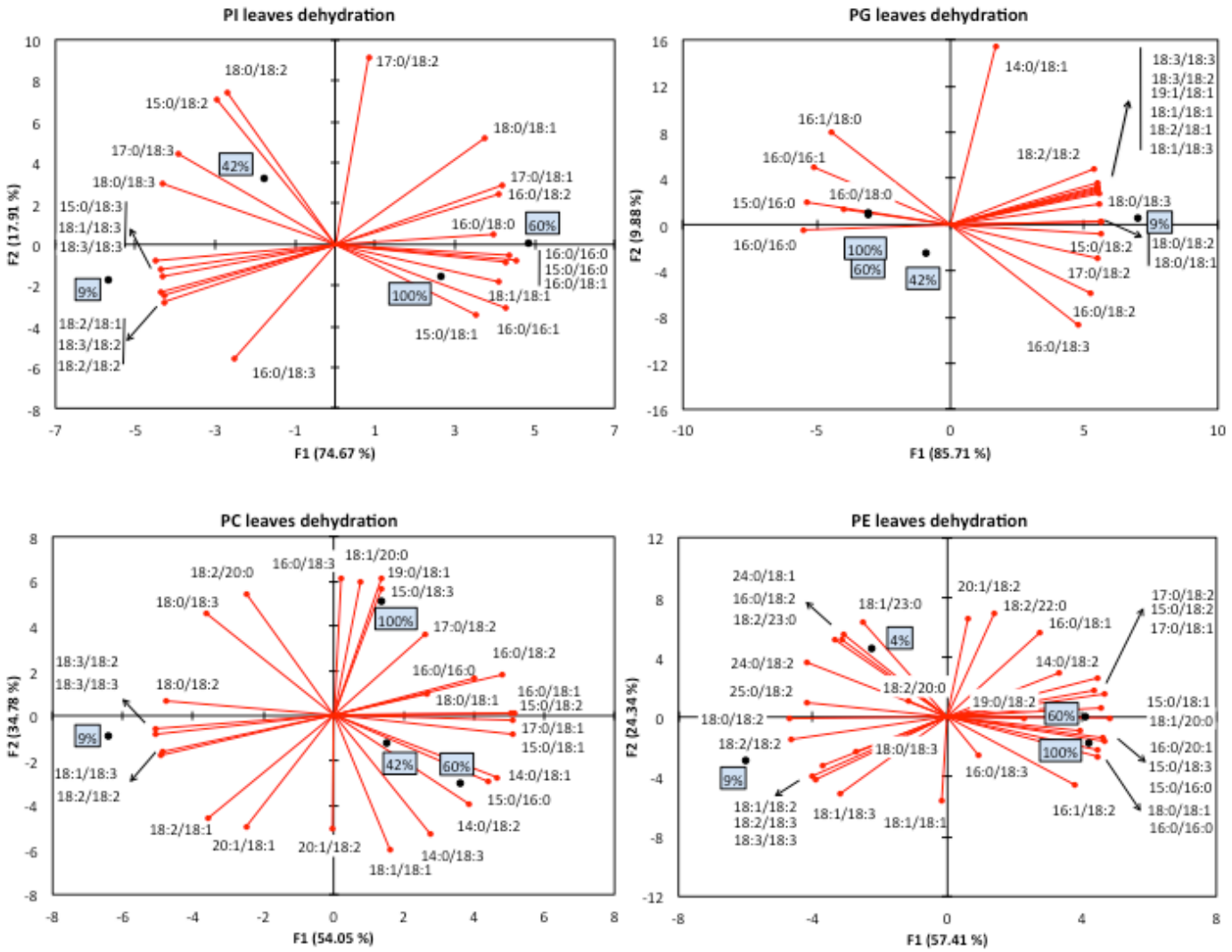

Figure 3.19: Changes associated with selected glycerolipid molecular species from leaves during dehydration experiments are vizualised by principal component analysis. Lipids were extracted at different points of the dehydration curves. Glycerolipid composition was analysed by multiple reaction monitoring mass spectrometry using a preset list of transitions. The results are expressed as % of total MRM transitions.

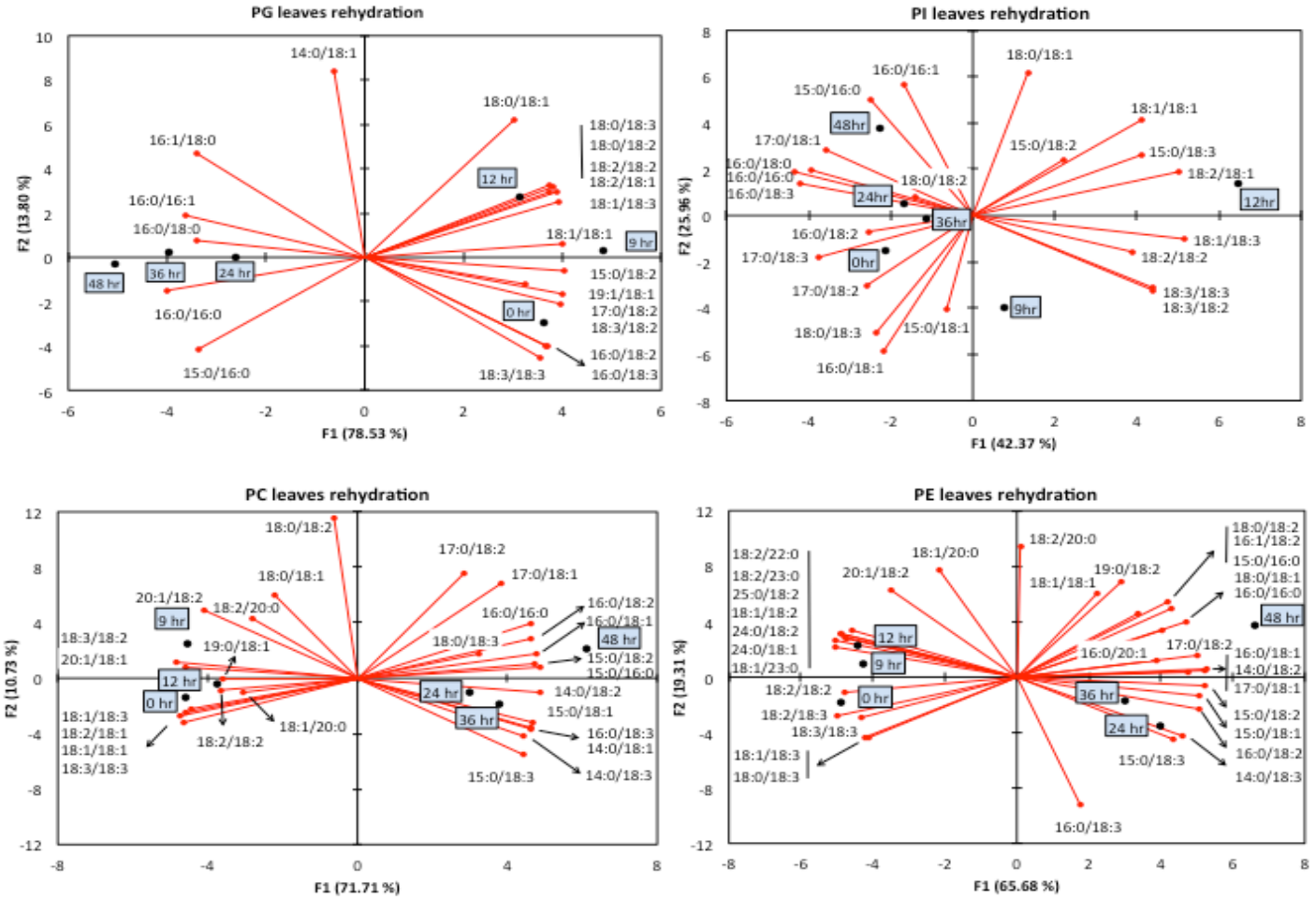

Figure 3.20: Changes associated with selected glycerolipid molecular species from leaves during rehydration experiments are vizualised by principal component analysis. Lipids were extracted at different points of the rehydration curves. Glycerolipid composition was analysed by multiple reaction monitoring mass spectrometry using a preset list of transitions. The results are expressed as % of total MRM transitions.

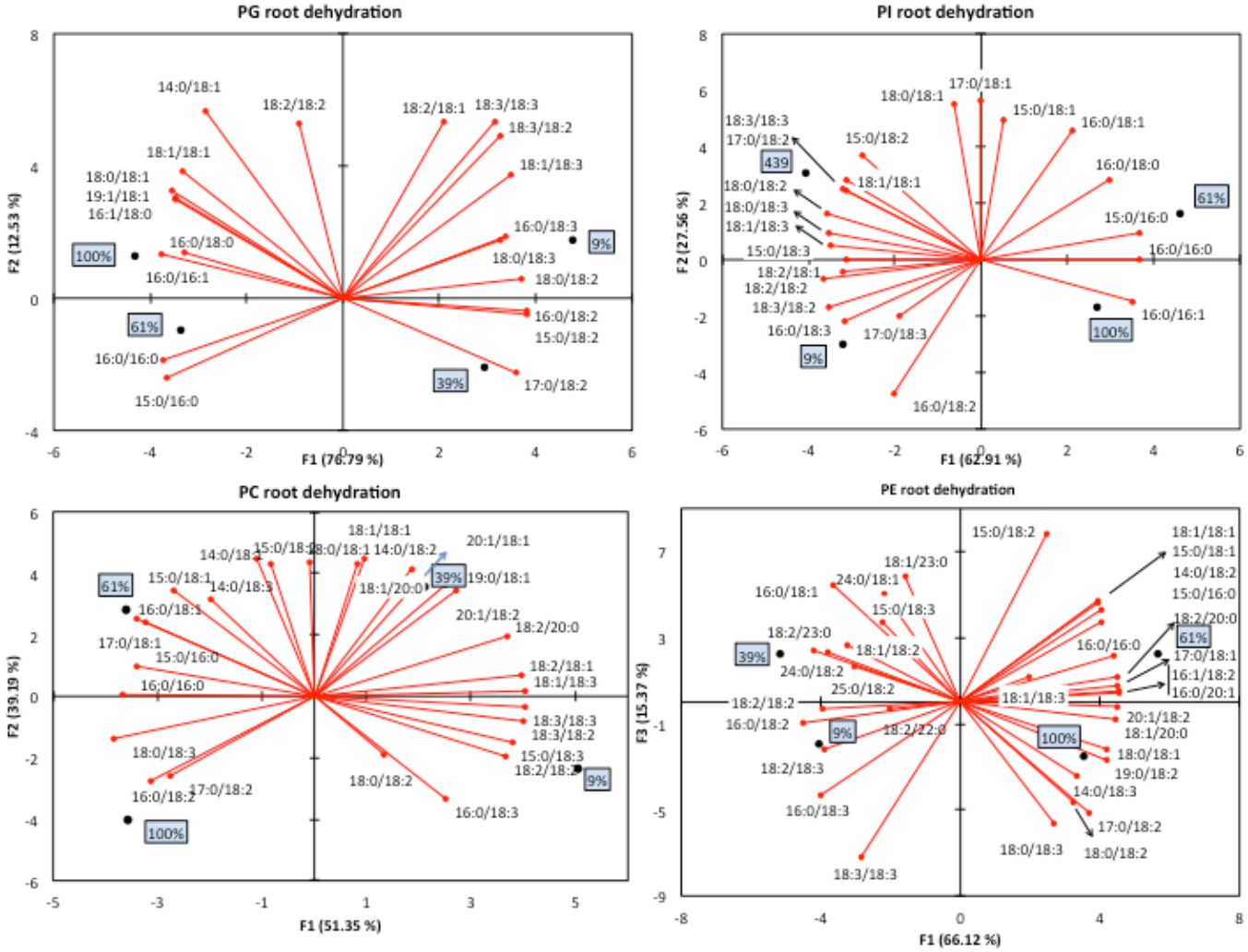

Figure 3.21: Changes associated with selected glycerolipid molecular species from roots during dehydration experiments are vizualised by principal component analysis. Lipids were extracted at different points of the dehydration curves. Glycerolipid composition was analysed by multiple reaction monitoring mass spectrometry using a preset list of transitions. The results are expressed as % of total MRM transitions.

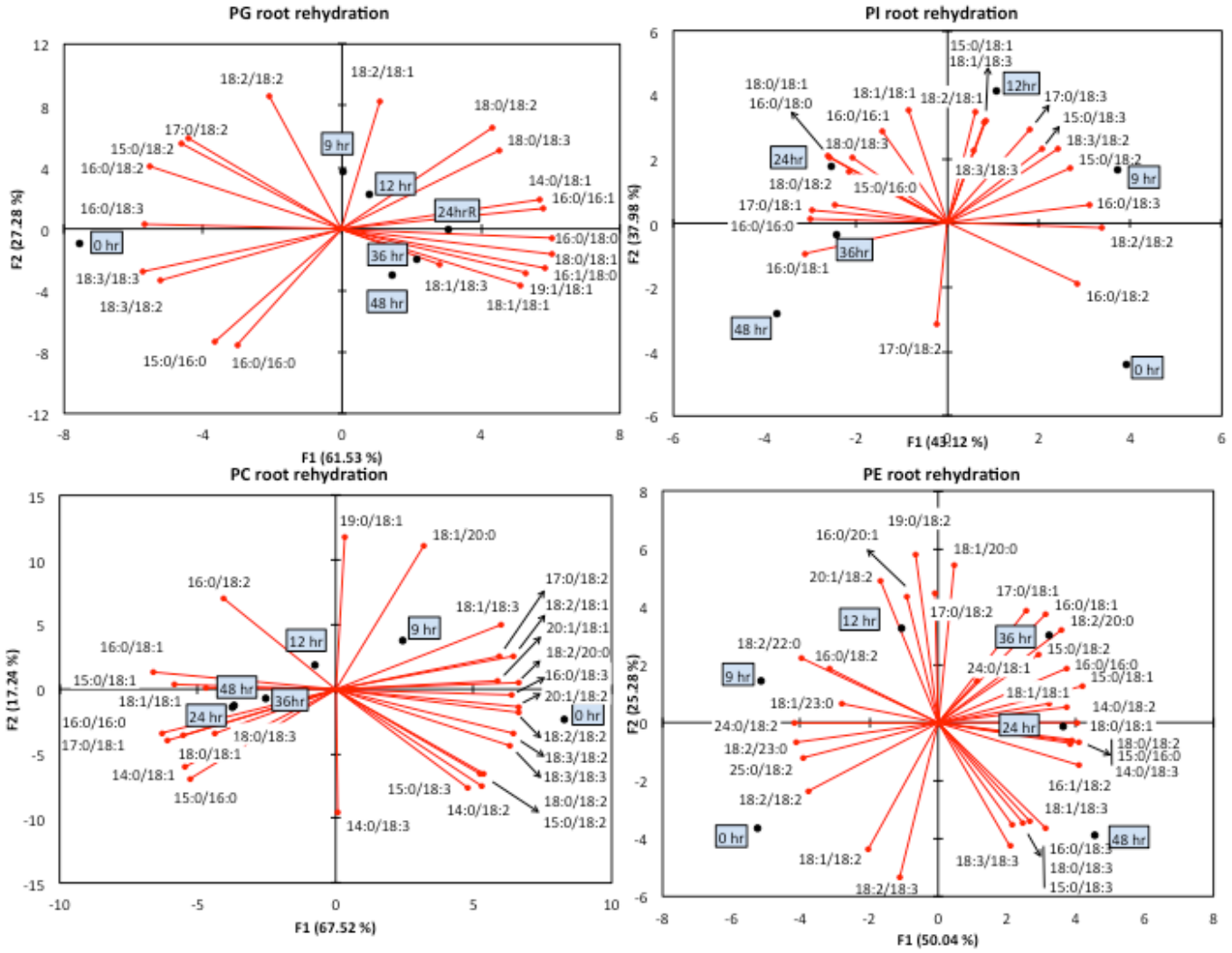

Figure 3.22: Changes associated with selected glycerolipid molecular species from roots during rehydration experiments are vizualised by principal component analysis. Lipids were extracted at different points of the rehydration curves. Glycerolipid composition was analysed by multiple reaction monitoring mass spectrometry using a preset list of transitions. The results are expressed as % of total MRM transitions.

3.2. Discussion

3.2.1. Fatty acids in roots and leaves of *X. humilis*

Anaylsis of roots and leaves is rarely performed in parallel and there are thus relatively few studies can be drawn upon on for comparison. This study shows that the poly-unsaturated fatty acid 18:3 was predominant in the leaves (Figure 3.16), while the 18:2-fatty acid was higher in the roots (Figure 3.17) in hydrated tissues of *X. humilis*. A high amount of 18:3-containing fatty acids has also been observed in the leaves of *X. scabrida* (Georgieva *et al.,* 2011). This fatty acid is a common diagnostic marker found in the thylakoid lipids produced by the prokaryotic pathway during galactolipid synthesis (Xu *et al.,* 2003; Warakanont *et al*., 2015). Therefore, high levels of 18:3-fatty acid in the leaf samples is corroborate by literature since the prokaryotic pathway involves the production of diacylglycerol, the precursor for galactolipids biosynthesis, which is restricted to the plastid of the leaves (Djafi *et al.,* 2013). Furthermore, predominant levels of 18:2-containing species in the roots of *X. humilis* is in agreement with the study performed by Lui and Huang (2005), who revealed that the roots of creeping bentgrass contain high amount of C18:2 (linoleic acid) compared to the leaves. The higher amount of 18:2-fatty acid in the roots of *X. humilis* may suggest lower activity in ω-3 fatty acid desaturases, which is responsible for the conversion of 18:2-fatty acid to 18:3-fatty acid (Mazliak, 1994). Therefore, it can be concluded that the roots and leaves differ in their fatty acids composition as far as the glycerophospholipids are concerned. Nevertheless, systematic and parallel studies of root and leaf lipidomics would be welcomed to corroborate these results, a prerequisite to elucidate the differences in biosynthetic pathways between organs. due to experimental limitation experienced when working with soil grown root tissues few studies, are available on the changes in root fatty acid composition of plants. Aeroponic cultivation systems and the use of high sensibility mass spectrometry devices should help overcome this limitation.

3.2.2. Effect of water deficit and rehydration on the levels of glycerophospholipids within the *X. humilis* plant

Lipid molecular species composition has a direct influence on the cell bilayer membrane structure and fluidity, which changes with water loss (Zheng *et al*., 2011). At normal growth conditions, plant leaves play important roles such as, supporting the photosynthetic organs, intercepting sunlight, facilitating the diffusion of carbon dioxide to chloroplasts, and monitoring the plant internal water status by regulating stomatal opening (Munne-Bosch and Alegre, 2004; Evans *et al*., 2009; Zimmermana *et al*., 2013). In desiccation sensitive plants it has been shown that dehydration of leaves to between 59-30% RWC triggers disruption of normal metabolic activities and ultimately leads to leaf senescence and plant death (Munne-Bosch and Alegre, 2004; Wehner *et al*., 2016). As one of the main factors associated with extensive water loss is membrane damage (Farooq *et al.,* 2009) it is clear that this species can prevent such damage during desiccation. One way that this damage appears to be circumvented is by changing the levels of saturation of fatty acids during desiccation in both root and leaf tissues. The nature of fatty acids involved in these changes may be of significance.

In hydrated tissues, significant amounts of mono-unsaturated molecular species including 16:0/18:1; 16:0/18:2 and 16:0/18:3 were observed within the membrane glycerophospholipid classes PC, PI and PE in both leaves and roots. Within the PG class significant amounts of mono-saturated molecular species such as 16:0/16:0 occurred in both tissues and 16:0/18:0 was found only in the leaves. A higher amount of 16:0/18:1; 16:0/18:2 and 16:0/18:3 within the PC, PI and PE of plasma membranes of well-watered plants has also been reported for rye and oat seedlings (Lynch and Steponkus, 1987; Uemura and Steponkus, 1994). It is thought that they are involved in the maintenance of liquid-crystalline property of the bio-membrane which is necessary for the optimum functioning of the plant cell. Using PC as an example, in response to desiccation in *X. humilis*, the proportion of 16:0/18:1-PC decreased with an increase in 18:2/18:3-PC, 18:1/18:3-PC, and 18:3/18:3-PC molecular species in the leaves (see Table 3.3). This is in agreement with Uemura and Steponkus, (1994) who also reported an increase in the levels of di-unsaturated species with decreasing

mono-saturated species during cold acclimation in rye. In the roots of *X. humilis*, the proportion of 16:0/18:2-PC also decreased with an increase in the 18:2/18:2-PC molecular species. The increase in these highly unsaturated molecular species has been associated with the fluidizing effect of the membrane (Murata and Los, 1997). This is important because a decrease in membrane fluidity has been associated with the loss in membrane permeability and the disruption of membrane-bound enzymes activities in plants (Mikami and Murata, 2003; Minorov *et al*., 2012). Thus, it appears that the increased desaturation in the molecular species within the lipid bilayers with increased desiccation in *X. humilis* would most likely enhance membrane fluidity. Furthermore, changes that occurred within the non-bilayer glycerophospholipid class PE during dehydration may suggest an involvement of PE in membrane stabilization during drought stress adaptation in *X. humilis*. Arbutin, an amphiphile in the presence of non-bilayer forming lipids such as MGDG or PE has been reported to stabilize the bilayer membrane by relaxing the inverted curvature stress during dehydration (Oliver *et al.,* 2001; 2002). Furthermore, accumulation of potential membrane stabilizers such as sugars (sucrose in particular), sugar alcohol (arabitol and mannitol), amino acids (glycine), and nucleotides (guanine and guanosine) have been reported in the root and leaf tissues of *X. humilis* during desiccation (Dace, 2014; Farrant *et al.,* 2017). These molecules have long been reported to play an important membrane protective role during desiccation in many resurrection plants (Whittaker *et al.,* 2001; Moore *et al.,* 2006; Farrant *et al.,* 2007; Yobi *et al.,* 2013).

3.2.3. Unsaturation of fatty acids during dehydration

Stearic (18:0), oleic (18:1), linoleic (18:2), linolenic (18:3) and palmitic (16:0) acids are the common constituents of the plant membrane lipids (16:0; Millar *et al.,* 1998; Rustan and Drevon, 2005). In response to drought stress, it has been reported that fatty acids acyl chain length and degree of unsaturation changes in various plants (Gigon *et al.,* 2004; Zhong *et al*., 2011; Gasulla *et al.,* 2013). Compared to other fatty acids, a high amount of 16:0-fatty acids was detected within the bilayer lipid classes PC, PI, and

PG, accounting for 23%, 38%, and 65% of the total fatty acids in fully hydrated leaves, respectively. In the fully hydrated roots, 16:0-fatty acids, accounted for 30%, 48%, and 64% of the total fatty acid in PC, PI, and PG, respectively. Because of the linearity of 16:0-fatty acid, high amounts of these fatty acids have been shown to induce membrane fluidity state, allowing for proper cellular metabolism and optimum functioning (Losa and Muratab, 2004). Upon dehydration, the proportion of 16:0-fatty acid decreased from PC (23 to 12%), PI (38 to 28%), and PG (65 to 34%) in the leaves, and PC (30 to 21%), PI (48 to 45%), and PG (64 to 46%) in the roots. The decrease in 16:0-fatty acid proportion was accompanied with an increase in the proportion of poly-unsaturated fatty acids (PUFA) such as 18:2 (in leaves and roots) and C18:3 (leaves). This pattern of fatty acid unsaturation within the glycerophospholipids is common in many plants subjected to various environmental stresses including salt (Harrathi *et al*., 2012), drought (Torres-Franklin *et al.,* 2009; Tarazona *et al*., 2015), chilling (Kodama *et al.,* 1995), and high temperature stress (Zheng *et al*., 2011). It has been proposed to play a role in a plant's acclimation to these stressors (Los and Murata, 2004). Within the resurrection plant *Sporobulus stapfianus*, leaf dehydration led to a decrease in the proportion of 16:0-fatty acids, with a concomitant increase in the proportion of 18:2- and 18:3-fatty acids within the PE and PC classes (Quartacci *et al.,* 1997). However, using PC as an example, during dehydration in an *Arabidopsis* mutant slightly more tolerant of water deficit, it was found that leaf dehydration had no effect on the proportion of 16:3-fatty acid, but the proportion of 18:3-fatty acid decreased (Gigon *et al.,* 2004). It can therefore be concluded that acclimation to water deficit is largely dependent on the ability of the plant to maintain higher levels of poly-unsaturated fatty acids such as 18:2 and 18:3 during such stress.

3.2.4. The occurrence of unusual fatty acids in *X. humilis*

Together with common fatty acids, unusual fatty acids with medium (C8-C14) and very long (C20-C30) acyl chains also occur naturally in seed oils (Badami and Patil, 1980; Millar *et al*., 2000; Voelker, 2001). Research has shown that these unusual fatty acids occur in very small amounts compared to common ones, and their roles in biological cells may differ (Moier *et al*., 2004; Zheng *et al*., 2016). Very long chained fatty acids (VLCFAs) in plants are synthesized in the endoplasmic reticulum by sequential addition of C2-moeties, derived from the malonyl-CoA into the pre-existing 18-carbon long chain fatty acid (Millar *et al*., 2000; Nobusawa and Umeda, 2012; Nobusawa *et al*., 2013). Four enzymatic reactions are involved in the synthesis of VLCFAs and are as follows: 1) condensation of Acyl-CoA with malonyl-CoA catalysed by ketoacyl-CoA synthase (KCS); 2) reduction of 3-ketoacyl-CoA synthase by 3-ketoacyl-CoA reductase (KCR); 3) dehydration of 3-hydroxyacyl-CoA by 3-hydroxyacyl-CoA dehydratase (HCD); and 4) reduction of enoyl-CoA by enoyl-CoA reductase (ECR; Bach *et al*., 2008; Nobusawa and Umeda, 2012; Nobusawa *et al*., 2013). It has been shown that the loss of KCR and/or HCD in *Arabidopsis* had a profound effect on the germination and seedling establisments of embryos, suggesting the important role of VLCFAs in plant growth promotion. Furthermore, Nobusawa and Umeda (2012) showed that VLCFAs play a crucial role in Z- ring formation, which regulates plastid division (Terbush and Osteryoung, 2012). In this study, the VLCFA were only present in both PC and PE, with 20:0- and 20:1-fatty acids present in both classes, and the 22:0-, 23:0-, 24:0- and 25:0-fatty acids exclusively present in PE. This is somewhat expected since PC is formed through the methylation of PE (Horl *et al.,* 2011). During dehydration, the proportion of 20:0-fatty acid decreased in both classes, except in the roots within PC. This decrease in 20:0-fatty acid during drought stress may stimulate the decrease in non-linear packing of fatty acids in membrane phase, thus inducing membrane flexibility (Cyril *et al*. 2002). Furthermore, the 22:0-, 23:0-, 24:0- and 25:0-fatty acids had an overall increase in proportion during dehydration. A similar trend was observed in the study by Millar *et al.* (2000), where the amount of VLCFAs increased in the transgenic plant of *A. thaliana* as the plant senesced. Resurrection plants are known to prevent senescence during dehydration (Griffiths *et al.,* 2014),

and while counter intuitive it could be possible that accumulation of VLCFAs may stabilise the membrane bilayer in *X. humilis* and prevent drought induced senescence.

Along with the increase in the amount of the unusual fatty acids of VLCFAs, the study also revealed the presence of medium chain fatty acids (MCFAs, C8-C14) which decrease during desiccation and increased on rehydration (Table 3.5; 3.13; 3.14). Trace amounts of MCFAs have been observed in leaf oils (Reynold *et al.,* 2015). Taken together, the study revealed that the *X. humilis* is able to activate the enzymes necessary for the biosynthesis of VLCFAs during dehydration, whilst inhibiting the synthesis of MCFAs. VLCFAs are rarely found in polar glycerolipids, but commonly present in triacylglycerol of seeds (Millar *et al.,* 1998). Their presence in the bilayer membrane has been suggested to play a role in facilitating bilayer curvature, due to their long hydrophobic tail interlocking with the opposite membrane leaflet (Schneiter *et al.,* 1996).

In conclusion, this chapter shows the important roles that lipids play in the ability of *X. humilis* to tolerate desiccation. This is indicated by the increase in poly-unsaturated fatty acids in both leaf and root tissues during dehydration. Hence the increased levels of fatty acid unsaturation in the fully dehydrated state must represent a drought triggered acclimation to improve membrane stability during water deficit. Furthermore, this data also revealed the involvement of unusual fatty acids, which also increased with the intensity of water loss and may also play important roles in membrane stabilization during such stress.

Chapter 4:

Chloroplast Membrane Lipid Analyses

4.1. Introduction

The survival of all life forms on earth ultimately depends on photosynthesis, which involves the production of organic compounds and oxygen from sunlight, carbon dioxide and water. In plants and green algae, the electron transfer processes essential to photosynthesis occur in the thylakoid membranes of the chloroplasts (Shimoni *et al.,* 2005). The photosynthetic thylakoid membranes in plants are known for their highly conserved lipid composition, namely galactolipids, sulfolipids and PG (Sakurai *et al.,* 2007). However, only galactolipids and PG were investigated in the present study.

Galactolipids are glycerolipids containing one or two galactose molecules attached to the *sn*-3 position glycerol backbone (Nakamura *et al*., 2013), synthesized within the chloroplast membrane (Marechal *et al.,* 2002) and make up 80% of the total membrane lipids (Dubots *et al.,* 2011; Myers *et al*., 2011). Monogalactosyldiacylglycerol (MGDG) and digalctosyldiacylglycerol (DGDG) are the two major components of the chloroplast envelope and thylakoid membranes, and are reported to be involved in the optimal functioning of the photosynthetic system of plants (Nakamura *et al*., 2010; Dubots *et al.,* 2011, Wang *et al*., 2014). MGDG is a non-bilayer forming lipid synthesized in the plastid membrane, by the action of MGDG synthase, which transfers galactose from uridine diphosphate galactose (UDP-galactose) to 1, 2-diacylglycerol (Jouhet *et al*., 2004; Torres-Franklin *et al.,* 2007; Nakamura *et al.,* 2010). Three MGDG synthase isomers have been detected in *Arabidopsis* i.e. MGD1, MGD2 and MGD3 (Awai et al., 2001). MGD1 synthase is localized in the inner envelope of the chloroplast, and knocking out this gene resulted in a fatal defect in photosynthesis (Kobayashi *et al*., 2007). Both the MDG2 and MDG3 are localized in the outer membrane of the chloroplast and double knock outs of these enzymes had no effect on the MDGD levels in *Arabidopsis* (Kobayashi *et al*., 2004). Previous studies showed a massive decrease in the levels of MGDG during dehydration in desiccation sensitive and tolerant species (Gigon *et al*., 2004;

Moellering *et al.,* 2010; Moellering *et al*., 2011; Gasulla *et al*., 2013; Li *et al*., 2014), and these decreases have been suggested to be a common adaptation to drought stress (Gigon *et al*., 2004; Gasulla *et al*., 2013). However, little is known about the changes in individual molecular species during water deficit or tolerance thereof. This study reports the changes in the molecular species within the MGDG in *X. humilis*.

DGDG, a bilayer forming galactolipid, is the second most abundant galactolipid found in plant leaves (Popova and Hincha, 2003; Deme *et al*., 2014), and consists of a second galactose moiety bound to a (1→6) α-glycosidic linkage between the two galactoses (Dormann and Benning, 2002). DGDG is synthesized either by the addition of galactose from UDP-galactose on MGDG through the action of the enzymes DGD1 and DGD2 (Kelly and Dormann, 2002; Kelly *et al*., 2003), or by the action of galactolipid-galactolipid galactosyltransferase where MGDG tranfers at second galactose to the other molecule of MDGD as follows: MGDG + MGDG gives DGDG + DAG (van Besouw and Wintermans, 1978). A considerable increase in the levels of DGDG during desiccation has been reported in homoiochlorophyllous resurrection plants, including *Paraisometrum mileense* and *Craterostigma plantagineum* (Gasulla *et al*., 2013; Li *et al*., 2014). However, data on the changes in the molecular species within DGDG during dehydration and rehydration is still lacking. The study thus also focused on determining which changes occur in order to understand the mechanisms of desiccation tolerance in *X. humilis*.

Dehydration in PDT species, including *X. humilis,* is associated with chlorophyll degradation and dismantling of thylakoid membranes (Tuba *et al.,* 1996; Sherwin and Farrant, 1998; Collett *et al*., 2003; Christ *et al.,* 2014), thereby potentially altering the composition and relative quantities of these galactolipids. Torres-Franklin *et al.,* (2007) showed that a variety of cowpea, more tolerant of mild water loss under drought stress showed an increase in DGDG content and its biosynthesis during drought, Gasulla et al (2013) reported a decline in MGDG and an increase of DGDG during desiccation of the homoiochlorophyllous resurrection plant *C. plantagineum*. For this reason, it can be hypothesized that both MGDG and DGDG are important for a plant's tolerance to water deficit stress and for recovery during re-watering. In this study, lipid molecular

species within the MGDG and DGDG were analysed, in order to understand, in part, the involvement of these photosynthetic lipids in the acquisition of desiccation tolerance.

4.2. Results

4.2.1. Confirmation of enrichment and purity of chloroplast isolates

The quantification of chloroplast lipid composition was performed on chloroplasts isolated from leaves of *X. humilis* at various stages of dehydration and rehydration by use of density centrifugation. In order to confirm the presence and enrichment of chloroplasts by the isolation protocol, western blot analysis was performed using anti-CRD1 as a marker. This antibody detects the protein CHL27, which is situated in both the chloroplast envelope and thylakoid membrane (Totty *et al.,* 2003; Canniffer *et al*., 2014). Immunoblot analysis showed the presence of CHL27 membrane proteins, but the levels appeared to decline during dehydration, with low levels being detected in dry leaves (Figure 4.1). A decline in the amount of protein visualized was initiated below 55% RWC. Upon rehydration, there was an increase in the amount of protein detected after 12 hours. The decline in amount of CHL27 protein during drying can possibly be attributed to a breakdown of thylakoid membranes during dehydration (see below), the faint signal being attributed to the remaining outer chloroplast membranes.

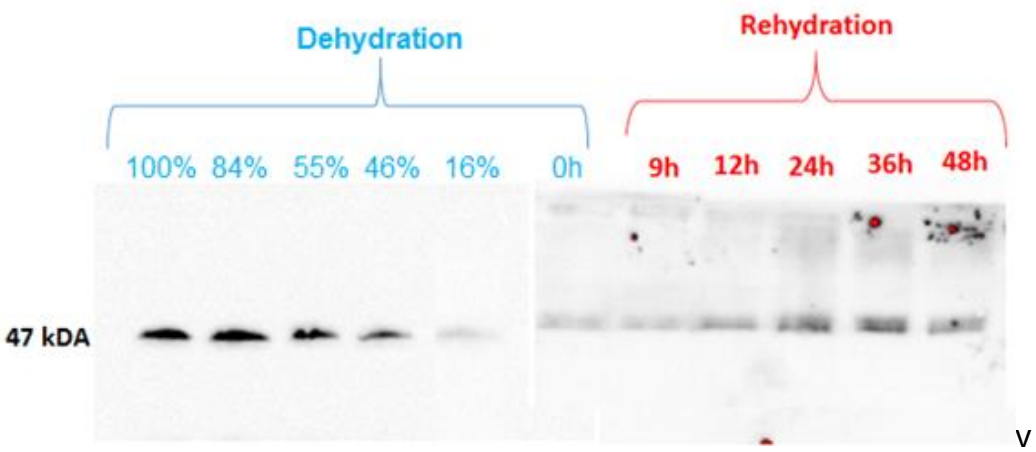

Figure 4.1: Western analysis of chloroplastic membrane protein levels during dehydration (in blue) and rehydration (in red) of *X. humilis* in RWC and hours respectively. 15 micrograms of total protein was probed with the CRD1 antibody. A band of 47 kDa molecular weight represented the chloroplast envelope membrane protein Equal loading of the gel was verified by Ponceau S staining of the membrane after protein transfer. The results shown are from one experiment representative of three.

To test for the purity of the isolated chloroplast, samples were blotted with ant-COX-2 (cytochrome oxidase subunit II; Figure 4.2), to check for presence of mitochondria contamination during chloroplast isolation (Pavlovic *et al.,* 2016). This is very important to eliminate false positive results during analyses, and since mitochondria have a similar structure to chloroplasts and also sediment at similar centrifugation speed (*g*), and tend to be co-extracted with the chloroplast (Islam and Takagi, 2010). Our results showed that the isolated chloroplasts were free from mitochondrial contamination, and therefore, ready for downstream experiments (Figure 4.2).

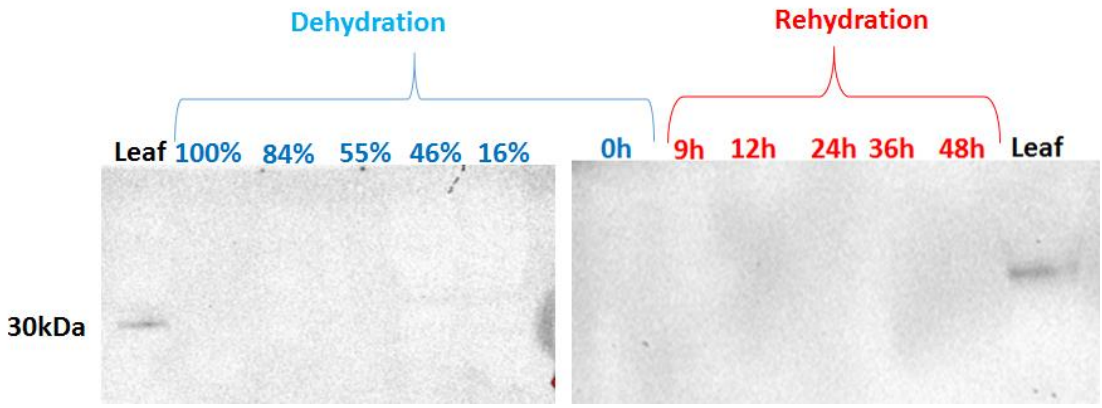

Figure 4.2: Western analysis of the mitochondrial membrane protein levels during dehydration (in blue) and rehydration (in red) of *X. humilis* in RWC and hours respectively. 15 micrograms of total protein was probed with ant-COX 2 (cytochrome oxidase subunit II). A band of 30 kDa molecular weight represented the COX II protein extracted from total hydrated leaf tissue. The results shown are from one experiment representative of three.

4.2.2. Changes in Chloroplast Ultrastructure during Dehydration and Rehydration

Being poikilochlorophyllous, *X. humilis* systematically disassembles thylakoid membranes during dehydration and reassemble these again during rehydration (Dace *et al*., 1998; Sherwin and Farrant, 1998; Farrant *et al.,* 2000; Ingle *et al*., 2008). In this study, transmission electron microscopy (TEM) was used to assess chloroplast structural changes during dehydration and rehydration in order to align these with observed lipid changes. In the fully hydrated state (Figure 4.3A), the chloroplasts were oblong in shape and had well-defined inner and outer membranes, stacked thylakoids and the presence of starch bodies, indicating metabolic activity. At 84% RWC, the grana appeared swollen, there was evidence of plastoglobuli formation and starch bodies had disappeared (Figure 4.3B). Dehydration to 55% RWC was associated with changes in the chloroplast shape, which became more oval in appearance, and further dissembling of the grana with most thylakoid appearing as isolated strands. The plastoglobuli appeared to have increased in number (Figure 4.3C). Photosynthesis, as measured by chlorophyll fluorescence and infra-red gas analysis, ceases below 60% RWC (Beckett *et al.,* 2012), which correlated with the observations in the present study. At 46% RWC, the remaining thylakoid strands appeared as small membrane-bound vesicles and plastoglobuli were clustered (Figure 4.3D). Further dehydration was associated with further vesiculation of thylakoids and clustering of plastoglobuli (Figure 4.3E). Upon rehydration (Figure 4.4), the vesicles appeared elongated and thylakoid re-assembly was evident such that by 12 hr they appeared as long strands, with little stacking into grana being evident (Figure 4.4I). Plastoglobuli were still evident. At this stage, chloroplasts had regained an elongated appearance. Apart from an apparent increase in starch, there was little further change in thylakoid appearance during further rehydration to 48 hr (96% RWC, Figure 4.4 J-K). The outer chloroplast membrane remained intact during dehydration and rehydration treatment.

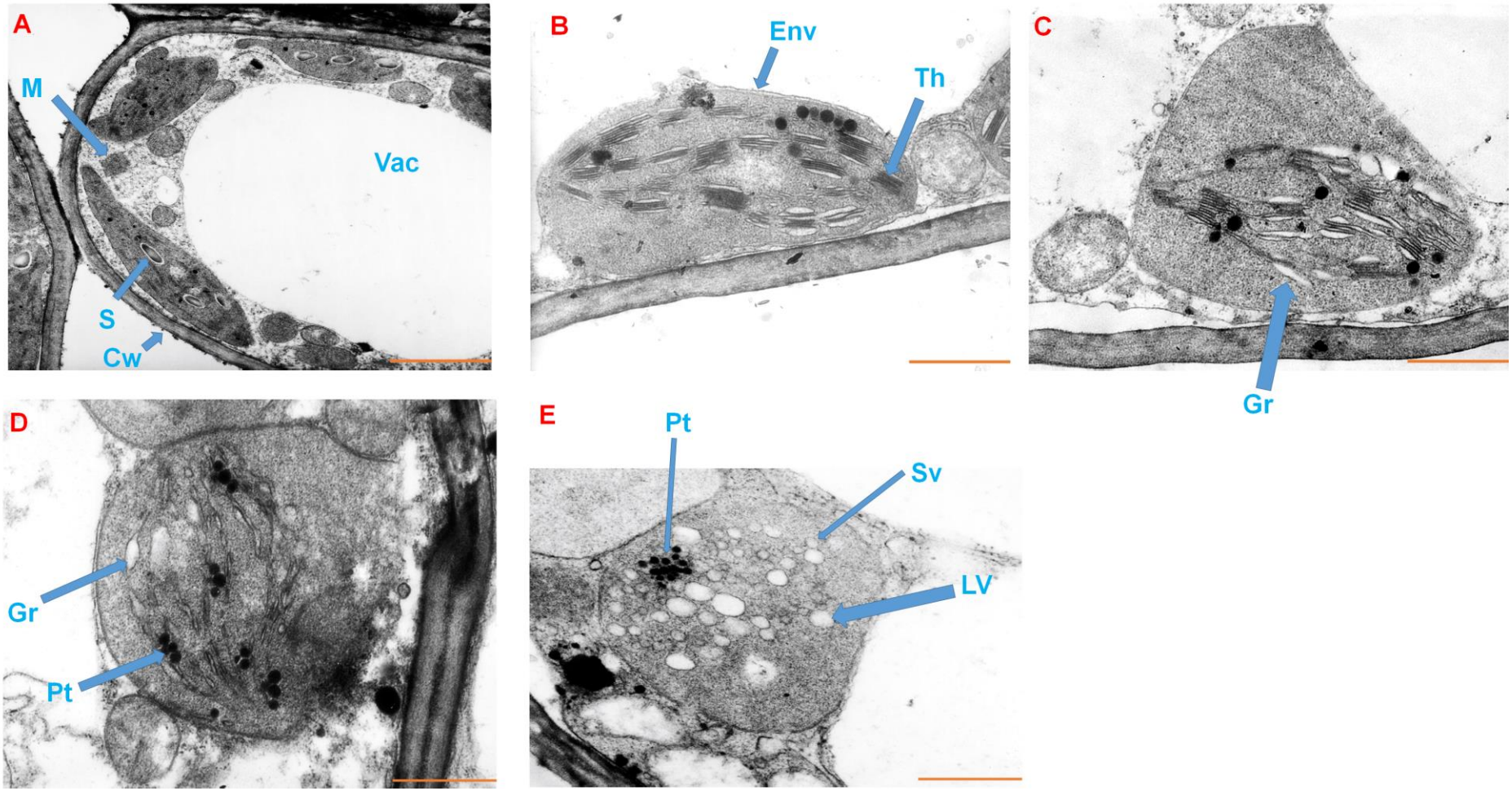

Figure 4.3: Transmission electron micrographs illustrating ultrastructural features of chloroplast during dehydration in *X. humilis*. A, 100%; B, 84%; C, 55%; D, 45%; E, 16%. Scale bars= 1µM. M, mitochondria; Vac, vacuole; S, starch grain; LV, large vesicles; Sv, oval vesicle; Pt, plastoglobuli; t, thylakoid; Cw, cell wall; Env, Envelope and Gr, grana.

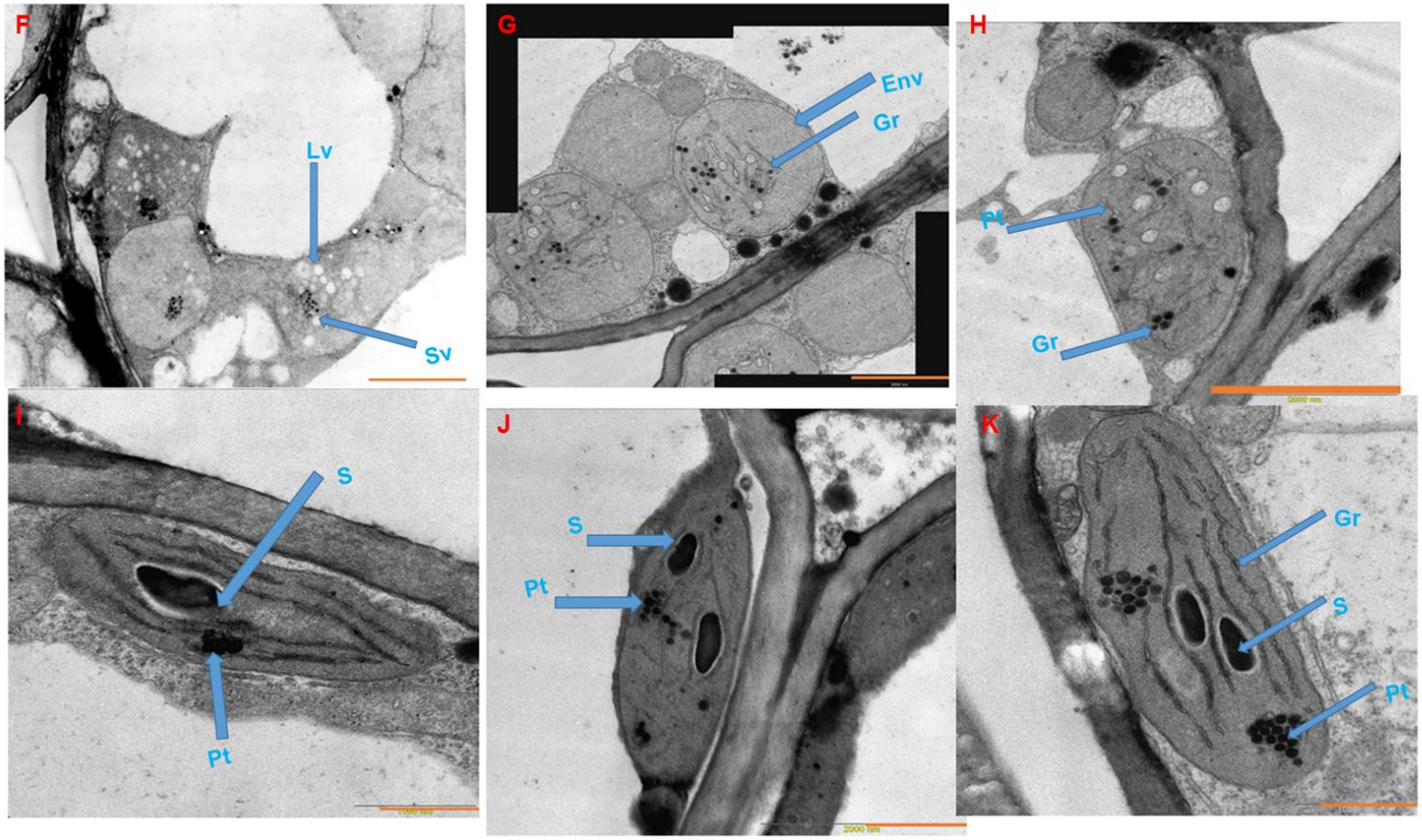

Figure 4.4: Transmission electron micrographs illustrating ultrastructural features of chloroplast during rehydration in *X. humilis*. F, 0hr (5%); G, 9hr (48%); H, 12hr (73%); I, 24hr (92%); J, 36hr (96%); K, 48hr (96%). Scale bars= 1µM. M, mitochondria; Vac, vacuole; S, starch grain; LV, large vesicles; Sv, oval vesicle; Pt, plastoglobuli; t, thylakoid; Cw, cell wall; and Gr, grana.

4.2.3. Lipid Molecular Species and Fatty Acid Composition in Chloroplasts during Dehydration and Rehydration Treatments

Total changes in galactolipids during drying was first assessed using TLC (Figure 3.3). When expressed relative to PC, there was a considerable decline in both species during drying, with a near disappearance of MGDG in the dehydrated state. During rehydration, the synthesis of both galactolipids was evident by 9 hr after rewatering. With levels being fully restored by 24 hr after rewatering.

4.2.3.1. MGDG

Based on the differences in the molecular species, two types of MGDG have been described: one containing 18:3 at both *sn*-1 and *sn*-2 positions on the glycerol backbone (18:3/18:3), and the other containing 18:3 at the sn-1 and 16:3 at sn-2 positions of the glycerol backbone (18:3/16:3; Joyard *et al*., 1998). Plants containing 18:3/18:3-MGDG are called 18:3 plants and those containing 16:3/18:3-MGDG are referred to as 16:3 plants. In this study, both the 18:3/18:3-MGDG and 16:3/18:3-MGDG (Table 4.1) molecular species were present, thus categorizing *X. humilis* as a 16:3 plant.

Chloroplast lipid composition was studied at five stages of drying, in which varying degrees of chloroplast dismantling had occurred (Figure 4.3) and six stages of rehydration during which reassembly of thylakoid was evident (Figure 4.4). The results obtained from MGDG extracted from chloroplast isolates from *X. humilis* leaves revealed that the 18:3/18:3-MGDG and 18:3/18:2-MGDG were predominant, accounting for 35% and 25% of the total lipids in the fully hydrated chloroplast, respectively (Table 4.1). The molecular species 16:0/16:1-MGDG, 18:0/18:3-MGDG, and 18:1/18:2-MGDG were minor, accounting for 0.93%, 0.95%, and 0.87% of the total MGDG, respectively. Dehydration was associated with no noticeable change in 18:3/18:3-MGDG; but rehydration was associated with an increase in the relative content of this MGDG species, that reached 52% of total MGDG content after 48 hr.

Conversely, a slight increase in 18:3/18:3-MGDG was observed during dehydration, but the amount of this species was lower in dry tissues than that initially present in fully hydrated tissues and there appeared to be little change in this species upon rehydration (supplementary figure 4.5). The minor molecular species 16:0/16:1-MGDG, 18:0/18:3-MGDG, and 18:1/18:2-MGDG had no noticeable change during both dehydration and rehydration. A slight decrease was detected in both 18:3/18:3-MGDG and 18:3/18:2-MGDG when the plant was maintained in the dehydrated state for 3 weeks. The 18:3/18:3-MGDG decreased from 36% to 32%, and 18:3/18:2-MGDG from 32% to 26%.

Seven fatty acids were detected within the chloroplastic MGDG pool (CHL-MGDG), including 16:0, 16:1, 16:3, 18:0, 18:1, 18:2, and 18:3 (Table 4.2). The 18:3 and 18:2 fatty acids accounted for 55% and 25% of the total fatty acids in MGDG, respectively. The 18:0 species occurred in the lowest amount, accounting for 0,7% of the total fatty acid, in fully hydrated CHL-MGDG. Dehydration resulted in only slight changes in the fatty acids within the CHL-MGDG pool. However, upon rehydration there was a considerable increase in 18:3 fatty acids, which increased from 53% (at 0hr) to 69% (after 48hr), and a decrease in 18:2 fatty acids, from 20% (at 0hr) to 13% (after 48hr). The increase in 18:3 fatty acid and decrease in 18:2 fatty acid during rehydration suggests that the 18:3-MGDG in *X. humilis* was formed by sequential desaturation of oleic acid (18:0) and linoleic (18:2) upon recovery.

Table 4.1: MGDG lipid molecular species (% of total MGDG MRM transitions) analysis of the *X. humilis* leaves during dehydration and rehydration within the chloroplast. The values highlighted in blue represent the plant during dehydration and the ones in red represent the plant during rehydration. Water content values are given as RWC in percentages at different sampling points.

CHL-MGDG	100%	84%	55%	46%	16%	0hr (5%)	9hr (48%)	12hr (73%)	24hr (92%)	36hr (96%)	48hr (96%)
16:0/16:1	0,93	0,95	0,68	0,69	0,53	0,92	0,62	0,9	0,83	0,69	0,63
16:3/18:3	4,76	3,94	4,91	5,42	5,59	5,39	5,32	6,52	9,19	8,71	7,75
16:1/18:3	3,07	2,7	2	1,73	1,74	1,98	2,43	3,23	4,38	3,24	3,23
16:1/18:2	1,62	1,84	1,17	1,26	1,11	1,49	1,38	1,05	1,05	0,74	0,79
16:0/18:3	5,36	3,23	1,45	2,44	1,83	3,61	2,82	3,69	2,87	2,8	2,98
16:1/18:1	0,92	1,15	0,69	0,71	0,62	1,15	1,37	1,22	0,91	0,51	0,48
16:0/18:2	2,65	2,39	1,09	1,32	1,59	1,93	1,36	1,24	0,7	0,71	0,8
16:0/18:1	1,18	1,39	0,63	0,76	0,83	1,72	1,2	1,22	0,6	0,39	0,32
18:3/18:3	35,49	30,07	35,75	38,52	36,39	32,08	33,44	40,67	48,26	51,85	51,67
18:3/18:2	26,72	27,75	31,21	26,86	32,12	26,09	24,9	21,22	20,17	21,26	22,38
18:2/18:2	7,74	11,14	9,71	8,97	8,83	8,97	4,72	2,58	2,05	2,46	3,07
18:1/18:3	3,98	4,72	4,09	3,67	3,66	3,76	9,59	9,15	5,6	4,03	3,4
18:2/18:1	3,78	6,24	4,73	4,44	2,88	6,94	5,46	3,1	1,67	1,49	1,55
18:0/18:3	0,95	0,77	0,96	1,3	1,6	2,23	2,4	2,58	0,96	0,75	0,59
18:1/18:1	0,87	1,72	0,94	0,92	0,69	1,79	2,98	1,62	0,76	0,37	0,34

Table 4.2: Fatty acids composition of chloroplastic MGDG class (%) of *X. humilis* leaves subjected to gradual dehydration and rehydration treatment. The values highlighted in blue represent the plant during dehydration and the ones in red represent the plant during rehydration. The observed % of MGDG fatty acid for a lipid class was calculated from the % of total MRM transitions. Water content values are given as RWC in percentages at different sampling points.

CHL-MGDG	100%	84%	55%	46%	16%	0h (5%)	9h (48%)	12h (73%)	24h (92%)	36h (96%)	48h (96%)
16:0	5,4	4,4	2,3	3,1	2,7	4,2	3,6	4,3	3,2	2,9	2,8
16:1	3,1	3,3	2,3	2,2	2,5	3,4	3,3	3,5	4,3	3	2,8
16:3	4,8	3,9	4,8	5,3	5,4	5,3	5,3	6,4	9,1	8,6	7,7
18:0	0,7	0,5	0,6	0,7	1	1	1,3	1,8	0,6	0,5	0,4
18:1	5,4	8	5,5	4,9	4	9,3	11,7	9,1	5,4	3,8	3,4
18:2	24,6	30,2	28,3	25,9	27,4	22,8	19,9	13,5	10,6	11,4	12,8
18:3	54,5	48,2	55,1	56,9	56,2	53,4	54,2	60,3	65,6	68,9	68,9

4.2.3.2. DGDG

In the fully hydrated state, the DGDG was predominated with 16:0/18:3-DGDG, 18:3/18:3-DGDG, and 18:3/18:2-DGDG molecular species, accounting for 27%, 25%, 17% of the total DGDG, respectively (Table 4.3). Species present in small amounts were 16:0/16:1-DGDG, 16:1/18:2-DGDG, and 18:1/18:1-DGDG, accounting for 0,7%, 0,7%, and 0,5%, respectively. A gradual decrease in the molecular species 16:0/18:3-DGDG and 16:0/18:2-DGDG was observed during dehydration, followed by an increase upon rehydration (supplementary figure 4.6). The polyunsaturated molecular species 18:3/18:3-DGDG and 18:3/18:2-DGDG increased with increasing water loss. Furthermore, as for the MGDG species, there was a progressive increase in 18:3/18:3-DGDG during maintenance in the dry state for a period of 3 weeks. Upon rehydration, the 18:3/18:3-DGDG content remained the same for at least 48 hours, but a slight decrease in 18:3/18:2-DGDG was noted. The minor molecular species had no noticeable changes during dehydration and rehydration treatment.

At 100% RWC, seven fatty acids were detected within the chloroplastic DGDG of *X. humilis* leaves, including 16:0, 16:1, 16:3, 18:0, 18:1, 18:2, and 18:3 fatty acids (Table 4.4). The fatty acids 18:3, 16:0, and 18:2 were the predominant ones in the fully hydrated CHL-DGDG, accounting for 49%, 24%, and 16%, respectively. During dehydration, the 16:0 fatty acid decreased from 24% to 10% (at fully dehydrated), followed by a gradual increase upon rehydration. The 18:3 fatty acid had a late increase, which started at 55% RWC, and continued to increase throughout dehydration and rehydration. The minor fatty acids at fully hydrated state, including 16:1, 16:3, 18:0, and 18:1, accounting for 2%, 2.6%, 1.6%, and 5.5%; had minor changes during both dehydration and rehydration treatments. This suggests that their levels remain stable during desiccation and recovery of *X. humilis*.

Table 4.3: DGDG lipid molecular species (% of total DGDG MRM transitions) analysis of the *X. humilis* leaves during dehydration and rehydration within the chloroplast. The values highlighted in blue represent the plant during dehydration and the ones in red represent the plant during rehydration. Water content values are given as RWC in percentages at different sampling points.

CHL-DGDG	100%	84%	55%	46%	16%	0h (5%)	9h (48%)	12h (73%)	24h (92%)	36h (96%)	48h (96%)
16:0/16:1	0,69	0,84	0,6	0,67	0,47	0,47	0,567	0,69	0,65	0,58	0,66
16:3/18:3	2,59	2,36	2,73	3,24	3,4	4,3	3,62	4,03	3,64	3,75	3,94
16:1/18:3	2,02	2,08	1,68	1,64	1,23	1,57	1,28	1,77	1,94	1,77	2,171
16:1/18:2	0,7	0,98	0,95	0,9	0,72	0,6	0,62	0,59	0,54	0,47	0,54
16:0/18:3	26,81	22,5	16,92	17,4	8,61	9,11	9,26	13,07	14,95	14,81	15,2
16:1/18:1	0,39	0,45	0,38	0,35	0,3	0,31	0,24	0,41	0,36	0,26	0,28
16:0/18:2	7,63	9,88	6,45	6,25	4,23	2,22	3,68	3,7	3,35	3,12	3,2
16:0/18:1	1,96	2,58	1,78	1,77	1,38	0,67	1,12	1,68	1,53	1,25	1,16
18:3/18:3	24,77	21,79	26,72	29,98	33,36	44,13	38,34	39,92	37,28	40,58	41,47
18:3/18:2	16,64	17,72	22,32	19,93	27,09	23,9	24,14	20	19	19,13	18,95
18:2/18:2	4,11	5,7	6,54	5,78	7,61	5,18	5,37	3,46	3,05	2,53	2,55
18:1/18:3	6,01	6,25	6,23	4,88	4,62	3,34	4,75	5,84	7,33	6,65	5,71
18:2/18:1	2,25	3,47	3,26	3,04	2,98	1,82	2,48	2,22	2,09	1,83	1,66
18:0/18:3	2,82	2,52	2,44	3,29	3,36	2,02	3,84	3,92	3,48	2,68	1,99
18:1/18:1	0,54	0,89	0,92	0,87	0,64	0,35	0,7	0,7	0,83	0,61	0,52

Table 4.4: Fatty acids composition of chloroplastic DGDG class (%) of *X. humilis* leaves subjected to gradual dehydration and rehydration treatment. The values highlighted in blue represent the plant during dehydration and the ones in red represent the plant during rehydration. The observed % of DGDG fatty acid for a lipid class were calculated from the % of total MRM transitions. Water content values are given as RWC in percentages at different sampling points.

CHL-DGDG	100%	84%	55%	46%	16%	0h (5%)	9h (48%)	12h (73%)	24h (92%)	36h (96%)	48h (96%)
16:0	24	22	16	16	10	8,3	9,4	12,7	13,1	12,8	12,9
16:1	2	2,3	1,9	1,8	1,4	1,6	1,5	1,9	1,8	1,6	1,9
16:3	2,6	2,3	2,7	3,2	3,4	4,2	3,6	4	3,6	3,7	3,9
18:0	1,6	1,6	1,5	1,9	2	1,3	2,3	2,4	2,1	1,7	1,2
18:1	5,5	6,7	6,2	5,2	4,2	3	4,3	5,3	6,1	5,3	4,6
18:2	16	20	21	19	23	16,2	18	13,6	12,5	11,6	11,5
18:3	49	45	50	53	56	65	61	60	61	63	64

4.2.3.3. Chloroplastic PG

PG is the only phospholipid documented in the thylakoid membranes of higher plants (Gaunaris *et al.,* 1986), which is synthesized through the acylation of glycerol 3-phosphate to lysophosphatidic acid by the action of glycerol 3-phosphate acyltransferase. The lysophosphatidic acid is further acylated to phosphatidic acid by the lysophosphatidic acid acyltransferase. The produced phosphatidic acid is converted to CDP-diacylglycerol by the action of CDP-diacylglycerol synthase, the product of which is further converted to phosphatidylglycerol phosphate (PGP) by the PGP-synthase. PGP is then dephosphorylated into PG by the enzyme PGP-phosphatase (Joyard *et al.,* 1998; Hagio *et al*., 2002). The chloroplastic PG (CHL-PG; Table 4.5) was predominated with saturated molecular species, including 16:0/16:0-PG, 16:0/18:0-PG, and 16:0/16:1-PG, accounting for 54%, 16%, and 11% of the PG in the fully hydrated chloroplast, respectively. During dehydration, a decrease in these saturated molecular species was noted. However, the decrease in 16:0/16:0-PG and 16:0/16:1-PG started when the plant RWC dropped to below 85%. Furthermore, a considerable decrease in 16:0/16:0-PG was observed when the plant was at 5% RWC, decreasing from 22% to 11%. All these molecular species, i.e. 16:0/16:0-PG, 16:0/18:0-PG, and 16:0/16:1-PG increased upon rehydration. Interestingly, an increase in non-fluidizing molecular species 16:0/18:3-PG, and 16:0/18:2-PG was observed during dehydration. The other polyunsaturated molecular species such as 18:3/18:3-PG, 18:3/18:2-PG, and 18:2/18:2-PG increased during dehydration, from 0.2%, 0.4%, 0.2%, 0.3%, and 0.4% at the fully hydrated state to 7%, 8%, 3%, 5%, and 4% of the total lipids at the fully dehydrated state, respectively (Supplementary Figure 4.7). Following rehydration, these polyunsaturated molecular species decreased reaching their lowest levels of 0.6%, 1%, 0.5%, 0.5%, and 0.5% after 48 h of re-watering.

Ten fatty acids were detected within the CHL-PG in the leaves of *X. humilis*, including 14:0, 15:0, 16:0, 16:1, 17:0, 18:0, 18:1, 18:2, 18:3, and 19:1 (Table 4.6). 16:0 was the major fatty acid accounting for 74% of the total fatty acids, followed by 16:1, which accounted for 11% in fully hydrated CHL-PG. Dehydration was associated with a

decrease in both 16:0 and 16:1 fatty acids, with the 16:0 reaching the lowest values when the RWC dropped below 9% RWC (0hr). The minor common fatty acids were 18:1, 18:2, 18:3, and 18:0, accounting for 1%, 3%, 2%, and 6% of the total fatty acids in fully hydrated CHL-PG, respectively. Upon dehydration, these fatty acids increased considerably, reaching their maximum values of 18:1 (9%), 18:2 (11%), 18:3 (16%), and 18:0 (21%) when the plant was at 5% RWC (0hr). A mirror image in the patterns of these fatty acids was observed upon rehydration.

Table 4.5: PG molecular species (% of the total PG MRM transitions) analysis of the *X. humilis* leaves during dehydration and rehydration within the chloroplast. The values highlighted in blue represent the plant during dehydration and the ones in red represent the plant during rehydration. Water content values are given as RWC in percentages at different sampling points.

CHL-PG	100%	84%	55%	46%	16%	0h (5%)	9h (48%)	12h (73%)	24h (92%)	36h (96%)	48h (96%)
15:0/16:0	5,26	3,77	3,7	4,1	4,8	2,45	4,49	4,46	5,31	5,31	5,53
14:0/18:2	0,11	0,04	0,14	0,18	0,85	1	0,46	0,33	0,17	0,17	0,13
14:0/18:1	0,91	0,86	0,96	1,11	0,74	1,56	0,83	0,78	0,85	0,85	0,82
16:0/16:1	11,17	12,26	10,62	13	5,04	2,9	5,1	6,12	10,22	10,22	11,52
16:0/16:0	53,75	53,17	45,86	33,1	22,46	11,34	22,21	32,67	39,18	39,18	40,99
15:0/18:2	0,19	0,23	0,41	0,58	1,44	1,84	1,33	0,79	0,35	0,35	0,39
16:1/18:2	1,18	1,29	1,56	2,96	1,72	2,37	1,53	1,21	1,33	1,33	1,5
16:0/18:3	2,73	2,75	5,62	7,33	10,52	14,71	12,66	12,61	9,66	9,66	8,42
16:0/18:2	3,55	3,36	4,93	8,2	10,07	11,19	8,05	6,2	4,91	4,91	4,89
16:1/18:0	1,23	3,25	2,77	2,57	1,92	1,59	1,84	2,96	3,48	3,48	3,15
16:0/18:0	15,99	15,98	18,55	13,77	13,51	7,63	13,79	15,25	17,4	17,4	17,56
17:0/18:2	0,09	0,14	0,2	0,52	0,89	0,84	0,58	0,41	0,17	0,17	0,17
18:3/18:3	0,21	0,23	0,49	0,52	3,03	7,24	3,41	2,4	1	1	0,57
18:3/18:2	0,43	0,52	0,74	1,36	5,18	7,64	5,27	3,07	1,53	1,53	0,99
18:2/18:2	0,22	0,43	0,42	0,79	1,79	2,67	1,51	1,11	0,67	0,67	0,45
18:1/18:3	0,28	0,31	0,45	1	2,21	5,34	2,61	1,85	0,86	0,86	0,53
18:2/18:1	0,34	0,18	0,35	0,89	2,16	4,21	2,15	1,47	0,68	0,68	0,47
18:0/18:3	0,27	0,31	0,71	0,98	2,39	3,43	2,61	1,54	0,91	0,91	0,63
18:1/18:1	0,5	0,39	0,39	4,4	4,17	4,8	4,73	2,44	0,43	0,43	0,47
18:0/18:2	0,15	0,11	0,55	0,64	2,13	2,29	1,67	0,84	0,53	0,53	0,36
18:0/18:1	0,23	0,29	0,42	1,05	1,91	2,16	2,01	1,02	0,26	0,26	0,35
19:1/18:1	0,23	0,13	0,17	0,93	1,08	0,83	1,15	0,45	0,11	0,11	0,11

Table 4.6: Fatty acids composition of chloroplastic PG class (%) of *X. humilis* leaves subjected to gradual dehydration and rehydration treatment. The values highlighted in blue represent the plant during dehydration and the ones in red represent the plant during rehydration. The observed % of PG fatty acid for a lipid class was calculated from the % of total MRM transitions. Water content values are given as RWC in percentages at different sampling points.

CHL-PG	100%	84%	55%	46%	16%	0h (5%)	9h (48%)	12h (73%)	24h (92%)	36h (96%)	48h (96%)
14:0	0,9	0,9	0,8	0,9	1	0,9	0,7	0,6	0,7	0,9	0,8
15:0	1,8	1,2	1,2	1,9	2,3	1,5	2,4	1,4	1,4	1,6	1,7
16:0	74,2	72,6	68,8	56,7	48,4	36	48	57,4	66,5	64,1	65,8
16:1	10,6	12,2	11,1	13,2	5,9	4,7	5,8	7,6	8,3	10,8	12
17:0	0,01	0,04	0,06	0,2	2	0,2	0,1	0,1	0,05	0,04	0,08
18:0	6	6	7,6	6,7	9,1	8,6	9,1	7,7	7	7,6	7,3
18:1	1	0,9	1,3	6,5	7,4	11,2	8,5	4,9	1,9	1,5	1,3
18:2	3	3,4	4,6	7,6	12,3	16	10,7	8	5,4	5,2	4,5
18:3	2,2	2,5	4,4	5,9	13	20,5	14,2	12	8,7	8,2	6,5
19:1	0,1	0,03	0,07	0,4	0,3	0,3	0,6	0,2	0,05	0,05	0,04

4.2.3.4. Chloroplastic PE

PE, a non-bilayer forming lipid, has never been reported in the chloroplast of so called drought tolerant (but desiccation sensitive) plants. However, Pillai and St. John (1981) reported the presence of PE in the chloroplast membranes of Atriazine-resistant biotypes of *Senecio vulgaris L*. Atriazine which was found to bind to the D-1 protein in photosynthetic electron transport, thereby inhibiting photosynthesis (Shimabukuro and Swanson, 1969). Their study showed that the chloroplasts from atriazine-resistant biotypes had higher amounts of PE than the chloroplast from susceptible varieties, suggesting the involvement of PE in the plant's resistance to atriazine herbicides. Furthermore, PE has also been shown to stabilize membranes during plastid biogenesis, since non-lamellar lipids are favoured over lamellar lipids during various environmental stresses (Escriba *et al*., 2008). Here we found the presence of PE molecular species during rehydration when chloroplast regeneration was apparent (Figure 4.3E; 4.4 F-K). In this study, significant amounts of 16:0/18:1-PE, 16:0/18:2-PE and 16:0 /18:3-PE molecular species were observed, accounting for 10%, 14%, and 15% of the total lipids, respectively. The 16:0/18:1-PE decreased upon rehydration, while the other two molecular species, 16:0/18:2-PE and 16:0/18:3-PE, increased (Supplementary Figure 4.8). The other molecular species were present in minute amounts and did not change during rehydration. At 16% RWC, 16:0, 18:2, 18:3, 18:1, and 18:0 were the most abundant fatty acids, accounting for 31%, 24%, 14%, 12%, and 12% of the total fatty acids, respectively (Table 4.8). These fatty acids had no significant change during rehydration.

Table 4.7: PE lipid molecular species (in weight %) analysis of the *X. humilis* leaves during dehydration and rehydration within the chloroplast. Dehydration was associated with undetectable values of PE molecular species. The values highlighted in blue represent the plant during dehydration and the ones in red represent the plant during rehydration. Water content values are given as RWC in percentages at different sampling points.

CHL-PE	100%	84%	55%	46%	16%	0h (5%)	9h (48%)	12h (73%)	24h (92%)	36h (96%)	48h (96%)
15:0/16:0					0,25	0,18	0,18	0,27	0,34	0,27	0,39
14:0/18:3					1,12	2,07	1,57	1,35	1,1	1,25	0,73
14:0/18:2					1,68	1,69	1,75	1,25	1,25	1,14	1,47
16:0/16:0					0,4	0,1	0,14	0,33	0,18	0,19	0,42
15:0/18:3					3,84	3,75	3,93	4,48	4,82	4,39	3,66
15:0/18:2					5,2	3,51	4,56	3,67	4,8	4,68	5,11
15:0/18:1					3,29	3,33	2,53	3,38	2,65	2,14	2,58
16:1/18:2					0,61	0,64	0,58	0,39	0,58	0,7	0,89
16:0/18:3					14,79	15,19	16,01	21,19	20,71	18,8	18,47
16:0/18:2					14,35	10,76	14,29	14,18	15,59	16,06	16,95
16:0/18:1					10,09	8,89	7,64	9,06	8,2	6,76	8,76
17:0/18:2					1,82	0,82	1,05	1,31	1,23	1,04	1,23
17:0/18:1					0,75	0,48	0,52	0,73	0,5	0,53	0,55
18:3/18:3					2,09	4,74	3,68	3,25	3,36	2,68	2,47
18:3/18:2					4,97	6,66	7,16	6,26	5,83	7,09	6,07
18:2/18:2					4,54	4,37	5,3	4,04	4,34	5,94	5,54
18:1/18:3					2,68	5,71	3,61	2,87	3,02	2,54	1,92
18:2/18:1					5,07	6,15	5,28	3,65	4,46	5,36	4,46
18:0/18:3					5,4	6,14	5,56	5,22	4,59	4,67	3,6
18:1/18:1					1,46	3,48	1,89	1,46	1,46	1,39	1,16
18:0/18:2					6,99	5,69	6,3	4,91	4,67	5,27	5,03
18:0/18:1					3,13	3,37	2,91	2,76	2,29	2,51	2,08
16:0/20:1					0,17	0,08	0,11	0,2	0,29	0,2	0,13
19:0/18:2					0,36	0,28	0,42	0,3	0,28	0,44	0,52

20:1/18:2	0,31	0,2	0,24	0,1	0,21	0,2	0,29
18:2/20:0	0,85	0,42	0,53	0,62	0,51	0,7	1,52
18:1/20:0	0,44	0,2	0,29	0,35	0,25	0,37	0,24
18:2/22:0	0,36	0,21	0,29	0,33	0,44	0,4	0,6
18:2/23:0	0,4	0,13	0,24	0,42	0,41	0,53	0,63
18:1/23:0	0,2	0,07	0,14	0,39	0,25	0,17	0,36
24:0/18:2	0,14	0,35	0,8	0,72	0,83	0,97	1,07
24:0/18:1	0,68	0,22	0,33	0,35	0,34	0,39	0,57
25:0/18:2	0,36	0,12	0,18	0,23	0,23	0,24	0,53

Table 4.8: Fatty acids composition of chloroplastic PE class (in weight %) of *X. humilis* leaves subjected to gradual dehydration and rehydration treatment. Dehydration was associated with undetectable values of PE fatty acids.The values highlighted in blue represent the plant during dehydration and the ones in red represent the plant during rehydration. Water content values are given as RWC in percentages at different sampling points.

CHL-PE	100%	84%	55%	46%	16%	0h (5%)	9h (48%)	12h (73%)	24h (92%)	36h (96%)	48h (96%)
14:0					0,4	0,7	0,7	0,5	0,4	0,3	0,5
15:0					2,3	1,9	1,9	2,3	2,3	2,2	2,1
16:0					30,9	27,8	30,3	35,8	35,5	32,9	36
16:1					0,5	0,4	0,4	0,3	0,5	0,5	0,8
17:0					0,5	0,2	0,3	0,3	0,3	0,3	0,4
18:0					12,1	11,5	11,3	9,8	8,9	9,6	8,4
18:1					12	15,8	11,5	11,3	10,5	9,8	9,3
18:2					24,4	20,7	24,5	19,9	22,3	25,5	26
18:3					13,5	18,6	16,5	16,5	16,3	15,9	13
19:0					0,1	0,05	0,1	0,09	0,09	0,1	0,2
20:0					0,3	0,2	0,3	0,4	0,3	0,3	0,7
20:1					0,2	0,09	0,1	0,1	0,2	0,2	0,1
22:0					0,1	0,05	0,07	0,1	0,07	0,1	0,1
23:0					0,4	0,14	0,3	0,6	0,6	0,5	0,7
24:0					0,7	0,2	0,3	0,3	0,3	0,5	0,5
25:0					0,2	0,03	0,03	0,1	0,08	0,1	0,1

4.2.3.5. Chloroplastic PC

PC has been reported to be asymmetrically distributed on the outer chloroplast membrane of pea (Cline *et al.,* 1981) and spinach plants (Block *et al.,* 1983). In the chloroplast of *X. humilis,* high amounts of 16:0/18:1-PC and 18:0/18:1-PC molecular species were found in the fully hydrated leaves, accounting for 26% and 14% of the total lipids, respectively (Table 4.9). The 18:1/18:1-PC, 16:0/18:2-PC, 16:0/18:3-PC and 15:0/18:1-PC were also present in significant amounts, accounting for 8%, 5%, 6%, and 6% of the total lipids in hydrated plant, respectively. The minor molecular species within the chloroplastic PC (CHL-PC) were 18:3/18:3-PC, 17:0/18:2-PC, 14:0/18:2-PC, 14:0/18:3-PC, and 15:0/16:0-PC, accounting 0,7%, 0,5%, 0,3%, 0,6%, 0,5%, and 0,3% of the total lipids, respectively. Upon dehydration, the molecular species 16:0/18:1-PC and 18:0/18:1-PC decreased to the lowest values of 9% (each) in fully dehydrated leaves (5% RWC; supplementary figure 4.9). These decreases started below 55%. The other three major molecular species, including 16:0/18:2-PC, 16:0/18:3-PC and 15:0/18:1-PC had no significant changes during both dehydration and rehydration. Within polyunsaturated molecular species, 18:0/18:3-PC, 18:2/18:1-PC, 18:1/18:3-PC, 18:2/18:2-PC 18:3/18:2-PC, 18:3/18:3-PC increased considerably during dehydration from 5%, 5%, 3%, 2%, 2%, and 0.7% in fully hydrated leaves to 8%, 10%, 10%, 5%, 7% and 7% in desiccated tissues (5% RWC; supplementary figure 4.9), respectively. Rehydration resulted in a decrease in these polyunsaturated molecular species.

Within the CHL-PC, the 18:1, 16:0, and 18:0 were the major fatty acids in fully hydrated leaves (Table 4.10), accounting for 35%, 29%, and 16% of the total fatty acids, respectively. Dehydration was associated with a decrease in the levels of these major fatty acids (18:1, 16:0, and 18:0), to 29%, 15%, and 15% in the fully dehydrated state, respectively. Minor fatty acids comprised of the 20:1, 20:0, 19:0, 17:0, and 14:0 species, accounting for less than 1% each of thet total fatty acids. These minor fatty acids did not change during dehydration and rehydration treatments. The polyunsaturated fatty acids, including 18:3 and 18:2 accounted for 6% and 9% in fully hydrated leaves, respectively, and increased extensively during dehydration reaching maximum values of 21% and 16% (5% RWC), respectively.

Table 4.9: PC lipid molecular species (in weight %) analysis of the *X. humilis* leaves during dehydration and rehydration within the chloroplast. The values highlighted in blue represent the plant during dehydration and the ones in red represent the plant during rehydration. Water content values are given as RWC in percentages at different sampling points.

CHL-PC	100%	84%	55%	46%	16%	0h (5%)	9h (48%)	12h (73%)	24h (92%)	36h (96%)	48h (96%)
15:0/16:0	0,26	0,28	0,26	0,21	0,27	0,14	0,17	0,2	0,25	0,08	0,16
14:0/18:3	0,46	0,34	0,35	0,35	0,83	1,18	1,24	1,49	0,87	1,15	1
14:0/18:2	0,64	0,31	0,35	0,5	0,63	0,55	0,68	0,48	0,75	0,88	0,93
14:0/18:1	2,24	1,83	1,39	1,44	1,29	1,25	0,98	1,22	0,06	1,06	1,21
16:0/16:0	0,31	0,72	0,29	0,2	0,26	0,12	0,23	0,27	0,15	0,17	0,19
15:0/18:3	1,37	1,17	1,15	1,67	2,54	1,87	2,53	3,15	3,33	3,17	2,81
15:0/18:2	1,64	1,87	1,34	1,03	1,88	1,08	1,65	1,56	2,28	2,61	2,77
15:0/18:1	6,23	5,57	5,01	4,19	3,7	2,65	2,48	3,18	3,81	3,77	4,24
16:0/18:3	6,06	5,3	4,7	5,9	7,72	6,83	9,58	13,07	13,8	11,7	10,39
16:0/18:2	5,4	7,82	7,3	7,55	5,99	3,94	5,32	5,11	6,99	8,22	9
16:0/18:1	25,53	25,09	19,04	15,45	11,37	8,9	8,45	11,52	11,07	11,18	13,09
17:0/18:2	0,48	0,6	0,6	0,73	0,9	0,45	0,61	0,59	0,73	0,7	0,83
17:0/18:1	1,94	2,01	1,56	2,28	1,22	0,67	0,76	0,93	0,73	0,98	1,02
18:3/18:3	0,68	0,32	1,28	1,11	3,66	7,15	6,7	5,44	4,68	3,54	2,1
18:3/18:2	1,47	1,48	2,03	2,5	4,79	7,04	7,6	6,06	6,2	5,25	4,73
18:2/18:2	1,75	2,57	3,63	4,07	4,09	4,1	3,77	2,63	2,85	3,62	3,65
18:1/18:3	2,48	2,35	4,51	3,86	6,31	10,36	9,23	8,73	7,97	7,19	5,8
18:2/18:1	5,1	5,21	6,79	7,68	7,51	10,07	7,79	6,25	6,72	8,12	8,08
18:0/18:3	4,45	3,47	5,17	4,96	8,66	7,67	8,64	8,4	7,62	7,53	6,31
18:1/18:1	7,79	7,27	7,83	9,99	6,02	9,62	5,93	5,45	5,64	5,33	6,32
18:0/18:2	3,43	4,4	4,77	5,55	6,32	3,68	4,95	3,99	4,11	4,98	5,79
18:0/18:1	14,07	14,18	16,22	13,78	11,41	9,18	8,58	8,23	6,63	6,46	7,25
19:0/18:1	1,73	1,68	1,34	1,98	0,78	0,44	0,59	0,71	0,57	0,62	0,48
20:1/18:2	0,17	0,05	0,19	0,31	0,29	0,21	0,17	0,17	0,17	0,29	0,36
20:1/18:1	0,31	0,6	0,52	0,45	0,37	0,25	0,35	0,24	0,16	0,3	0,46

18:2/20:0	1,01	0,6	0,86	0,93	0,47	0,27	0,41	0,3	0,36	0,52	0,57
18:1/20:0	3	1,85	1,51	1,32	0,72	0,35	0,58	0,66	0,51	0,53	0,44

Table 4.10: Fatty acids composition of chloroplastic PC class (in weight %) of *X. humilis* leaves subjected to gradual dehydration and rehydration treatment. The values highlighted in blue represent the plant during dehydration and the ones in red represent the plant during rehydration. Water content values are given as RWC in percentages at different sampling points.

CHL-PC	100%	84%	55%	46%	16%	0h (5%)	9h (48%)	12h (73%)	24h (92%)	36h (96%)	48h (96%)
14:0	0,4	5	0,3	0,5	0,4	0,4	0,5	0,6	0,4	0,5	0,6
15:0	1,7	1,3	1,7	0,9	1,5	1,1	1,3	1,4	1,7	1,5	1,9
16:0	28,5	31,9	23,6	23	20	15,3	18,1	23,2	24,7	24,1	25,5
17:0	0,4	0,5	0,3	0,8	0,4	0,2	0,2	0,3	0,2	0,3	0,4
18:0	16,4	16	20,5	19	19,4	15,7	16,8	15,8	14,1	14,4	15
18:1	35	31,7	30,9	30,5	25,2	29,4	23,8	24,1	22,9	24,2	23,7
18:2	9,1	10,7	13,5	14,5	16,4	15,8	16,2	12,6	14,9	17,2	17,3
18:3	6,2	5,8	8	9,4	15,8	21,7	22,4	21,6	20,5	17,2	14,5
19:0	0,6	0,4	0,5	0,5	0,2	0,1	0,2	0,1	0,2	0,1	0,1
20:0	0,7	0,4	0,4	0,3	0,2	0,1	0,1	0,1	0,1	0,2	0,1
20:1	0,3	0,3	0,2	0,4	0,2	0,1	0,1	0,1	0,1	0,2	0,4

4.2.3.6. Chloroplastic PI

Although PI is not a common chloroplastic lipid, it has been found on the outer envelope chloroplast membrane of spinach (Bovet *et al*., 2001; Siegenthaler *et al*., 1997) and Arabidopsis (Okazaki *et al.,* 2015). These authors suggested that is possibly involved in the regulation of chloroplast division. In this study, fully hydrated leaves had predominantly 16:0/18:3-PI, 16:0/18:2-PI, and 16:0/18:1-PI within the chloroplastic PI, accounting for 26%, 20%, and 12% of the total lipids, respectively (Table 4.11). Dehydration was associated with a decrease in 16:0/18:2-PI, and 16:0/18:1-PI molecular species to 11% and 5% of total lipids in fully dehydrated leaves. These increased slightly during rehydration. The molecular species16:0/18:3-PI fluctuated during dehydration. Furthermore, a significant amount of 15:0/16:0-PI, 18:0/18:3-PI, 16:0/16:0-PI, and 18:0/18:2-PI was also detected, accounting for 9%, 6%, 5%, and 4% of the total lipid, respectively (Table 4.11). The levels of most saturated molecular species, including 16:0/16:0-PI and 15:0/16:0-PI decreased from 5% and 9% in fully hydrated leaves to 0.4% and 0.7% in fully hydrated leaves, respectively (supplementary figure 4.10). With the exception of 18:2/18:2-PI, which remained unchanged during drying and rehydration, the unsaturated molecular species had a large increase upon dehydration and decreased again during rehydration. For example, the molecular species 18:3/18:3-PI, 18:3/18:2-PI, 18:1/18:3-PI, and 18:0/18:3-PI increased during dehydration from 0.3%, 0.3%, 0.8%, and 6% to 6%, 4%, 3%, and 14% of the total lipids in the fully dehydrated state (5% RWC), respectively (supplementary figure 4.10). The reverse pattern was observed upon rehydration.

Our data revealed eight fatty acids within the CHL-PI, including 15:0, 16:0, 17:0, 18:0, 18:1, 18:2, and 18:3 (Table 4.12). 16:0 was the predominant fatty acid, accounting for 40% of the total fatty acids within the hydrated plant. Furthermore, significant amounts of 18:3, 18:2, 18:1, 15:0, and 18:1 fatty acids were also observed, accounting for 17%, 14%, 9%, 9%, and 7% of the total lipids, respectively. Dehydration was associated with an overall decrease in 16:0, 18:1, and 15:0 fatty acids, reaching their lowest values of 27%, 7%, and 6% at the RWC of 5%, respectively. An increase in 18:3 fatty acids was noted from 17% in fully hydrated tissue to 32% when the plant was in the

fully dehydrated state (5% RWC). Rehydration was associated with the reverse of these patterns.

Table 4.11: PI lipid molecular species (in weight %) analysis of the *X. humilis* leaves during dehydration and rehydration within the chloroplast. The values highlighted in blue represent the plant during dehydration and the ones in red represent the plant during rehydration. Water content values are given as RWC in percentages at different sampling points.

CHL-PI	100%	84%	55%	46%	16%	0h (5%)	9h (48%)	12h (73%)	24h (92%)	36h (96%)	48h (96%)
15:0/16:0	8,57	11,28	5,93	5,73	3,49	0,7	2,06	3,75	2,7	1,76	3,46
16:0/16:1	0,87	0,89	0,64	0,77	0,82	0,57	0,62	0,92	0,87	0,9	0,88
16:0/16:0	4,84	5,95	2,53	2,19	1,62	0,42	1,49	2,21	1,85	1,35	2,9
15:0/18:3	3	3,2	4,81	4,26	5,65	6,56	5,98	5,68	4,1	3,73	3,78
15:0/18:2	1,75	1,38	1,8	2,12	2,89	1,78	2,15	1,81	1,64	2,3	1,82
15:0/18:1	1,99	1,46	1,87	1,91	1,76	1,74	1,49	1,66	1,83	1,59	1,48
16:1/18:3	0,48	0,64	1,05	0,47	1,07	2,51	0,65	0,95	3,21	0,69	1,36
16:0/18:3	25,9	21,74	25,45	24,99	29,1	30,34	33,06	38,15	33,01	24,86	28,56
16:0/18:2	19,55	20,29	14,36	15,75	13,07	10,63	13,21	11,68	13,04	14,51	15,57
16:0/18:1	11,67	10,77	8,41	7,61	5,99	5	5,08	7,23	7,13	7,57	7,12
16:0/18:0	1,86	1,72	2,42	2,32	1,12	0,59	1,05	1,16	1,47	2,99	1,57
17:0/18:3	1,65	1,87	2,68	2,77	2,99	2,69	3,29	2,85	2,94	3,16	2,57
17:0/18:2	1,26	1,68	1,29	1,49	1,11	0,99	1,19	1,3	1,2	1,75	1,73
17:0/18:1	0,68	0,68	0,93	0,83	0,58	0,39	0,45	0,58	0,62	1,84	0,69
18:3/18:3	0,26	0,2	1,45	1,73	2,51	5,69	3,17	1,72	1,81	1,44	0,79
18:3/18:2	0,34	0,58	1,24	1,68	2,47	3,61	2,93	1,48	1,75	3,9	1,27
18:2/18:2	0,27	0,24	0,46	0,64	0,61	0,66	0,56	0,34	0,6	1,41	0,48
18:1/18:3	0,82	0,82	1,65	1,1	1,63	2,95	2,11	1,32	2,39	1,01	1,69
18:2/18:1	0,91	1,01	1,09	0,72	1,1	1,42	1,14	0,86	1,31	2,02	1,16
18:0/18:3	5,67	5,39	10,01	9,59	12,21	13,58	11,22	9,24	9,64	10,23	11,28
18:1/18:1	1,09	0,54	0,79	1,1	0,6	1,13	0,63	0,5	0,96	1,01	0,86
18:0/18:2	3,89	4,93	5,81	6,92	5,63	4,49	4,78	2,93	4,12	7,02	6,42
18:0/18:1	2,69	2,75	3,3	3,32	2,16	1,67	1,7	1,7	1,83	2,98	2,56

Table 4.12: Fatty acids composition of chloroplastic PI class (in weight %) of *X. humilis* leaves subjected to gradual dehydration and rehydration treatment. The values highlighted in blue represent the plant during dehydration and the ones in red represent the plant during rehydration. Water content values are given as RWC in percentages at different sampling points.

CHL-PI	100%	84%	55%	46%	16%	0h (5%)	9h (48%)	12h (73%)	24h (92%)	36h (96%)	48h (96%)
15:0	8,5	10	8,3	8,3	7,3	5,5	6,1	7,3	5,6	5	5,9
16:0	40,3	38,6	31,9	31,3	30,2	26,6	31,2	35	32,9	26,9	33,4
16:1	1	1,2	1,4	0,8	1,4	2,3	0,7	1,3	3,7	1,1	1,7
17:0	1,6	1,9	2	1,8	2,1	1,8	2,3	2,1	1,9	2,8	1,8
18:0	7,2	6,5	10,5	11,2	10,5	10,2	9,1	7,3	8,3	10,6	10,9
18:1	9,4	8,9	9,1	8,7	6,8	7,5	6,2	6,6	7,9	10,8	7,7
18:2	13,6	15,4	13,6	13,6	12,7	11,1	12,7	9,8	11,6	16,8	14
18:3	17,1	15,9	21,1	22,3	26,4	31,9	28,7	27,9	26,3	23,6	22,9

4.3. Discussion

In this study, changes in the composition of chloroplast membrane lipids during dehydration and rehydration *of X. humilis* was investigated using LC-MS/MS in the MRM mode. Drought has been well known to severely reduce the photosynthetic capabilities of plants either by reducing carbon dioxide assimilation into the plant or resulting in damage of their chloroplast membranes (Liu *et al.,* 2005; Ashraf and Harris, 2013). Changes in the chloroplast membrane lipids have been reported during water loss in many plants including cotton and cow pea (Pham Thi *et al.,* 1990), *A. thaliana* (Ecotype Columbia: Gigon *et al.,* 2004), as well as in the resurrection plants *C. plantagineum* and *Lindernia brevidens* (Gasulla *et al*., 2013). However, information on the role that membrane lipids play during water deficit is scarce and contradictory; and depends on the plant species under investigation, as well as the degree of drought stress imposed. Cumulatively, the reported results suggest a decrease in membrane lipids as a common trend across plant species, resulting from a decrease in membrane quantity during drought stress. Previous studies using TEM have reported the controlled dismantling of thylakoid membranes in *Xerophyta* species during dehydration and re-assembly during rehydration (Tuba *et al.,* 1998; Farrant, 2000; Ingle *et al.,* 2008; Farrant *et al.,* 2015). However, knowledge of the composition and changes in molecular species and/or fatty acids within the chloroplast membrane lipids (i.e. phospholipids and galactolipids) during desiccation is not available for such species. To study these changes, intact chloroplasts were extracted from *X. humilis* leaves during drought stress treatment.

Our TEM studies confirmed previously reported changes in chloroplast internal structure during dehydration and rehydration of *X. humilis* (Figure 4.3). In particular, it was apparent that dismantling of thylakoid membranes during dehydration was accompanied by increased evidence of plastoglobuli, which was reversed on rehydration. The relationship between plastoglobuli and the thylakoid membranes has been implied in several studies (reviewed in Austin II *et al.,* 2006). Increased numbers of plastoglobuli in chloroplasts has been reported in plants exposed to various environmental stresses such as high CO_2 concentrations (Sallas *et al.,* 2003); high

salt concentration (Sam *et al.,* 2003); microgravity growth conditions (Kochubey *et al.,* 2004), as well as drought (Munne-Bosch and Alegre, 2004). A variety of lipidic compounds have been found contained in the isolated plastoglobuli fractions and include, among others, MGDG, DGDG, free fatty acids, carotenoids, chlorophylls, triacylglycerols, proteins as well as enzymes (Kaup *et al.,* 2002; Austin II *et al.,* 2006). However, the precise role of plastoglobuli still remains unclear, but their accumulation and increase in size during thylakoid membrane dismantling, and their subsequent reduction in number and size upon thylakoid re-organisation, has led to the speculation that they may be temporary storage bodies for thylakoid lipid metabolites. We propose that they play this role in *X. humilis*; the breakdown products of thylakoid disassembly during dehydration being stored for re-use in re-assembly thereof during rehydration.

In fully hydrated tissues, our data showed that the chloroplast membrane lipid composition comprised of significant amounts of unsaturated molecular species, such as 18:3/18:3-MGDG (Table 4.1), which is due to considerable amounts of linolenic acid (18:3; Table 4.2). Higher amounts of MGDG associated linolenic acid has been previously reported in the chloroplast membrane of *Vigna unguiculata* which is relatively tolerant to drought stress (Pham Thi *et al.,* 1990); and in the desiccation tolerant resurrection plants *C. plantagineum* and *L. brevidens* (Gasulla *et al.,* 2013). During dehydration of *X. humilis*, there were no significant changes in DGDG and MGDG molecular species 18:3/18:3 and 18:2/18:2; while the levels of 16:0/18:2 and 16:0/18:3 decreased. The maintenance of 18:3/18:3 and 18:2/18:2 molecular species during dehydration may suggest a better protection of 18:2 and 18:3 fatty acids against lipid peroxidation in *X. humilis*, since unsaturated fatty acids are susceptible to lipid peroxidation (Liu and Huang, 2004). Furthermore, it has been shown that unsaturated fatty acids protect the photosynthetic acitivities (Laskay and Lehoczki, 1986; Routaboul *et al.,* 2000), however the mechanisms involved is not clearly elucidated. and this protection may be due to the activation of NADPH oxidase by PUFA (Elmayan T and Simon-Plas, 2007). The decrease in saturated molecular species such as 15:0/16:0 and 16:0/16:0 during dehydration, may indicate accelerated palmitic acid (16:0) catabolism in *X. humilis.* Upon rehydration, an increase in both 18:3 and 18:2 fatty acids were observed within MGDG, which exceeded the control levels after 48hr post re-watering. This may suggest increased fatty acyl desaturases activity, as the

enzyme is responsible for unsaturated fatty acid synthesis (Uttaro, 2006). PG is the only predominant phospholipid found in the thylakoid membranes (Hagio *et al.,* 2002), directly involved with the activities of PS I (Jordan et al., 2001) and PS II (Hagio et al., 2000). During dehydration, a decrease in saturated (16:0/16:0-PG) and mono-unsaturated (16:0/16:1-PG) molecular species, and an increase in poly-unsaturated molecular species such as 18:3/18:3-PG and 18:2/18:3-PG was observed in *X. humilis*. This may be due to increased activities of *FAD* desaturases (Lou *et al.,* 2014), which facilitates the biosynthesis of unsaturated fatty acids to maintain membrane stability during drought (Gigon *et al.,* 2004; Zhao *et al*., 2011; Zhong *et al.,* 2011), and cold adaptation (Yurchenko *et al*., 2014; Liu *et al.,* 2015). Similar trends have been reported in *Telfairia occidentalis* seeds maintained at higher temperatures, which also had increased accumulation of polyunsaturated fatty acids (Nkang *et al.,* 2003). Furthermore, tolerance to cold stress has also been associated with the increased levels of polyunsaturated fatty acids in the chloroplast membranes (Iba, 2002). Our data also revealed the presence of unusual chloroplastic lipid such as PE, PC and PI. The PC and PI lipids were detected during dehydration and rehydration treatments, whereas the PE signals were detected only when the plant was fully dehydrated and upon early rehydration. The presence of these unusual chloroplastic lipids may either suggest chloroplast contamination by other cellular organelles or the involvements of these lipids during membrane protection. However, PC and PI being bilayer lipids have been previously reported to be confined in the outer chloroplast membrane of various plants such as spinach, pea and *A. thaliana* (Cline *et al.,* 1981; Block *et al.,* 1983; Okazaki *et al.,* 2015). It is likely that this is true for X. *humilis* and thus one would expect their presence to be evident throughout the dehydration and rehydration process, since the outer chloroplastic envelope is maintained as shown by transmission electron microscopy (Figure 4.3 and 4.4). The brief appearance of PE in chloroplasts from fully dehydrated tissues and its retention through the early stages of rehydration, if real, is unique and intriguing. The formation of stromules (i.e. stroma filled tubules), in plants under temperature, pathogenic and water deficit stresses have been reported (Gary *et al.,* 2012; Caplan *et al.,* 2015; Xiao *et al.,* 2012), suggesting their potential role in stress signalling (Schattat *et al.,* 2011). These structures extend from the main plastidic body to the cytosol (Kohler et al., 1997). During plant response to environmental stimuli, aggregation of stromules with other cellular organelles such

as ER has been also been documented, providing evidence of their role as conduits for exchange of metabolites or genetic information (Ho and Theg, 2016). Thus, the presence of PE in dehydrated and rehydrating leaves maybe due to the close association of these stromules with other cellular organelles, may suggest the involvement of PE during chloroplast regeneration. Similarly, PE, a non-bilayer forming lipid, has also been reported to be involved with protection of photosynthesis during chemical stress such as application of triazine (Pillai and St. John, 1981). Furthermore, in *Rhodobacter sphaeroides,* the efficient formation of photosynthetic membranes and light capturing complexes requires the presence of PE (Kim *et al.,* 2007). Although the exact mechanism of action is not well understood, the presence of PE in dry tissues and upon rehydration can therefore suggests its involvement in reformation of the thylakoid membranes and recovery of photosynthetic efficiency upon rehydration. It has been shown that the interaction of PE with LacY facilitates the proper folding of LacY, needed for proper cell functioning (Bogdanov and Dowhan, 1999). To the best of our knowledge; this is the first study in which these lipids are reported in chloroplasts of a resurrection plant. Dehydration was associated with increase in unsaturated molecular species in both PC and PI, and rehydration associated with the maintenance of these unsaturated molecular species in all lipid classes (i.e. PE, PI and PC). This is important since unsaturated fatty acids are known to prevent membrane fusion of adjacent membranes, due to their non-linear packing which could results in irreversible damage to the cell membrane (Crowe *et al.,* 1992).

In conclusion, the data presented here showed that chloroplast membrane lipids are highly unsaturated in fully hydrated leaves, and are maintained at higher levels of unsaturation during dehydration and rehydration. The accumulation of unsaturated fatty acids has also been reported in plants subjected to both high and low temperatures; and may represent a common mechanism used by plants to adapt to various environmental stresses. The minor changes in the levels of unsaturated fatty acids, especially 18:3 and 18:2, have been reported in ozone-treated *A. thaliana* leaves (Yaeno *et al*., 2004). The authors further revealed that 18:3 fatty acid stimulated the activity of NADPH oxidase in ozone-treated *A. thaliana* leaves. Therefore, the presence of 18:3 in higher amounts may suggest the involvement of this fatty acid in the protection of photosynthetic apparatus during dehydration and rehydration.

Furthermore, the presence of poly-unsaturated MGDG and PE containing molecular species in the chloroplast suggests the involvement of the non-bilayer lipids in tolerance of desiccation. The presence of PE may introduce a negative curvature stress, due to the nature of lipid-packaging which facilitates adjacent membrane fusion, as well as the proper functioning of peripheral membrane (Holthuis and Menon, 2014). However, the presence of PE, PI and PC could represent contamination of the chloroplast suspension with other cellular organelles, which is one limitation of this study. Furthermore, if so, the degree of contamination cannot be determined, since MRM is only able to detect the molecular species of the lipids, but not their quantity. Future studies should include more rigorous testing for possible cellular contaminants in chloroplast isolates. However, the results presented in this chapter may allow researchers to speculate what the role of the individual molecular species and/or fatty acids in preservation of chloroplast structure during desiccation and in preparation for the re-assembly of fully functional chloroplasts on rehydration.

Chapter 5:

General Conclusion and Future Perspectives

Lipids, being the main structural components of bio-membranes, play important roles in the structure and function of plant cells. Changes in lipid molecular species in leaf tissues during dehydration and rehydration has only been documented for a few HDT species (Quartacci *et al*., 2002; Oliver *et al.,* 2011b; Gasulla *et al.,* 2013). This study expands on our knowledge of the role of molecular species and/or fatty acids during desiccation tolerance in the PDT species, *X. humilis*. It revealed that, dehydration is associated with significant increases in levels of unsaturated fatty acids in both roots and leaves. The same trend was reported in the freezing tolerant Arabidopsis (Tarazona *et al.,* 2015) and in orthodox seeds (Liu *et al.,* 2006). Therefore, it can be suggested that this increase in unsaturated levels in *X. humilis* has an important role in vegetative desiccation tolerance in this species. While not a trivial exercise, increasing the ability of desiccation sensitive plants to form unsaturated fatty acids in response to water deficit stress may facilitate increased tolerance of water loss. Furthermore, the presence of unusual fatty acids, and changes in their levels during dehydration suggests *X. humilis* employs unique pathways to survive desiccation stress. These unique pathways, if further investigated, could be used to improve drought tolerance in crop plants.

Desiccation of drought sensitive plants is associated with ROS damage of the chloroplast membranes (Halliwell, 1987), and has also been shown to decrease the levels of lipid unsaturation (Zhong *et al.,* 2011). Therefore, within the *X. humilis* chloroplast, maintenance and/or increase in chloroplast membrane lipid unsaturation during dehydration might prevent damage to outer chloroplast membranes and prevent further lipid oxidation. Poly-unsaturated fatty acids such as 18:3 in the chloroplast membranes have been shown to maintain the fluid-state of membranes, which is necessary for the optimum functionality of the chloroplast. This is true for *B. hygroscopica* tissues (Navari-izzo et al., 2000), where membrane fluidity decreased with an increase in fatty acid unsaturation levels during drying, and increased again with decreasing fatty acid unsaturation levels during re-watering. The authors

suggested that maintenance of membrane fluidity was necessary for plant membrane functioning in *B. hygroscopica* during desiccation.

The main ultrastructural observations of this study (Chapter 4) was that during dehydration of leaf tissues the unstacking and disappearance of the thylakoid membranes occurs, concomitantly with the appearance and an increase in size and numbers of plastoglobuli. This has led us to suggest that *X. humilis* stores metabolites required for their reformation during rehydration in the plastoglobuli. Consistent with this, is the disappearance of the plastoglobuli during thylakoid membrane re-organization upon rehydration. Furthermore, the chloroplast envelope was preserved during the dehydration/rehydration treatments, which is usually damaged in drought-sensitive plants (Gaurine *et al.,* 1986).

In summary, the above data showed that *X. humilis* maintains higher levels of unsaturated fatty acids such as 18:2 and 18:3, which are susceptible to lipid peroxidation, in both leaves and roots during drying, and decreases them during re-watering. This supports the finding that maintenance of membrane fluidity is essential for a plant's tolerance to desiccation, as well as inferring that *X. humilis* has mechanisms which limits this lipid peroxidation. The pathways involved in the protection of these highly unsaturated fatty acids in *X. humilis* could be provided by various antioxidant systems and/or presence of different sugars (*inter alia*) and requires further analysis. Furthermore, the reason for the presence of unusual fatty acids including, medium chain fatty acids such as 14:0 and VLCFAs, such as 20:0-, 22:0-, 24:0- and 26:0-fatty acids needs elucidation. Fatty acids with odd-numbered carbons were also detected. These unusual fatty acids fluctuated during dehydration and rehydration, also suggesting their potential role desiccation tolerance in *X. humilis*. Besides the study done by Narayanan *et al*. (2016), where odd-numbered fatty acids where found to be esterified to phosphoglycerolipids, this study is the only reported to date that shows the presence of these unusual fatty acids in vegetative plants. Their specific role in desiccation tolerance requires further investigation. The inability to quantify the individual glycerophospholipids of the bilayer during dehydration and rehydration was the major limitation of the study. In future, this quantification needs to

be done, in order to obtain a complete picture of the roles of each individual glycerophospholipids during acquisition of desiccation tolerance.

References

Abdi H., Williams L.J. (2010). Principal component analysis. *Overview*.2(4): 433-459.

Allakhverdiev S.I., Kinoshita M., Inaba M., Suzuki I., Murata N. (2001). Unsaturated fatty acids in membrane lipids protect the photosynthetic machinery against salt-induced damage in *Synechococcus. American Society of Plant Physiologists*. 125(4): 1842-1853.

Akıncı Ş. and Lösel D.M. (2012). Plant water-stress response mechanisms, water stress," I. Md. and M. Rahman, Eds., Water Stress, Intech Europe. Pp: 15-42.

Allwood J. W., Goodacre R. (2010). An introduction to liquid chromatography–mass spectrometry instrumentation applied in plant metabolomic analyses. *Phytochem Anal.* 21: 33–47.

Alpert P. (2006). The limits and frontiers of desiccation tolerant life. *Integrative and Comparative Biology*. 45: 685-695.

Anjum S.A., Xie X., Wang L., Saleem M.F., Man C., Lei W. (2011). Morphological, physiological and biochemical responses of plants to drought stress. *Afr. J. Agr. Res*. 6: 2026-2032.

Austin II J.R., Frost E., Vidi P-A., Kessler F., Staehelin L.A. (2006). Plastoglobules are lipoprotein subcompartments of the chloroplast that are permanently coupled to thylakoid membranes and contain biosynthetic enzymes. *The Plant Cell*. 18: 1693–1703.

Ashraf M., Harris P.J.C. (2013). Photosynthesis under stressful environments: An overview. *PHOTOSYNTHETICA*. 51 (2): 163-190.

Aslam M., Zamir M.S.I., Afzal I., Yaseen M., Mubeen M., Shoaib A. (2013). Drought stress, its effect on maize production and development of drought tolerance through potassium application. *Cercetări Agronomice în Moldova.* 2(154): 99-114.

Ataei S., Braun V., Challabathula D., Bartels D. (2016). Differences in LEA-like 11-24 gene expression in desiccation tolerant and sensitive species of *Linderniaceae* are due to variations in gene promoter sequences. *Functional Plant Biology*. 43(7): 695-708.

Awai K., Maréchal E., Block M. A., Brun D., Masuda T., Shimada H., Takamiya K., Ohta H., Joyard J. (2001). Two types of MGDG synthase genes, found widely in both 16:3 and 18:3 plants, differentially mediate galactolipid syntheses in photosynthetic and nonphotosynthetic tissues in *Arabidopsis thaliana*. *Proc. Natl. Acad. Sci. U.S.A.* 98: 10960–10965.

Bach L, Michaelson LV, Haslam R, Bellec Y, Gissot L, et al. (2008). The very long-chain hydroxy fatty acyl-CoA dehydratase PASTICCINO2 is essential and limiting for plant development*. Proc Natl Acad Sci U S A.* 105: 14727–14731.

Badami R.C., Patil K.B. (1980). Structure and occurrence of unusual fatty acids in minor seed oils.Prog. *Lipid Res*. 19: 119–153.

Bahama R.C., Patil K.B. (1980). Structure and occurrence of unsual fatty acids in minor seed oils. *Prog Lipid Res*. 19(3-4): 119-53.

Bailey D.M., Davies B., Young I.S., Jackson M.J., Davison G.W., Isaacson R., Richardson R.S. (2003). EPR spectroscopic detection of free radical outflow from an isolated muscle bed in exercising humans. *Journal of Applied Physiology*. 94: 1714-1718.

Bailly, C., Leymarie, J., Lehner, A., Rousseau S., Come, D., Corbineau F. (2004). Catalase activity and expression in developing sunflower seeds as related to drying. *Journal of experimental Botany*. 55: 475-483.

Bajji M., Lutts S., Kinet J.M. (2001). Water deficit effects on solute contribution to osmotic adjustment as a function of leaf ageing in three durum wheat (*Triticum durum Desf*.) cultivars performing differently in arid conditions. *Plant Science*. 160(4): 669-681.

Bartels D., Salamina F. (2001). Desiccation tolerance in the resurrection plant *Craterostigma plantagineum.* A contribution to the study of drought tolerance at the molecular level*. Plant Physiol*. 127(4): 1346-53.

Barak S., Farrant J.M. (2016). Extremophyte adaptations to salt and water stress. *Functional Plant Biology.* 43(7): v-x.

Bazinet R.P., Layé S. (2014). Polyunsaturated fatty acids and their metabolites in brain function and disease. *Natural Review in Neuroscience.* 15(12): 771-85.

Beckett M., Loreto F., Velikova V., Brunetti C., Di Ferdinando M., Tattini M., Calfapietra C., Farrant J.M. (2012). Photosynthetic limitations and volatile and non-volatile isoprenoids in the poikilochlorophyllous resurrection plant *Xerophyta humilis* during dehydration and rehydration. *Plant Cell Environ*. 35: 2061–2074.

Block M.A., Dome A.J., Joyard J., Douce R. (1983). Preparation and characterization of membrane fractions enriched in outer and inner envelope membranes from spinach chloroplasts. II. Biochemical characterization*. J. Biol. Chem*. 258: 13281-13286.

Bogdanov M., Umeda M, Dowhan W. (1999). Phospholipid-assisted refolding of an integral membrane protein.Minimum structural features for phosphatidylethanolamine to act as a molecular chaperone. *J.Biol.Chem.* 274: 12339-12345.

Boundless (2016). “The Plasma Membrane and the Cytoplasm.” *Boundless Biology.* Retrieved 25 Sep. 2016

from https://www.boundless.com/biology/textbooks/boundless-biology-textbook/cell-structure-4/eukaryotic-cells-60/the-plasma-membrane-and-the-cytoplasm-314-11447/

Bovet L., Müller M.O., Siegenthaler P.A. (2001). Three distinct lipid kinase activities are present in spinach chloroplast envelope membranes: Phosphatidylinositol phosphorylation is sensitive to wortmannin and not dependent on chloroplast ATP. *Biochem. Biophys. Res. Commun*. 289: 269–275.

Berjak P. (2006). Unifying perspectives of some mechanism basic to desiccation tolerance across life forms. *Seed Science Research.* 16: 1-15.

Bernacchia G., Salamini F., Bartels D, (1996). Molecular characterization of the rehydration process in the resurrection plant *Craterostigma plantagineum*. *Plant physiology*. 111: 1043-1050.

Brügger B. (2014). Lipidomics: analysis of the lipid composition of cells and subcellular organelles by electrospray ionization mass spectrometry. *Annu Rev Biochem.* 83:79-98.

Bryant G., Koster K.L., Wolfe J. (2001). Membrane behaviour in seeds and other systems at low water content: the various effects of solutes*. Seed Science Research*. 11: 17–25.

Canniffe D.P., Chidgey J.W., Hunter C.N. (2014). Elucidation of the preferred routes of C8-vinyl reduction in chlorophyll and bacteriochlorophyll biosynthesis. *Biochem J*. 462(3): 433-40.

Caplan J.L., Kumar A.S., Park E., Padmanabhan M.S., Hoban K., Modla S. (2015). Chloroplast stromules function during innate immunity. *Developemental Cell*. 34(1): 45-57.

Caverzan A., Casassola A., Brammer S. (2016). Antioxidant responses of wheat plants under stress. *Genetics and Molecular Biology*. 39(1): 1-6.

Chace D.H. (2001). Mass spectrometry in the clinical laboratory. *Chem Rev*. 101: 445–477.

Chambers P., Moron V., Okoola R., Philippon N., Gitau W. (2009). Components of rainy seasons' variability in equatorial East Africa: onset, cessation, and rainfall frequency and intensity. *Theor. Appl. Climatol.* 98: 237-240.

Charuvi D., Nero R., Shimoni E., Naveh L., Zia A., Adam Z. (2015). Photoprotection conferred by changes in photosynthetic protein levels and organization during dehydration of a homoiochlorophyllous resurrection plant. *Plant Physiology*. 167: 1554-1565.

Christ B., Egert A., Süssenbacher I., Kräutler B., Bartels D., Peters S., Hörtensteiner S. (2014). Water deficit induces chlorophyll degradation via the 'PAO/phyllobilin' pathway in leaves of homoio- (*Craterostigma pumilum*) and

poikilochlorophyllous (*Xerophyta viscosa*) resurrection plants. *Plant Cell Environ***.** 37: 2521–2531.

Collett H., Butowt R., Smith J., Farrant J., Illing N. (2003). Photosynthetic genes are differentially transcribed during the dehydration-rehydration cycle in the resurrection plant, *Xerophyta humilis*. *Journal of Experimental Botany*. 54: 2593–2595.

Clover J. (2003). Food security in sub-Saharan Africa. *African security review*. 12(1): 1-15.

Cline K., Andrews J., Mersey B., Newcomb E.H., Keegstra K. (1981). Separation and characterization of inner and outer envelope membranes of pea chloroplasts. *Proc. Natl. Acad. Sci. USA.* 78: 3595–3599.

Crowe J.H., Crowe L.M. (1992b). Anhydrobiosis: a strategy for survival. *Adv. Space Res*. 12: 239-247.

Cyril J., Powell G.L., Duncan R.R., Baird W.V. (2002). Changes in membrane polar lipid fatty acids of seashore paspalum in response to low temperature exposure. *Crop Science*. 42: 2031-2037.

Dace H., Sherwin H.W., Illing N., Farrant J.M. (1998). Use of metabolic inhibitors to elucidate mechanism of recovery from dessication stress in the resurrection plant *Xerophyta humilis*. *Plant Growth Regulation*. 24: 171–177.

Dace H. (2014). The metabolomics of desiccation tolerance in *Xerophyta humilis*. Thesis, University of Cape Town.

Djafi N., Vergnolle C., Cantrel C., Wietrzyñski W., Delage E., Cochet F., et al. (2013). The Arabidopsis DREB2 genetic pathway is constitutively repressed by basal phosphoinositide-dependent phospholipase C coupled to diacylglycerol kinase. *Front. Plant Sci*. 4: 307.

Dashty M. (2014). A Quick Look at Biochemistry: Lipid Metabolism. *Journal of Diabetes Metabolism*. 2: 324.

Dinakar C., Djilianov D., Bartels D. (2012). Photosynthesis in desiccation-tolerant plants: energy metabolism and antioxidative stress defense. *Plant Science*. 182: 29-41.

Dinakar C., Bartels D. (2013). Desiccation tolerance in resurrection plants: new insights from transcriptome, proteome, and metabolome analysis. *Plant Science*. 4(482): 1-14.

Djafi N., Vergnolle C., Cantrel C., Wietrzyñski W., Delage E., Cochet F., et al. (2013). The Arabidopsis DREB2 genetic pathway is constitutively repressed by basal phosphoinositide-dependent phospholipase C coupled to diacylglycerol kinase. *Front. Plant Sci*. 4: 307.

Djilianov D., Genova G., Parvanova D., Zapryanova N., Konstantinova T., Atanassov A. (2005). In vitro culture of the resurrection plant *Haberlea rhodopensis. Plant Cell Tissue and Organ Culture*. 80: 115–118.

Dörmann P., Benning, C. (2002). Galactolipids rule in seed plants*. Trends Plant Sci*. 7**:** 112–118.

Dowhan W., Bogdanov M. (2002). In: Biochemistry of Lipids, Lipoproteins and Membranes. Vance DE, Vance JE, editors.36: 1–35.

Dubots E., Audry M., Yamaryo Y., Bastien O., Ohta H., Breton C., Marechal E., Block M.A. (2010) .Activation of the chloroplast monogalactosyldiacylglycerol synthase MGD1 by phosphatidic acid and phosphatidylglycerol. *J Biol Chem.* 285: 6003–6011.

Dure L., Crouch M., Harada J.J., Ho T., Mundy J., Quatrano R.S., Thomas T.L., Sung Z.R. (1989). Common amino acid sequence domains among the LEA proteins of higher plants. *Plant Molecular Biology.* 12: 475–486.

Elstner E.F. (1982). Oxygen activation and oxygen toxicity. *Annual Review in Plant Physiology*. 33: 75-96.

Escriba P.V., Gonzalez-Ros J.M., Goni F.M., Kinnunen P.K., Vigh L., Sanchez-Magraner L., Fernandez A.M., Busquets X., Horvath I., Barcelo-Coblijn G. (2008). Membranes: a meeting point for lipids, proteins and therapies*. J Cell Mol Med*. 12: 829-875.

Essaghi S., Hachmi M., Yessef M., Dehhaoi M. (2016). Leaf shrinkage: a predictive indicator of the potential variation of the surface area-volume ratio according to the leaf moisture content. *SpringerPlus*. 5: 1229

Evans J.R., Kaldenhoff R., Genty B., Terashima I. (2009). Resistances along the CO_2 diffusion pathway inside leaves. *J. EXP. Bot.* 60: 2235-2248.

Eyster K.M. (2007). The membrane and lipids as integral participants in signal transduction: lipid signal transduction for the non-lipid biochemist. *Adv Physiol Educ*. 31: 5–16.

Fahy E., Subramaniam S., Brown H.A., Glass C.K., Merrill A.H. Jr, Murphy R.C., Raetz C.R., Russell D.W., Seyama Y., Shaw W., Shimizu T., Spener F., van Meer G.,VanNieuwenhze M.S., White S.H., Witztum J.L., Dennis E.A. (2005). A comprehensive classification system for lipids. *Journal of Lipid Research*. 46(5): 839-61.

Farooq M., Wahid, A., N. Kobayashi N., Fujita D., Basra S.M.A. (2009). Plant drought stress: effects, mechanisms and management. *Agronomy for Sustainable Development*. 29 (1): 185-212.

Farrant J.M. (2000). Comparison of mechanisms of desiccation tolerance among three angiosperm resurrection plants. *Plant Ecology.* 151: 29–39.

Farrant J.M., Willigen C.V., Loffell D.A., Bartsch S., Whittaker A. (2003). An investigation into the role of light during desiccation of three angiosperm resurrection plants. *Plant, Cell and Environment.* 26: 1275–1286.

Farrant J.M., Brandt W., Lindsey G.G. (2007). An overview of Mechanisms of Desiccation Tolerance in Selected Angiosperm Resurrection Plants. *Plant Stress.* 1(1): 72-84.

Farrant J.M, Lehner A., Cooper K., Wisedel S. (2009). Desiccation tolerance in the vegetation tissues of the fern *Morhia caffrorum* is seasonally regulated. *The Plant Journal.* 57: 65-79.

Farrant J.M., Cooper K., Nell H. (2012). Desiccation tolerance. *Plant stress physiology*. Pp: 238–265.

Farrant M.J., Cooper K., Hilgart A., Abdalla K.O., Bentley J., Thomson J.A., Dace H.J.W., Peton N., Mundree S.G., Rafudeen M.S. (2015). A molecular physiological review of vegetative desiccation tolerant in the resurrection plant *Xerophyta viscosa* (Baker). *Planta*. 244 (2): 407-426.

Farrant M.J et al., (2017). A footprint of desiccation tolerance in the genome of *Xerophyta viscosa. Nature Plants*. 3:17038

Foyer C.H., Lelandais M., Kunert K.J. (1994). Oxidative stress in plants. *Physiology Plant*. 92: 696–717.

Furt F., Simon-Plas F., Mongrand S. (2011). Lipids of the plant plasma membrane. In: Murphy AS, Peer W, Shulz B (eds) The plant plasmamembrane. Springer, Berlin Heidelberg. Pp: 3–30.

Gaff D.F. (1971). Desiccation tolerant flowering plants in Southern Africa. *Science*. 174: 1033-1034.

Gaff D.F., Blomstedt C.K., Neale A.D., Le T.N., Hamill J.D., Ghasempour H.R. (2009). *Sporobolus stapfianus*, a model desiccation-tolerant grass. *Functional Plant Biology.* 36: 589–599.

Gaff D.F., Oliver M. (2013). The evolution of desiccation tolerance in angiosperm plants: a rare yet common phenomenon. *Functional Plant Biology*. 40(4). 315-328.

Gary J.C., Hansan M.R., Shaw D.J., Graham K., Dale R., Smallman P. (2012). Plastid stromules are induced by stress treatment acting through abscisic acid. *Plant*. 69(3): 387-98

Gasulla F., vom Dorp K., Dombrink I., Zanhringer U., Gisch N., Dormann P. (2013). The role of lipid metabolism in the acquisition of desiccation tolerance in *Craterostigma plantagineum:* a comparative approach. *Plant Journal*. 75(5): 726-741.

Gechev T.S., Benina M., Obata T., Tohge T., Sujeeth N., Minkov I., Hille J., Temanni M.R., Marriott A.S., Bergström E., Thomas-Oates J., Antonio C., Mueller-Roeber B., Schippers J.H., Fernie A.R., Toneva V. (2013). Molecular mechanisms of desiccation tolerance in the resurrection glacial relic *Haberlea rhodopensis*. *Cell and Molecular Life Sciences*. 70(4): 689-709.

Georgieva K., Ivanova A., Doncheva S., Petkova S., Stefano D., Peli E., Tuba Z (2011). Fatty acid content during reconstitution of the photosynthetic apparatus in the air-dried leaves of *Xerophyta scabrida* after rehydration. *Biologia Plantarum*. Pp: 1-5.

Gigon A., Matos A-R., Laffray D., Zuily-Fodil Y., Pham-Thi. (2004). Effects of drought stress on lipid metabolism in the leaves of *Arabidopsis thaliana* (Ecotype Columbia). *Annuls of Botany*. 94: 345-351.

Gimbel K.F., Felsmann K., Baudis M., Puhlmann H., Gessler A., Bruelheide H., Kayler Z., Ellerbrock R.H., Ulrich A., Welk E., Weiler M. (2015). Drought in forest understory ecosystems- a novel rainfall reduction experiment. *Biogeosciences*. 12: 961-975.

Gounaris K., Barber J., Harwood J.L. (1986). The thylakoid membranes of higher plant chloroplasts. *Biochemical Journal*. 237: 313–326.

Griffiths C.A., Gaff D.F., Neale A.D. (2014). Drying without senescence in resurrection plants. *Front Plant Sci*. 5: 36.

Gross R.W., Han X. (2011). Lipidomics at the Interface of Structure and Function in Systems Biology. *Chem Biol.* 18(3): 284–291.

Gürsoy M., Balkan A., Ulukan H. (2012). Ecophysiological responses to stresses in plants: A general approach. *Pak J Biol Sci* 15: 506–516.

Hagio M., Sakurai I., Sato S., Kato T., Tabata S., Wada H. (2002). Phosphatidylglycerol is essential for the development of thylakoid membranes in *Arabidopsis thaliana*. *Plant Cell Physiol.* 43: 1456–1464.

Halliwell B., Gutteridge J.M.C. (1999). Free radicals in biology and medicine, 3rd edn. Oxford: Clarendon Press.

Hammond-Kosack K.E., Jones J.D.G. (2000). Response to plant pathogens. In: Buchannan B,Gruissem W, Jones R , editors. Biochemistry and molecular biology of plants. *American Society of Plant Physiologists*. Pp: 1102-1157.

Han X. (2001). Quantitative analysis and molecular species fingerprinting of triacylglyceride molecular species directly from lipid extracts of biological samples by electronspray ionization tanderm mass spectrometry. *Anal Biochem*. 295: 88-100.

Han X.L., Gross R.W. (2005). Shotgun lipidomics: multidimensional MS analysis of cellular lipidomics. *Expert Revie in Proteomics*. 2: 253-264.

Han X., Rozen S., Boyle S., Hellegers C., Cheng H., Burke J.R., Welsh-Bohmer K.A., Doraiswamy P.M., Kaddurah-Daouk R. (2011). Metabolomics in early alzheimer's disease: Identification of altered plasma sphingolipidome using shotgun lipidomics. *PLoS ONE*. 6(7): e21643.

Han X., Yang K., Groos R.W. (2012). Multi-dimensional mass spectrometry-based shotgun lipidomics and novel strategies for lipidomic analysis. *Mass Spectrometry Review*. 31: 134-78.

Hannun Y.A., Obeid L.M. (2008). Principles of bioactive lipid signalling: lessons from sphingolipids. *Nature Reviews Molecular Cell Biology*. 9(2): 139-50.

Hardy M., Dziba L., Kilian W., Tolmy J. (2011). Rainfed farming system in south Africa. *Springer Science and Business*. Pp: 395-432.

Harrathi J., Hosni K., Karray-Bouraoni N., Attia H., Marzouk B., Magne C., Lachaal M. (2012). Effect of salt stress on growth, fatty acids and essential oils in sanfflower (*Carthamus tinctorius* L.). *Acta Physiol Plant*. 34(1): 129-137.

Hincha D.K., Hagemann M. (2004). Stabilization of model membranes during drying by compatible solutes involved in the stress tolerance of plants and microorganisms. *Biochemical* Journal. 383(2): 277-83.

Hoekstra F.A., Golovina E.A., Buitink J. (2001). Mechanisms of plant desiccation tolerance. *Trends in Plant Science.* 6(9): 431-8.

Höfler K., Migsch H., Rottenburg W. (1941). Über die Austrocknungresistenz landwirtschaftlicherKulturpflanzen. *Forschungsdienst. Organ Deut. Landwirtschaftswiss.* 12: 50–61.

Ho¨ lzl G., Do¨ rmann P. (2007). Structure and function of glycoglycerolipids in plants and bacteria. Prog. *Lipid Res.* 46: 225–243.

Holthuis J.C.M., Menon A.K. (2014). Lipid landscapes and pipelines in membrane homeostasis. *Nature.* 510: 48–57.

Hopfgartner G., Varesio E., Tschappat V., Grivet C., Bourgogne E., Leuthold L.A. (2004). Triple quadrupole linear ion trap mass spectrometer for the analysis of small molecules and macromolecules. *Journal of Mass Spectrometry*. 39: 845-855.

Horl G., Wagner A., Cole L.K., Malli R., Reicher H., Kotzbeck P., Ko¨ feler H., Ho¨ fler G., Frank S., Bogner-Strauss J.G., Sattler W., Vance D.E., Steyrer E. (2011). Sequential synthesis and methylation of phosphatidylethanolamine promote lipid

droplet biosynthesis and stability in tissue culture and in vivo. *The Journal of Biological Chemistry*. 286: 17338–17350.

Hou J., Acharya L., Zhu D., Chen J. (2016). An overview of bioinformatics methods for modeling biological pathways in yeast. *Brief Functional Genomics.* 15(2): 95-108.

Hsiao T.C. (1973). Plant Responses to Water Stress. *Annual Review of Plant Physiology*. 24(1): 519-570.

Hsu F-F., Turk J., Thukkani AK., Messner M.C., Wildsmith K.R., Ford D.A. (2003). Characterization of alkylacyl, alk-1-enylacyl and lyso subclasses of glycerophosphocholine by tandem quadrupole mass spectrometry with electrospray ionization. *J Mass Spectrom.* 38: 752–763.

Hsu C.C., Chen C.L., Chen J.J., Sung J.M. (2003). Accelerated aging-enhanced lipid peroxidation in bitter gourd seeds and effects of priming and hot water soaking treatments. *Sci Hortic-Amsterdam*. 98: 201-212.

Ingle R.A., Collett H., Cooper K., Takahashi Y., Farrant J.M., Illing N. (2008). Chloroplast biogenesis during rehydration of the resurrection plant *Xerophyta humilis*: parallels to the etioplast-chloroplast transition. *Plant Cell Environ*. 31: 1813–1824.

Ingram J., Bartels D. (1996). The molecular basis of dehydration tolerance in plants. *Plant Molecular Biology*. 47: 377–403.

Islam S., Takagi S. (2010). Co-localization of mitochondria with chloroplasts is a light-dependent reversible response. *Plant Signal Behav.* 5: 146–152.

Jiang X., Cheng H., Yang K., Gross R.W., Han X. (2007). Alkaline methanolysis of lipid extracts extends shotgun lipidomics analyses to the low abundance regime of cellular sphingolipids. *Anal Biochem*. 371: 135–145.

Joyard J., Teyssier E., MieÁge C., Seigneurin-Berny D., MareÂ chal E., Block M., Dorne A.-J., Rolland N., Ajlani G. and Douce R. (1998). The biochemical machinery of plastid envelope membranes. *Plant Physiol*. 118: 715-723.

Jorge T. F., Rodrigues J. A., Caldana C., Schmidt R., van Dongen J. T., Thomas-Oates J., et al. (2015). Mass spectrometry-based plant metabolomics: metabolite responses to abiotic stress. *Mass Spectrom. Rev.* 35: 620–649.

Jordan P., Fromme P., Witt H.T., Klukas O., Saenger W., Krauß N. (2001). Three-dimensional structure of cyanobacterial photosystem I at 2.5 Å resolution. *Nature.* 411: 909–917.

Jouhet J., Mare´ chal E., Baldan B., Bligny R., Joyard J., Block M.A. (2004). Phosphate deprivation induces transfer of DGDG galactolipid from chloroplast to mitochondria. *J. Cell Biol*. 167: 863–874.

Jouhet J. (2013). Importance of the hexagonal lipid phase in biological membrane organization. *Front Plant Sci.* 4(494): 1-15.

Kaup M.T., Froese C.D., Thompson J.E. (2002). A role for diacylglycerol acyltransferase during leaf senescence. *Plant Physiol*. 129: 1616–1626.

Karupaiah T., Sundram K. (2007). Effects of stereospecific positioning of fatty acids in triacylglycerol structures in native and randomized fats: a review of their nutritional implication. *Nutrition and Metabolism*. 4:16.

Kelly A.A., Dörmann P. **(2002).** *DGD2*, an *Arabidopsis* gene encoding a UDP-galactose-dependent digalactosyldiacylglycerol synthase is expressed during growth under phosphate-limiting conditions. *J. Biol. Chem*. 277**:** 1166–1173.

Kelly A.A., Froehlich J.E., Do¨rmann P. (2003). Disruption of the two digalactosyldiacylglycerol synthase genes DGD1 and DGD2 in Arabidopsis reveals the existence of an additional enzyme of galactolipid synthesis. *Plant Cell*. 15: 2694–2706.

Kim Y-J., Ko I-J., Lee J-M., Kang H-Y., Kim Y.M., Kaplan S., Oh J-I. (2007). Dominant Role of the cbb3 Oxidase in Regulation of Photosynthesis Gene Expression through the PrrBA System in *Rhodobacter sphaeroides* 2.4.1*. Journal Bacteriology*. Pp: 5617–5625.

Klose C., Ejsing C.S., Garcia-Saez A.J., Kaiser H.J., Sampaio J.L., Surma M.A., Shevchenko A., Schwille P., Simons K. (2010). Yeast lipids can phase-separate into micrometer-scale membrane domains. *J Biol Chem*. 285: 30224–30232.

Kobayashi K., Awai K., Takamiya K., Ohta H. (2004). Arabidopsis type B monogalactosyldiacylglycerol synthase genes are expressed during pollen tube growth and induced by phosphate starvation. *Plant Physiol*. 134: 640–648.

Kobayashi K., Kondo M., Fukuda H., Nishimura M., Ohta H. (2007). Galactolipid synthesis in chloroplast inner envelope is essential for proper thylakoid biogenesis, photosynthesis, and embryogenesis. *Proc. Natl Acad. Sci. USA.* 104: 17216–17221.

Kochubey S.M., Adamchuk N.I., Kordyum E.I., Guikema J.A. (2004). Microgravity affects the photosynthetic apparatus of Brassica rapa L. *Plant Biosyst*. 138: 1–9.

Kodama H., Hamada T., Horiguchi G., Nishimura M., Iba K. (1995). Fatty acid desaturation during chilling acclimation is one of the factors involved in conferring low-temperature tolerance to young tobacco leaves. *Plant Physiol.* 107: 1177-1185.

Kofeler H.C., Fauland A., Rechberger G.N., Trotzmuller M. (2012). Mass spectrometry based lipidomics: an overview of technological platforms. *Metabolites.* 2(1): 19-38.

Kohler R.H., Hanson M., Wildman S. (1997). Pictures in cell biology: Plastid interconnections imaged by fluorescence and phase contrast. *Trends in Cell Biology*. 7: 392.

Korfmacher W.A. (2005). Using Mass Spectrometry for Drug Metabolism Studies, ed Korfmacher WA (CRC Press, Boca Raton, FL), Pp: 1–34.

Knittelfelder O.L., Weberhofer B.P., Eichmann T.O., Kohlwein S.D., Rechberger G.N. (2014). A versatile ultra-high performance LC-MS method for lipid profiling. *J Chromatogr B: Analyt Technol Biomed Life Sci*. 951–952:119–128.

Kushnir M.M., Rockwood A.L., Roberts W.L., Yue B., Bergquist J., Meikle A.W. (2011). Liquid chromatography tandem mass spectrometry for analysis of steroids in clinical laboratories. *Clin Biochem*. 44: 77-88.

Kumar D., Sigh P., Yusuf M.A., Upadhyaya C.P., Roy S.D., Hohn T., Sarin N.B. (2003). The *Xerophyta viscosa* aldose reductase (ALDRXV4) confers enhanced drought and salinity tolerance to transgenic tobacco plants by scavenging methylglyoxal and reducing the membrane damage. *Molecular Biotechnology.* 54 (2): 292-303.

Kumiko Okazaki K., Miyagishima S-Y., Hajime Wada H. (2015). Phosphatidylinositol 4-Phosphate Negatively Regulates Chloroplast Division in Arabidopsis. *Plant Cell*. 27(3): 663–674.

Lang E.G.E., Mueller S.J., Hoernstein S.N.W., Porankiewicz-Asplund J., Vervliet-Scheebaum M., Reski R. (2011). Simultaneous isolation of pure and intact chloroplasts and mitochondria from moss as the basis for subcellular proteomics. *Plant Cell Rep*. 30: 205–215.

Lange V., Picotti P., Domon B., Aebersold R. (2008). Selected reaction monitoring for quantitative proteomics: a tutorial*. Molecular Systems Biology*. 4: 222.

Larsen A., Uran S., Jacobsen P.B., Skotland T. (2001). Collision-induced dissociation of glycerol phospholipids using electrospray ion-trap mass specretrometry. *Rapid Commun Mass Spectrom.* 15(24): 2393-8.

Le N.T., Blomstedt C.K., Kuang J., Tenlen J., Gaff D.F., Hamill J.D., Neale A.D. (2007). Desiccation-tolerance specific gene expression in leaf tissue of the resurrection plant *Sporobolus stapfianus*. *Functional Plant Biology*. 34, 589–600.

Li L., Han J., Wang Z., Liu J., Wei J., Xiong S., Zhao Z. (2014). Mass Spectrometry Methodology in Lipid Analysis. *International Journal of Molecular Sciences*. 15: 10492-10507.

Li J., Wang X., Zhang T., Wang C., Huang Z., Luo X. (2015). A review on phospholipids and their main applications in drug delivery systems. *Asian Journal of Pharmaceutical Sciences*. 10: 81-98.

Liljenberg C.S. (1992). The effects of water deficit stress on plant membrane lipids. *Prog Lipid Res.* 31: 335-343.

Liu X., Huang B. (2004). Changes in fatty-acid composition and saturation in leaves and roots of creeping bentgrass exposed to high soil temperatures. *Amer. Soc. Hort. Sci*. 129: 795-801.

Liu W., Li W., He Q., Daud M.K., Chen J., Zhu S. (2015). Characterization of 19 genes encoding membrane-bound fatty acid desaturases and their expression profiles in *Gossypium raimondii* under low temperature. *PLoS One.* 10(4): e0123281.

Losa D., Muratab N. (2004). Membrane fluidity and its roles in the perception of environmental signals. *Biochim Biophys Acta.* 1666: 142-157.

Lou Y., Schwender J., Shanklin J (2014). FAD2 and FAD3 Desaturases Form Heterodimers That Facilitate Metabolic Channeling *in Vivo. The Journal of Biological Chemistry.* 289: 17996-18007.

Lynch D.V., Steponkus P.L. (1987). Plasma membrane lipid alterations associated with cold acclimation of winter rye seedling (*Secale cereal* L. cv Puma). *Plant Physiol*. 83: 761-767.

Mani D.R., Abbatiello S.E., Carr S.A. (2012). Statistical characterization of multiple-reaction monitoring mass spectrometry (MRM-MS) assays for quantitative proteomics. *BMC Bioinformatics*. 13(16): 1-18.

Martin B., Ruiz-Torres N.A. (1992). Effects of water-deficit stress on photosynthesis, its component limitations, and on water use efficiency in wheat (*Triticum aestivum L.*). *Plant physiology.* 100: 733-739.

Martinelli T. (2008). In situ localization of glucose and sucrose in dehydrating leaves of *Sporobolus stapfianus*. *J. Plant Physiol.* 165: 580–587.

Maréchal, E., N. Azzouz, C.S. de Macedo, M.A. Block, J.E. Feagin, R.T. Schwarz, and J. Joyard. (2002). Synthesis of chloroplast galactolipids in apicomplexan parasites. *Eukaryot. Cell*. 1:653–656.

Mazliak P. (1994). Desaturation processes in fatty acid and acyl lipid biosynthesis. *J. Plant Physiol.* 143: 399-406**.**

Mello-Silva R. (2005). Morphological analysis, phylogenies and classification in Velloziaceae. *Botanical Journal of the Linnean Society.* 148: 157-173.

Mello-Silva R., Santos D.Y.A.C., Salatino M.L.F., Motta L.B., Cattai M.B., Sasaki D., Lovo J., Pita P.B., Rocini C., Rodrigues C.D.N., Zarrie M., Chase M.W. (2011). Five vicarious genera from Gondwana: the Velloziaceae as shown by molecules and morphology. *Annals of Botany.* 108: 87-102.

Merrill A.H., Dennis E.A., McDonald J.G., Fahy E. (2013). Lipidomics technologies at the end of the first decade and the beginning of the next. *Advances in Nutrition*. 4: 565-567.

Mikami K., Murata N. (2003). Membrane fluidity and the perception of environment signals in cyanobacteria and plants. *Prog Lipid Res*. 42(6): 527-43.

Millar A.A., Wrischer M., Kunst L. (1998). Accumulation of very long chain fatty acids in membrane glycerolipids is associated with dramatic alterations in plant morphology. *American Society of Plant Physiologists.* 10(11): 1889-1902.

Millar A., Smith M.A., Kunst L. (2000). All fatty acids are not equal: discrimination in plant membrane lipids. *Trends in Plant Science*. 5: 95-101.

Mittler R. (2002). Oxidative stress, antioxidants and stress tolerance. *Trends in Plant Science*. 7: 405–410.

Mitra J., Xu G., Wang B., Li M., Deng X. (2013). Understanding desiccation tolerance using the resurrection plant *Boea hygrometrica* as a model system. *Plant Science*. 4(446): 1-10.

Mironov K.S., Sidorov R.A., Trofimova M.S., Bedbenov V.S., Tsydendambae V.D., Allakhverdiev S.I., Los D.A. (2012). Light-dependent cold-induced fatty acid unsaturation, changes in membrane fluidity, and alterations in gene expression in *Synochocystis*. *Biochim Biophys Acta.* 1817(8): 1352-9.

Moellering E.R., Muthan B., Benning C. (2010). Freezing tolerance in plants requires lipid remodeling at the outer chloroplast membrane*. Science.* 330: 226-228.

Moellering E.R., Benning C. (2011). Galactoglycerolipid metabolism under stress: a time for remodeling. *Trends Plant Sci*. 16: 98-107.

Moire L., Rezzonico E., Geopfert S., Poirier Y. (2004). Impact of unusual fatty acid synthesis on futile cycling through beta-oxidation and on gene expression in transgenic plants (1 [w]). *Plant Physiol*. 134: 432-442.

Moore J.P., Nguema-Ona E., Chevalier L.M., Lindsey G.G., Brandt W., Lerouge P., Farrant J.M., Driouich A. (2006). The response of the leaf cell wall to desiccation in the resurrection plant *Myrothamnus flabellifolia. Plant Physiology*. 141: 651-662.

Moore J.P., Lindsey G.G., Farrant J.M., Brandt W.F. (2007a). An overview of the biology of the desiccation-tolerant plant *Myrothamnus flabellifolia*. *Annals of Botany*. 99: 211-217.

Moore J.P., Hearshaw M., Ravenscroft N., Lindsey G.G., Farrant J.M., Brandt W.F. (2007b). Desiccation-induced ultrastructural and biochemical changes in the leaves of the resurrection plants *Myrothanmus flabellifolia. Australian Journal of Botany*. 55: 482-491.

Moore J.P., Le N.T., Brandt W.F., Driouich A., Farrant J.M. (2009). Towards a systems-based understanding of plant desiccation tolerance. *Trends in Plant Science*. 14(2): 110–117.

Moore J.P., Nguema-Ona E.E., Vicré-Gibouin M., Sørensen I., Willats W.G.T., Driouich A., Farrant J.M. (2012). Arabinose-rich polymers as an evolutionary strategy to plasticize resurrection plant cell walls against desiccation. *Planta.* 237: 739–754.

Moyankova D., Mladenov P., Berkov S., Peshev D., Georgieva D., Djilianov D. (2014). Metabolic profiling of the resurrection plant *Haberlea rhodopensis* during desiccation and recovery. *Physiol. Plant.* 152 675–687.

Munne-Bosch S., Alegre L. (2004). Die and let live: leaf senescence contributes to plant survival under drought stress. *Functional Plant Biology*. 31: 203-216.

Murakami Y., Tsuyama M., Kobayashi Y., Kodama H., Iba K. (2000). Trienoic fatty acids and plant tolerance of high temperature. *Science*. 287: 476–479.

Murata N., Los D.A. (1997). Membrane fluidity and temperature perception. *Plant Physiol.* 115: 875-879.

Myers M.Y., Farrant J.M. (2010). Preliminary characterization of floral response of *Xerophyta humilis* to desiccation, vernalisation, photoperiod and light intensity. *Plant Growth Regul*. 62: 213-216.

Myers A.M, James M.G, Lin Q., Yi G., Stinard P.S., Hennen-Bierwagen T.A., Becraft P.W. (2011). Maize *opaque5* encodes monogalactosyldiacylglycerol synthase and specifically affects galactolipids necessary for amyloplast and chloroplast function. *Plant Cell.* 23: 2331–2347.

Nakamura Y., Shimojima M., Ohta H., Kobayashi K. (2010). Biosynthesis and function of monogalactosyldiacylglycerol (MGDG), the signature lipid of chloroplasts. *The Chloroplasts: Basics and Applications*. Pp: 185–202.

Nakamura Y. (2013). Phosphate starvation and membrane lipid remodeling in seed plants. *Progress in Lipid Research*. 52: 43–50.

Navari-Izzo F., Quartacci M.F., Pinzino C., Rascio N., Vazzana C., Sgherri C.L.M. (2000). Protein dynamics in thylakoids of the desiccation-tolerant plant Boea hygroscopica during dehydration and rehydration. *Plant Physiology*. 124(3): 1427-1436.

Nobusawa T., Umeda M. (2012). Very-long-chain fatty acids have an essential role in plastid division by controlling Z-ring formation in *Arabidopsis thaliana*. *Genes Cells*.17: 709–719.

Nobusawa T., Okushima Y., Nagata N., Kojima M., Sakakibara H., Umeda M. (2013). Synthesis of Very-Long-Chain Fatty Acids in the Epidermis Controls Plant Organ Growth by Restricting Cell Proliferation. *PLoS Biol*. 11(4): e1001531.

Ntuli T.M. (2012). Drought and Desiccation-Tolerance and Sensitivity in Plants, Botany, Dr. John Mworia (Ed.), ISBN: 978-953-51-0355-4, InTech, Available from: http://www.intechopen.com/books/botany/droughtand-desiccation-tolerance-and-sensitivity-in-plants.

O'Donnell V.B., Murphy R.C., Watson S.P. (2014). Platelet lipidomics: a modern day perspective on lipid discovery and characterization in platelets. *Circ Res*. 114(7): 1185–1203.

Ohtake S., Schebor C., de Pablo J.J. (2006). Effects of trehalose on the phase behavior of DPPC-cholesterol unilamellar vesicles. *Biochimica et Biophysica Acta*. 1758: 65-73.

Oliver A.E., Hincha D.K., Tsvetkova N.M., Vigh L., Crowe J.H. (2001). The effect of arbutin on membrane integrity during drying is mediated by stabilization of the lamellar phase in the presence of nonbilayer-forming lipids. *Chem Phys Lipids*. 111: 37-57.

Oliver A.E., Hincha D.K Crowe J.H. (2002). Looking beyond sugars: the role of amphiphilic solutes in preventing adventitious reactions in anhydrobiotes at low water contents. *Comparative Biochemistry and Physiology*. 131(3): 515-525.

Oliver M.J., Jain R., Balbuena T.S., Agrawal G., Gasulla F., Thelen J.J. (2011a). Proteome analysis of leaves of the desiccation-tolerant grass, *Sporobolus stapfianus*, in response to dehydration. *Phytochemistry.* 72: 1273–1284.

Oliver M.J., Guo L., Alexander D., Ryals J., Wone B., Cushman J. (2011b). A sister group metabolomic contrast using untargeted global metabolomic analysis delineates the biochemical regulation underlying desiccation tolerance in *Sporobolus stapfianus*. *Plant Cell*. 23: 1231–1248.

Oliver M.J., Guo L., Alexeander D.C., Ryals J.A., Wone B.W.M., Cushman J.C. (2011). A Sister Group Contrast Using Untargeted Global Metabolomics Analysis Delineates the Biochemical Regulation Underlying Desiccation Tolerance in *Sporobulus stapfianus*. *The Plant Cell*. 23: 1231-1248.

Okazaki Y., Otsuki H., Narisawa T., Kobayashi M., Sawai S., Kamide Y., Kusano M., Aoki T., Hirai M.Y., Saito K. (2013). A new class of plant lipid is essential for protection against phosphorus depletion. *Nat. Commun.* 4:1510.

Pham-Thi A.T., Da Silva J.V., Mazliak P. (1990). The role of membrane lipids in drought resistance of plants. *Bulletin de la Société Botanique de France. Actualités Botaniques*. 137(1): 99-114.

Phillips J.R., Fisher E., Baron M., van den Dries N., Facchinelli F., Kutzer M., Rahmanzadeh R., Remus D., Bartels D. (2008). *Lindernia brevidens*: a novel desiccation-tolerant vascular plants, endemic to ancient tropical rainforests. *The Plant Journal*. 54: 938-948

Pillai P., St. John. J.B. (1981). Lipid composition of chloroplast membranes from weed biotypes differentially sensitive to triazine herbicides. *Plant Physiol*. 68: 585-587.

Pitt J.J. (2009). Principles and Applications of Liquid Chromatography-Mass Spectrometry in Clinical Biochemistry*. Clinical Biochemistry Review*. 30(1): 19–34.

Popova, A.V., Hincha D.K. (2003). Intermolecular interactions in dry and rehydrated pure and mixed bilayers of phosphatidylcholine and digalactosyldiacylglycerol: a Fourier-transform infrared spectroscopy study. *Biophys. J.* 85: 1682–1690.

Quartacci M.F., Forli M., Rascio N., Dalla Vecchia F., Bochicchio A., Navari-Izzo F. (1997). Desiccation-tolerant *Sporobolus stafinanus*: lipid composition and cellular ultrastructure during dehydration and rehydration. *Journal of Experimental Botany*. 48: 1269-1279.

Quartacci M.F., Glisic O., Stevanovic B., Navari-Izzo F. (2002). Plasma membrane lipids in the resurrection plant *Ramonda serbica* following dehydration and rehydration. *Journal of Experimental Botany.* 53(378): 2159-2166.

Quehenberger O., Armando A. M., Brown A. H., Milne S. B., Myers D. S., Merrill A. H., et al. (2010). Lipidomics reveals a remarkable diversity of lipids in human plasma. *J. Lipid Res.* 51: 3299–3305.

Rafsanjani A., Brulé V., Tamara L. Western T.L., Pasini D. (2015). Leaf metabolite profile of the Brazilian resurrection plant *Barbacenia purpurea* Hook. (*Velloziaceae*) shows two time-dependent responses during desiccation and recovering*. Fronteirs in Plant Science.* 5:96.

Rainteau D., Humbert L., Delage E., Vergnolle C., Cantrel C., Maubert M. A., Lanfranchi S., Maldiney R., Collin S., Wolf C., Alain Zachowski A., Ruelland E. (2012). Acyl Chains of Phospholipase D transphosphatidylation products in arabidopsis cells: a study using multiple reaction monitoring mass spectrometry. *PLoS ONE.* 7(7): 1-15.

Rakic T., Gajic G., Maja Lazarevic M., Stevanovic B. (2015). Effects of different light intensities, CO2 concentrations, temperatures and drought stress on photosynthetic activity in two paleoendemic resurrection plant species *Ramonda serbica* and *R. nathaliae*. *Environmental and Experimental Botany.* 109: 63-72.

Reyes J. L., Rodrigo M.-J., Colmenero-Flores J. M., Gil J.-V., Garay-Arroyo A., Campos F., Salamini F., Bartels D., Covarrubias A. A. (2005). Hydrophilins from distant organisms can protect enzymatic activities from water limitation effects in vitro. *Plant Cell Environment*. 28(6): 709-718.

Reynolds K.B., Taylor M.C., Zhou X-R., Vanhercke T., Wood C.C., Blanchard C.L., Singh S.P., Petrie J.R. (2015). Metabolic engineering of medium-chain fatty acid biosynthesis in *Nicotiana benthamiana* plant leaf lipids. *Front Plant Sci.* 6: 164.

Routaboul J-M., Fischer S.F., Browse J. (2000). Trienoic fatty acids are required to maintain chloroplast function at low temperatures. *Plant Physiology*. 124(4): 1697-1705.

Ruelland E., Vaultier M.N., Zachowski A., Hurry V. (2009). Cold signalling and cold acclimation in plants. *Advances in Botany Research*. 49: 36-150.

Rustan A.C., Drevon C.A. (2005). Fatty acids: structure and properties. London: Encyclopedia of life science, NATURE publishing. http://www.wls.els.net.

Sakurai I., Mizusawa N., Ohashi S., Kobayashi M., Wada H. (2007). Effects of the lack of phosphatidylglycerol on the donor side of photosystem II. *Plant Physiol*. 144:1336–1346.

Sallas L., Luomala E.M., Utriainen J., Kainulainen P., Holopainen J.K. (2003). Contrasting effects of elevated carbon dioxide concentration and temperature on

Rubisco activity, chlorophyll fluorescence, needle ultrastructure and secondary metabolites in conifer seedlings. *Tree Physiol*. 23: 97–108.

Sam O., Ramirez C., Coronado M.J., Testillano P.S., Risueno M.C. (2003). Changes in tomato leaves induced by NaCl stress: Leaf organization and cell ultrastructure. *Biol. Plant*. 47: 361–366.

Sampaio J. L., Gerl M. J., Klose C., Ejsing C. S., Beug H., Simons K., Shevchenko A. (2011). Membrane lipidome of an epithelial cell line. *Proc. Natl. Acad. Sci. U.S.A.* 108, 1903–1907.

Schattat M., Barton K., Bandisch B., Klosgen R.B., Mathur J. (2011). Plastid stromule branching coincides with contiquous endoplasmic recticulum dynamics. *Plant Physiology*. 155(4): 1667-1677.

Schneiter R., Hitomi M., Ivessa A.S., Fasch E-V., Kohlwein S.D., Tartakoff A.M. (1996). A yeast acetyl coenzyme A carboxylase mutant links very-long-chain fatty acid synthesis to the structure and function of the nuclear membrane pore complex. *Mol. Cell. Biol.* 16: 7161–7172.

Scoffoni C., Vuong C., Diep S., Cochard H., Sack L. (2014). Leaf shrinkage with dehydration: coordination with hydraulic vulnerability and drought tolerance. Plant Physiology. 164(4): 1772-1788.

Selivanov V.A., Votyakova T.V., Pivtoraiko V.N., Zeak J., Sukhomlin T., Trucco M., Roca J., Cascante M. (2011). Reactive oxygen species production by forward and reverse electron fluxes in the mitochondrial respiratory chain. Plos Computational Biology. 7(3): e1001115.

Serhan C.N. (2005). Mediator lipidomics. Prostaglandins Other Lipid Mediators. 77: 4-14.

Sharma P., Jha A.B., Dubey R.S., Pessarakli M. (2012). reactive oxygen species, oxidative damage, and antioxidative defense mechanism in plants under stressful conditions. *Journal of Botany*. Pp: 1-26.

Shackleton C. (2010): Clinical steroid mass spectrometry: A 45-year history culminating in HPLC-MS/MS becoming an essential tool for patient diagnosis. *J Steroid Biochem Mol Biol*. 121: 481–490.

Shaner R. L., Allegood J. C., Park H., Wang E., Kelly S., Haynes C. A., et al. (2009). Quantitative analysis of sphingolipids for lipidomics using triple quadrupole and quadrupole linear ion trap mass spectrometers. *J. Lipid Res*. 50: 1692–1707.

Sherwin H.W., Farrant J.M. (1996). Differences in rehydration of three different desiccation-tolerant species. *Annals of Botany*. 78: 703–710.

Slotte J.P. (2013). Molecular properties of various structurally defined sphingomyelins-correlations of structure with function. *Progress in Lipid Research.* 52(2): 206-219.

Smirnoff N. (1993). The role of active oxygen in the response of plants to water deficit and desiccation. *New Phytologist*. 125: 27–58.

Suarez-Rodriguez M.C., Edsgä D., Hussain S.S., Alquezar D., Rasmussen M., Gilbert T., Nielsen B.H., Bartels D., Mundy J. (2010). Transcriptome of the desiccation-tolerant resurrection plant *Craterostigma plantagineum. Plant Journal.* 63: 212-28.

Suguiyama V.F., Silva E.A., Meirelles S.T., Centeno D.C., Braga M.R. (2014). Leaf metabolite profile of the Brazilian resurrection plant *Barbacenia purpurea* Hook. (*Velloziaceae*) shows two time-dependent responses during desiccation and recovering. *Frontiers in Plant Science.* 5 (96): 1-13.

Sherwin H.W., Farrant J.M. (1998). Protection mechanisms against excess lightintheresurrection plants *Craterostigma wilmsii* and *Xerophyta viscosa*. *Plant Growth Regulation*. 24: 203–210.

Shimabukuro R.H., Swanson H.R. (1969). Atrazine metabolism, selectivity, and mode of action. *Journal of Agricultural and Food Chemistry*. 17(2): 199-205.

Shimoni E., Rav-Hon O., Ohad I., Brumfeld V., Reich Z. (2005). Three-dimensional organization of higher-plant chloroplast thylakoid membranes revealed by electron tomography. *Plant Cell*. 17: 2580–2586.

Siegenthaler P.A., Müller M.O., Bovet L. (1997). Evidence for lipid kinase activities in spinach chloroplast envelope membranes*. FEBS Lett.* 416: 57–60.

Tarahovsky Y.S. (2008). Plant polyphenols in cell-cell interaction and communication. *Behaviour.* 3(8): 609–611.

Tarazona P., Feussner K., Feussner I. (2015). An enhanced plant lipidomics method based on multiplexed liquid chromatography-mass spectrometry reveals additional insight into cold- and drought-induced membrane remodelling. *Plant Journal*. 84: 621-633.

Tenchov B., Koynova R. (2012). Cubic phases in membrane lipids. *Eur. Biophys*. *J*. 41: 841–850.

Tenchov B.G., MacDonald R.C., Lentz B.R. (2013). Fusion peptides promote formation of bilayer cubic phases in lipid dispersions. An x-ray diffraction study. *Biophys. J.* 104: 1029–1037.

TerBush A.D., Osteryoung K.W. (2012). Distinct functions of chloroplast FtsZ1 and FtsZ2 in Z-ring structure and remodeling. *J. Cell Biol.* 199: 623–637.

t'Kindt R., Scheltema R.A., Jankevics A., Brunker K., Rijal S., Dujardin J.-C., Breitling R., Watson D.G., Coombs G.H., Decuypere S., Geary T.G. (2010).

Metabolomics to unveil and understand phenotypic diversity between pathogen populations. *PLoS Neglected Tropical Diseases*, 4 (11): e904.

Toldi O., Tuba Z., Scott P. **(2009).** Vegetative desiccation tolerance: is it a goldmine for bioengineering crops? *Plant Science*. 176:187–199.

Tottey S., Block M.A., Allen M., Westergren T., Albrieux C., Scheller H.V., Merchant S., Jensen P.E. (2003). Arabidopsis CHL27, located in both envelope and thylakoid membranes, is required for the synthesis of protochlorophyllide. *Proc Natl Acad Sci USA*. 100:16119–16124.

Torres-Franklin M.L., Gigon A., de Melo D.F., Zuily-Fodil Y., Pham-Thi A.T., (2007). Drought stress and rehydration affect the balance between MGDG and DGDG synthesis in cowpea leaves. *Physiol Plant*. 131: 201–210.

Touchstone J.C. (1995). Thin-layer chromatographic procedures for lipid separation. *J. Chromatogr*. 1218: 2754-2774.

Tsugawa H., Ohta E., Izumi Y., Ogiwara A., Yukihira D., Takeshi Bamba T., Fukusaki E., Arita M. (2014). MRM-DIFF: data processing strategy for differential analysis in large scale MRM-based lipidomics studies. *Front Genet*. 5: 471.

Tuba Z., Lichtenthaler H.K., Csintalan Z., Nagy Z., Szente K. (1996). Loss of chlorophylls, cessation of photosynthetic CO# assimilation and respiration in the poikilochlorophyllous plant *Xerophyta scabrida* during dessication. *Physiologia Plantarum*. 96: 383–388.

Tuba, Z., Proctor, M.C.F., Csintalan, Z. (1998). Ecophysiological responses of homoiochlorophyllous and poikilochlorophyllous desiccation tolerant plants: a comparison and an ecological perspective. *Plant Growth Regul*. 24: 211-217.

Tuba z (2008). Notes on the poikilochlorophyllous desiccation tolerant plants. *Acta Biologica Szegediensis.* 52(1): 111-13.

Tunnacliffe A., Wise M.J. (2007). The continuing conundrum of the LEA proteins**.** *aturwissenschaften*. 94:791–812.

Uemura M., Steponkus P.L. (1994). A contrast of the plasma membrane lipid composition of oat and rye leaves in relation to freezing tolerance. *Plant Physiol.* 104: 479-496.

Uttaro D.U. (2006). Biosynthesis of polyunsaturated fatty acids in lower eukaryotes. *Life.* 58(10): 563-571.

Valko M., Rhodes C.J., Moncol J., Izakovic M., Mazur M. (2006). Free radicals, metals and antioxidants in oxidative stress-induced cancer. *Chemico- Biological Interaction.* 160: 1–40.

van Besouw A., Wintermans J.F.G.M. (1978). Galactolipid formation in chloroplast envelopes: I. Evidence for two mechanisms in galactosylation. Biochim. Biophys. Acta - *Lipids and Lipid Metabolism*. 529: 44-53.

van den Dries N., Facchinelli F., Giarola V., Phillips J. R., Bartels D. (2011). Comparative analysis of LEA-like 11-24 gene expression and regulation in related plant species within the *Linderniaceae* that differ in desiccation tolerance. *New Phytol.* 190 (1): 75–88.

van Meer G., de Kroon A.I.P.M. (2011). Lipid map of the mammalian cell. *Journal of Cell Science*. 124: 5-8.

Vertucci C.W., Farrant J.M. (1995). Acquisition and loss of desiccation tolerance. In: Kigel J, Galili G (Eds) Seed Development and Germination, Marcel Dekker Press Inc., New York. Pp: 237-271.

Voelker T. (2001). Variations in the biosynthesis of seed-storage lipids. *Annual Review of Plant Physiology and Plant Molecular Biology.* 52(1): 335-361.

Wallis J.G., Browse J. (2002). Mutants of Arabidopsis reveal many roles for membrane lipids. *Progress in Lipid Research*. 41: 54–278.

Wang C., Wang M., Zhou Y., Dupree J.L., Han X. (2014). Alterations in mouse brain lipidome after disruption of CST gene: A lipidomics study. *Molecular Neurobiology*. 50(1): 88-96.

Wang L-Z., Goh S-H., Wong AL-A., Thuya W-L., Lau J-YA., Wan S-C., Lee S.C., Ho P.C., Goh B.C. (2015). Validation of a rapid and sensitive LC-MS/MS method for determination of exemestane and its metabolites, 17β-hydroxyexemestane and 17β-Hydroxyexemestane-17-O-β-D-Glucuronide: application to human pharmacokinetics study. *PLoS ONE* 10(3): 1-13.

Wang m., Wang C., Han R.H., Han X. (2016). Novel advances in shotgun lipidomics for biology and medicine. *Progress in Research*. 61: 83-108.

Wang S., Uddin M. I., Tanaka K., Yin L., Shi Z., Qi Y., Mano J., Matsui K., Shimomura N., Sakaki T., Deng X., Zhang S. (2014). Maintenance of chloroplast structure and function by overexpression of the rice MONOGALACTOSYLDIACYLGLYCEROL SYNTHASE gene leads to enhanced salt tolerance in tobacco. *Plant Physiol.* 165(3): 1144-1155.

Warakanont J., Tsai C.H., Mitchel E.J., Murphy G.R. III., Hsueh P.Y., Roston R.L., Sears B.B., Benning C. (2015). Chloroplast lipid transfer processes in *Chlamydomonas reinhardtii* involving a TRIGALACTOSYLDIACYLGLYCEROL 2(TGD2) orthologue. *Plant Journal*. 84: 1005-1020.

Wehner G., Balko C., Humbeck K., Zyprian E., Ordon F. (2016). Expression profifiling of genes involved in drought stress and leaf senescence in juvenile barley. *BMC Plant Biol.* 16(3): 1-12.

Welti R., Shah J., Li W., Li M., Chen J., Burke J.J., Fauconnier M.L., Chapman K., Chye M.L., Wang X. (2007). Plant lipidomics: Discerning biological function by profiling plant complex lipids using mass spectrometry. *Front Biosci*. 12: 2494–2506.

Wenk M.R. (2005). The emerging field of lipidomics. Natural Reviews in Drug Discoveries. 4(7): 594-610.

Wenk M.R. (2010). Lipidomics: new tools and applications**.** *Cell*.143(6): 888-95.

Whittaker A., Bochicchio A., Vazzana C., Lindsey G., Farrant J.M. (2001). Changes in leaf hexokinase activity and metabolites levels in response to drying in the desiccation-tolerant species *Sporobolus stapfianus* and *Xerophyta viscosa. Journal of Experimental Botany.* 52: 961-969.

Williams W.P., Brain A.P.R., Cunningham B.A., Wolfe D.H. (1997). X-ray diffraction study of bilayer phase transitions in aqueous disersion of di-polyenoic phosphatidylethnalamines. *Biochimica et Biophysica Acta (BBA)-Biomembranes*. 1326(1):103-114.

Williams B., Njaci I., Moghaddam L., Long H., Dickman M.B., Zhang X., Mundree S. (2015). Trehalose accumulation triggers autophagy during plant desiccation. Plos Genetics. 11(12): e1005705.

Wolf C., Quinn P.J. (2008). Lipidomics: practical aspects and applications. *Progress in Lipid Research*. 47(1): 15-36.

Xiao Y., Savchenko T., Baidoo E.E., Chehab W.E., Hayden D.M., Tolstikov V (2012). Retrograde signaling by the plastidial metabolite MecPP regulates expression of nuclear stress-response genes. *Cell.* 149(7): 1525-35.

Xiao L., Yanga G., Zhanga L., Yang X., Zhao S., Ji Z., Zhou Q., Hu M., Wang Y., Chen M., Xu Y., Jin H., Xiao X., Hu G., Bao F., Hu Y., Wan P., Li L., Deng X., Kuang T., Xiang C., Zhu J-K, Oliver M.J., He Y. (2015). The resurrection genome of *Boea hygrometrica*: A blueprint for survival of dehydration*. PNAS*. 112(18): 5833-5837.

Xu C., Fan J., Riekhof W., Froehlich J.E., Benning C. (2003). A permease-like protein involved in ER to thylakoid lipid transfer in Arabidopsis. *EMBO J.* 22: 2370-2379.

Yaeno T., Mutsuda O., Iba K. (2004). Role of chloroplast trienoic fatty acids in plant disease defense responses. *The Plant Journal*. 40: 931-941.

Yang K., Jenkins C.M., Dilthey B., Gross R.W. (2015). Multidimensional mass spectrometry-based shotgun lipidomics analysis of vinyl ether diglycerides. *Anal Bioanal Chem*. 407: 5199.

Yobi A., Wone B.W.M., Xu W., Alexander D.C., Guo L., Ryals J.A., Oliver M.J., Cushman J.C. (2013). Metabolomic profiling is *Selaginella lepidophylla* at various hydration states provides new insights into the mechanistic basis of desiccation tolerance. *Mol. Plant.* 6(3): 369-85.

Yordanov I., Velikova V., Tsonev T. (2003). Plant responses to drought and stress tolerance. *Bulg Journal of Plant Physiology*. Pp: 187-206.

Yurchenko O.P., Park S., Ilut D.C., Inmon J.J., Millhollon J.C., Liechty Z., Page J.T., Jenks M.A., Chapman K.D., Udall J.A., Gore M.A.,Dyer J.M. (2014). Genome-wide analysis of the omega-3 fatty acid desaturase gene family in *Gossypium. BMC Plant Biology***.**14**:** 312**.**

Zech M., Mayr C., Tuthorn M., Leiber-Sauheitl K., Glaser B. (2014). Oxygen isotope ratios (18O/16O) of hemicellulose-derived sugar biomarkers in plants, soils and sediments as paleoclimate proxy I: Insight from a climate chamber experiment. *Geochimica et Cosmochimica Acta*. 126: 614–623.

Zhai S.M., Gao Q., Xue H.W., Sui Z.H., Yang A.F., Zhang J.R. (2012). Overexpression of the phosphatidylinositol synthase gene from *Zea mays* in tobacco plants alters the membrane lipids composition and improves drought tolerance. *Planta*. 235: 69-84.

Zheng G., Tian B., Zhang F., Tao F., Li W. (2011). Plant adaptation to frequent alterations between high and low temperatures: remodelling of membrane lipids and maintenance of unsaturation levels. *Plant, Cell and Environment*. 34: 1431–1442.

Zheng X., TianluChen T., Aihua Zhao A., Wang X., Xie G., Huang F., Liu J., Zhao Q., Wang S., Wang C., Zhou M., Panee J., He Z., Jia W. (2016). The Brain Metabolome of Male Rats across the Lifespan. *Scientific Reports*. 6(24125): 1-12.

Zhong D., Du H., Wang Z., Huang B. (2011). Genotypic variation in fatty acid composition and unsaturation levels in Bermudagrass associated with leaf dehydration tolerance. *J. Amer. Soc. Hort. Sci.* 136(1): 35-40.

Zhou L, Liao Y, Yin P, Zeng Z, Li J, Lu X, Zheng L, Xu G. (2014). Metabolic profiling study of early and late recurrence of hepatocellular carcinoma based on liquid chromatography-mass spectrometry. *J Chromatogr B Analyt Technol Biomed Life Sci.* 966: 163–170.

Zhu Y., Wang B., Zhang Z-N., Xu T., Huang L-C., Zhang X-F., Xu G-H., Li W-L., Wang Z., Wang L., Liu Y-X., Deng X. (2015). Global Transcriptome analysis reveals acclimation-primed processes involved in the acquisition of desiccation tolerance in *Boea hygrometrica. Plant and Cell Physiology Advance.* Pp: 1-13.

Zimmermann U., Bitter R., Marchiori P.E.R., Ruger S., Ehrenberger W., Sukhorukov V.L., Schuttler A., Ribeiro R.V. (2013). A non-invasive plant-based probe for continuous monitoring of water stress in real time: a new tool for irrigation

scheduling and deeper insight into drought and salinity stress physiology. *Theor. Exp. Plant Physiol*. 25(1): 2-11.

SUPPLEMENTAL FIGURES:

Changes associated with selected glycerolipid molecular species from roots and leaves during dehydration and rehydration experiments. Lipids were extracted at different points of the dehydration and rehydration curves. Glycerolipid composition was analysed by multiple reaction monitoring mass spectrometry using a preset list of transitions. The results are expressed as % of total MRM transitions. The lipid classes studied are phosphatidylcholine (PC; figure 3.8; 3.9), phosphatidylethanolamine (PE; figure 3.12; 3.13), phosphatidylglycerol (PG; figure 3.14; 3.15), phosphatidylinositol (PI; figure 3.10; 3.11), monogalactosyldiacylglycerol (MGDG; figure 4.5), digalactosyldiacylglycerol (DGDG; figure 4.6), chloroplastic PG (figure 4.7), chloroplastic PE (figure 4.8), chloroplastic PI (figure 4.10), and chloroplastic PC (figure 4.10). Data for leaves are shown for one lipid class before the data for roots.

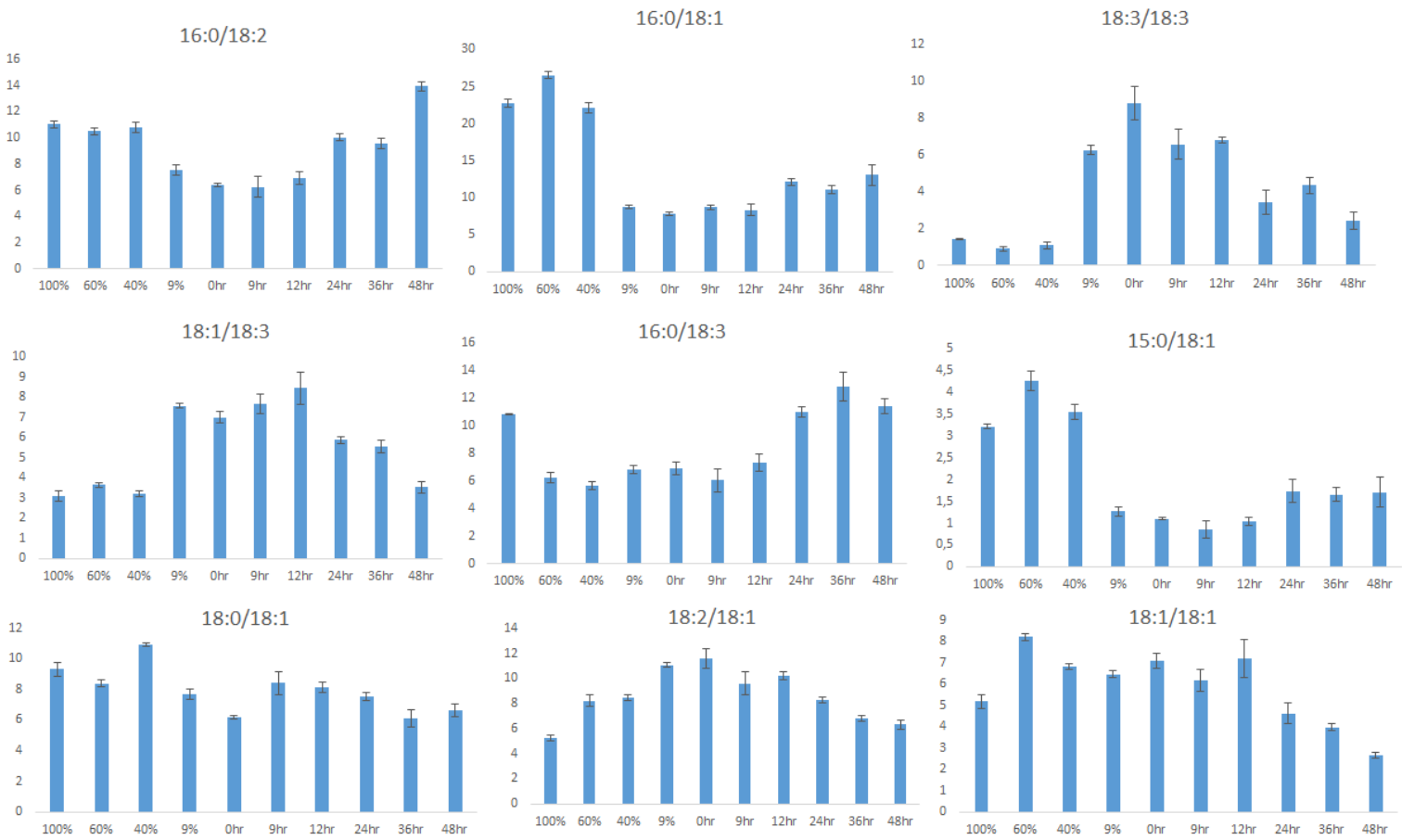

Figure 3.8: Changes in selected PC species (% of total MRM transition signal) within *X. humilis* leaves subjected to dehydration and rehydration treatments. Lipids were analysed by searching for the transitions listed in Table 3.1.

Figure 3.9: Changes in selected PC species (% of total MRM transition signal) of *X. humilis* roots subjected to dehydration and rehydration treatments. Lipids were analysed by searching for the transitions listed in Table 3.1.

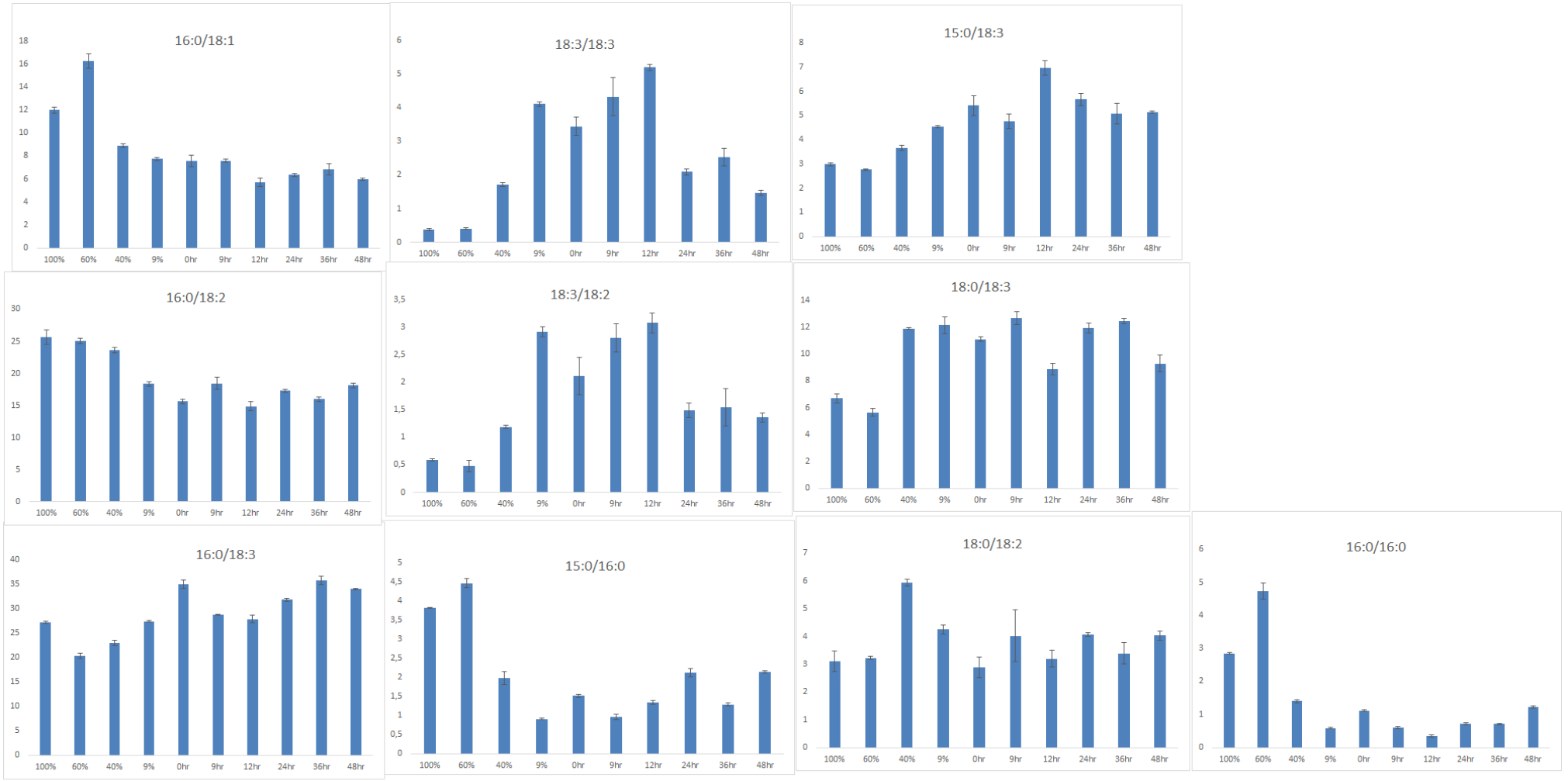

Figure 3.10: Selected PI molecular species (% of total MRM transition signal) of *X. humilis* leaves subjected to dehydration and rehydration treatments. Lipids were analysed searching for the transitions listed in Table 3.1.

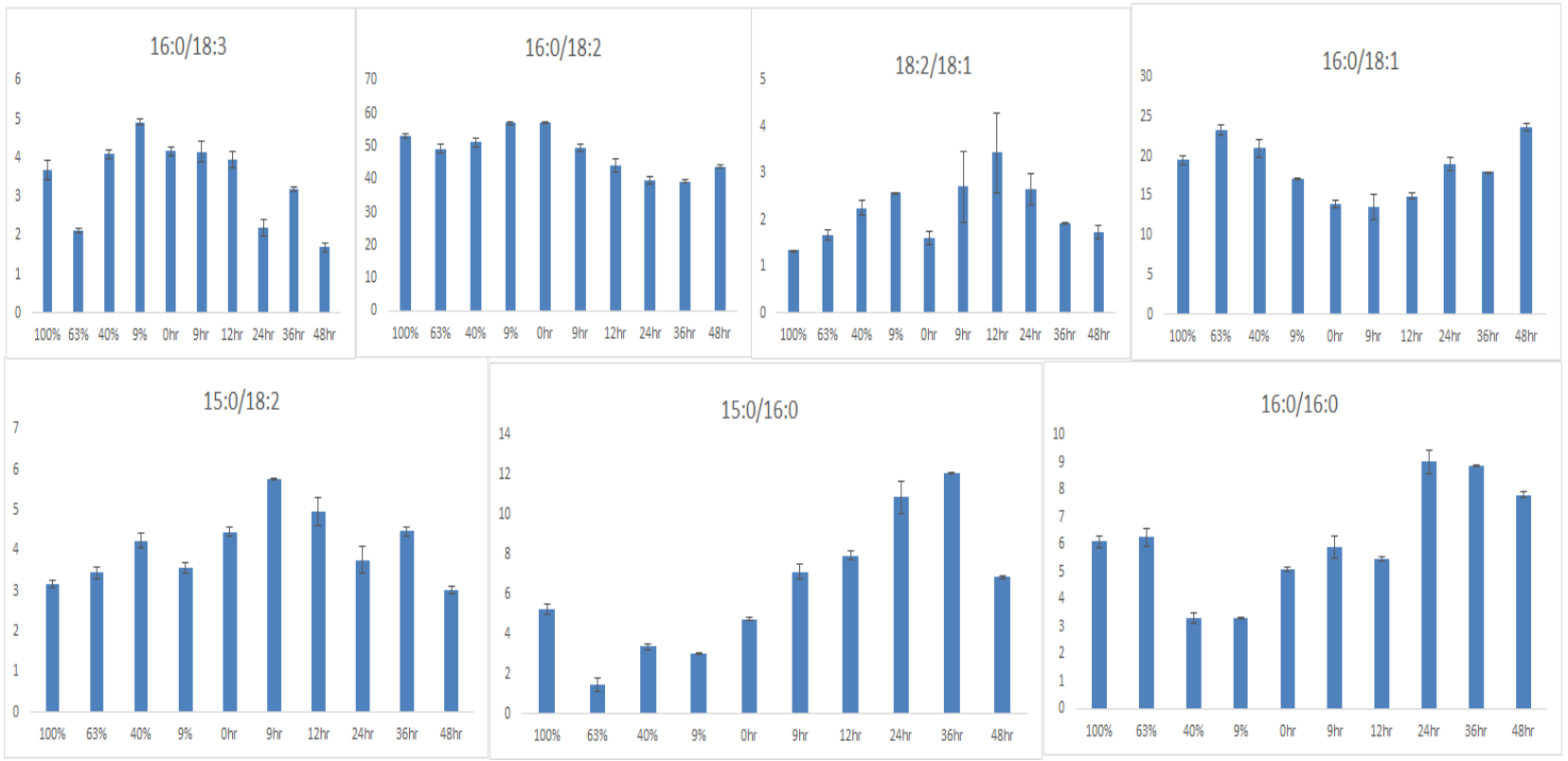

Figure 3.11: Selected PI molecular species (% of total MRM transition signal) in roots of *X. humilis* roots subjected to dehydration and rehydration treatments. Lipids were analysed searching for the transitions listed in Table 3.1.

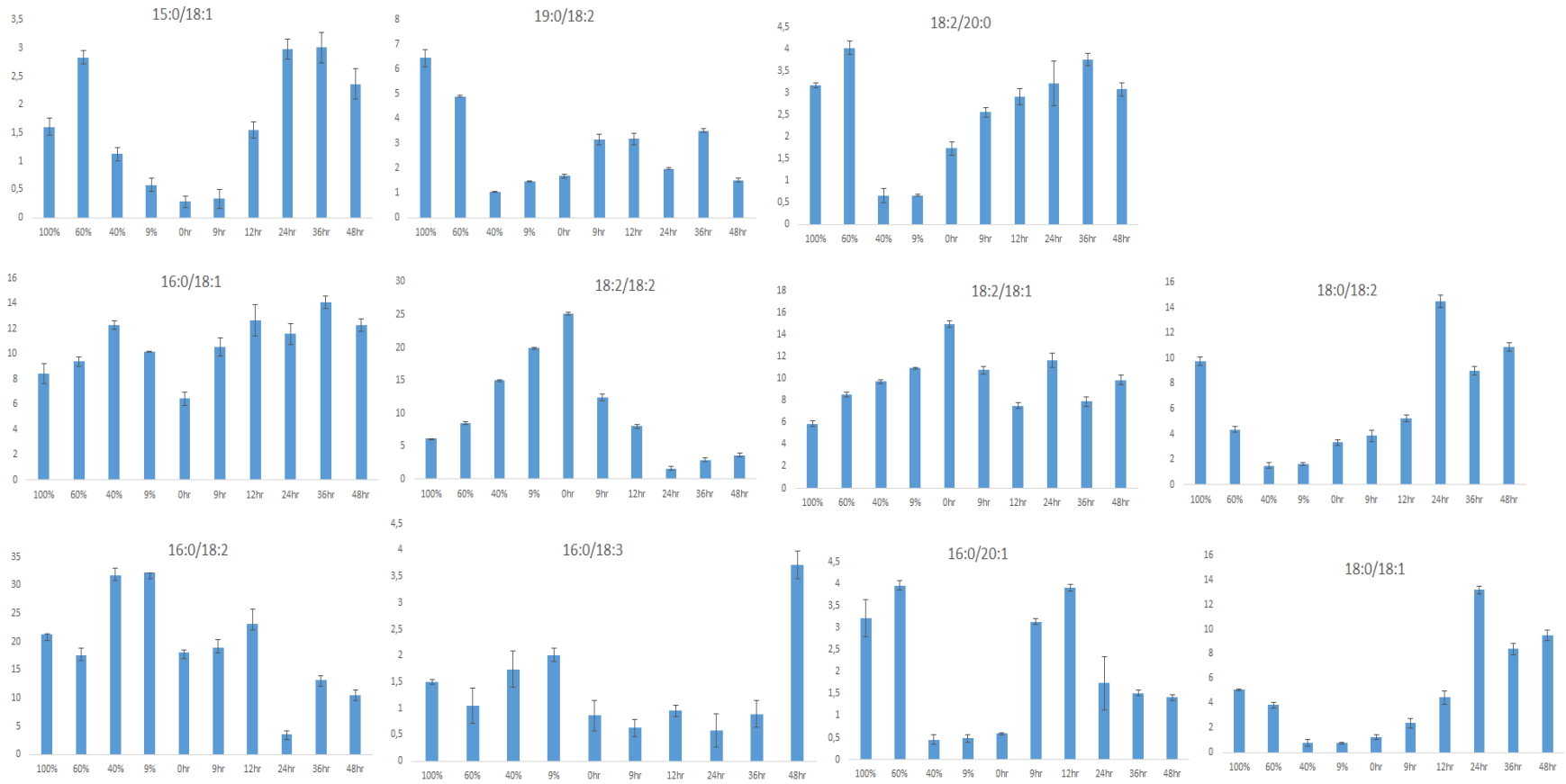

Figure 3.12: Selected PE lipid molecular species (% of total MRM transition signal) in leaves of *X. humilis* subjected to dehydration and rehydration treatments. Lipids were analysed searching for the transitions listed in Table 3.1.

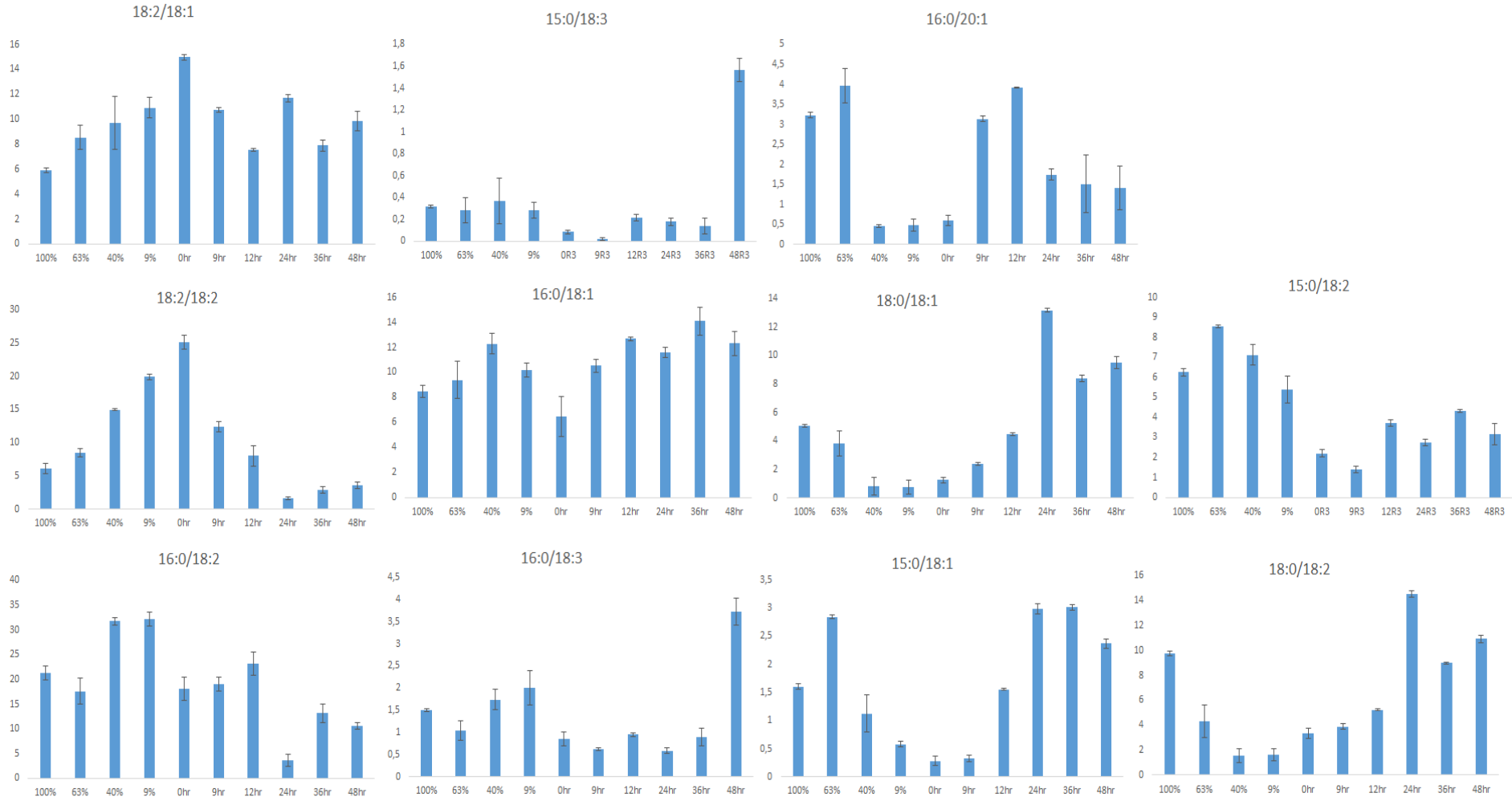

Figure 3.13: Selected PE lipid molecular species (% of total MRM transition signal) in roots of *X. humilis* subjected to dehydration and rehydration treatments. Lipids were analysed searching for the transitions listed in Table 3.1.

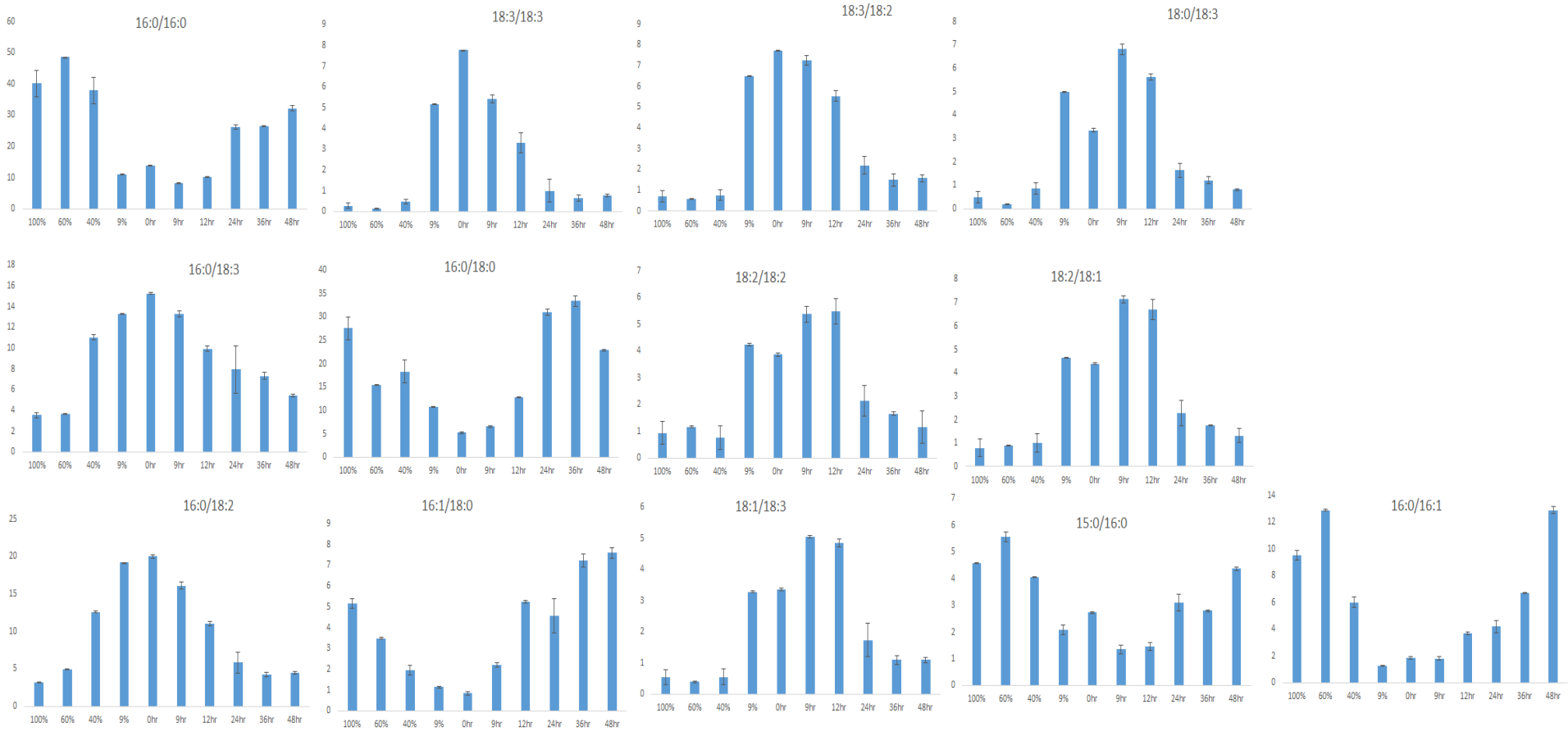

Figure 3.14: Selected PG molecular species PG (% of total MRM transition signal) of *X. humilis* leaves subjected to dehydration and rehydration treatments. Lipids were analysed searching for the transitions listed in Table 3.1.

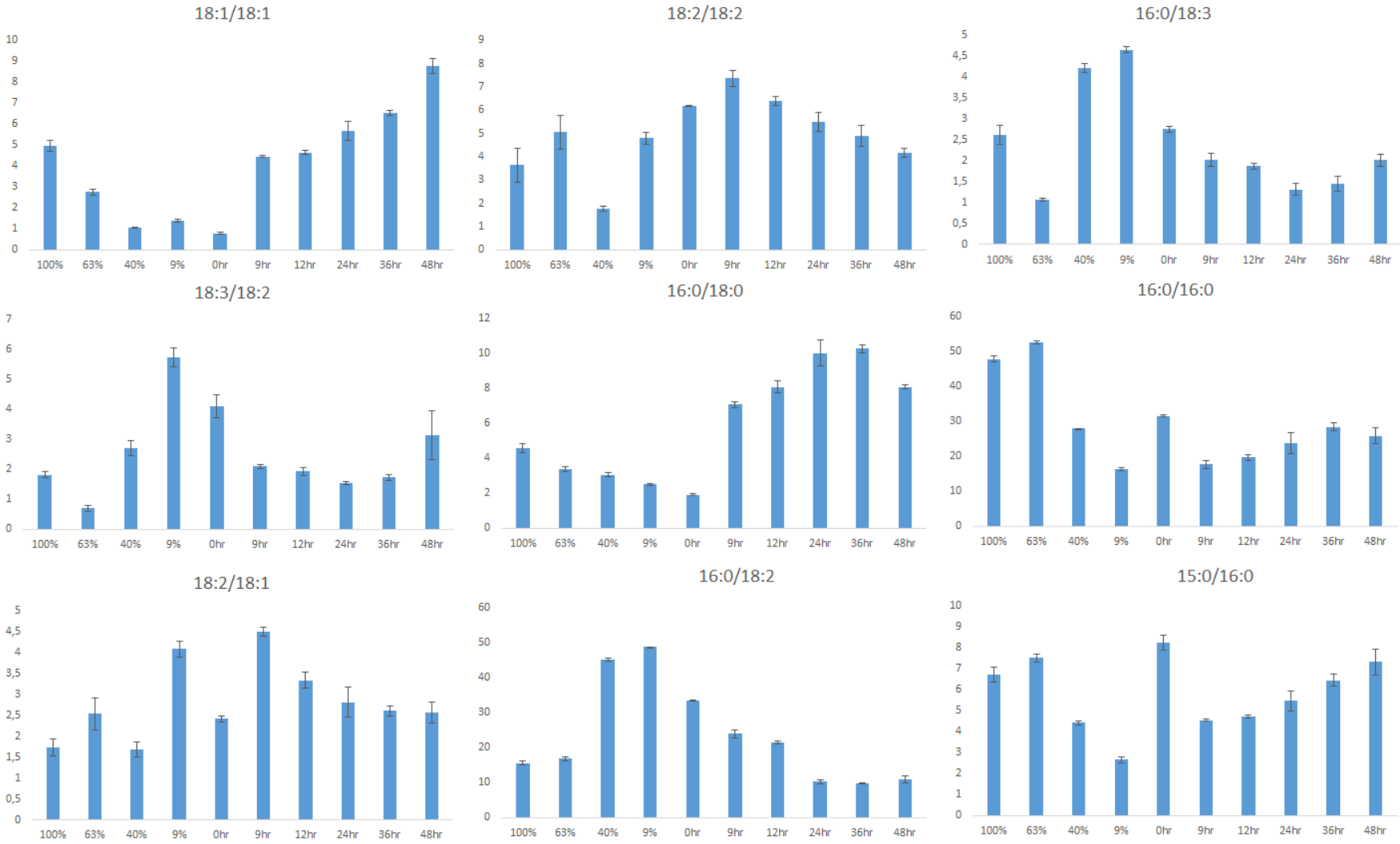

Figure 3.15: Selected PG molecular species (% of total MRM transition signal) in roots of *X. humilis* subjected to dehydration and rehydration treatments. Lipids were analysed searching for the transitions listed in Table 3.1.

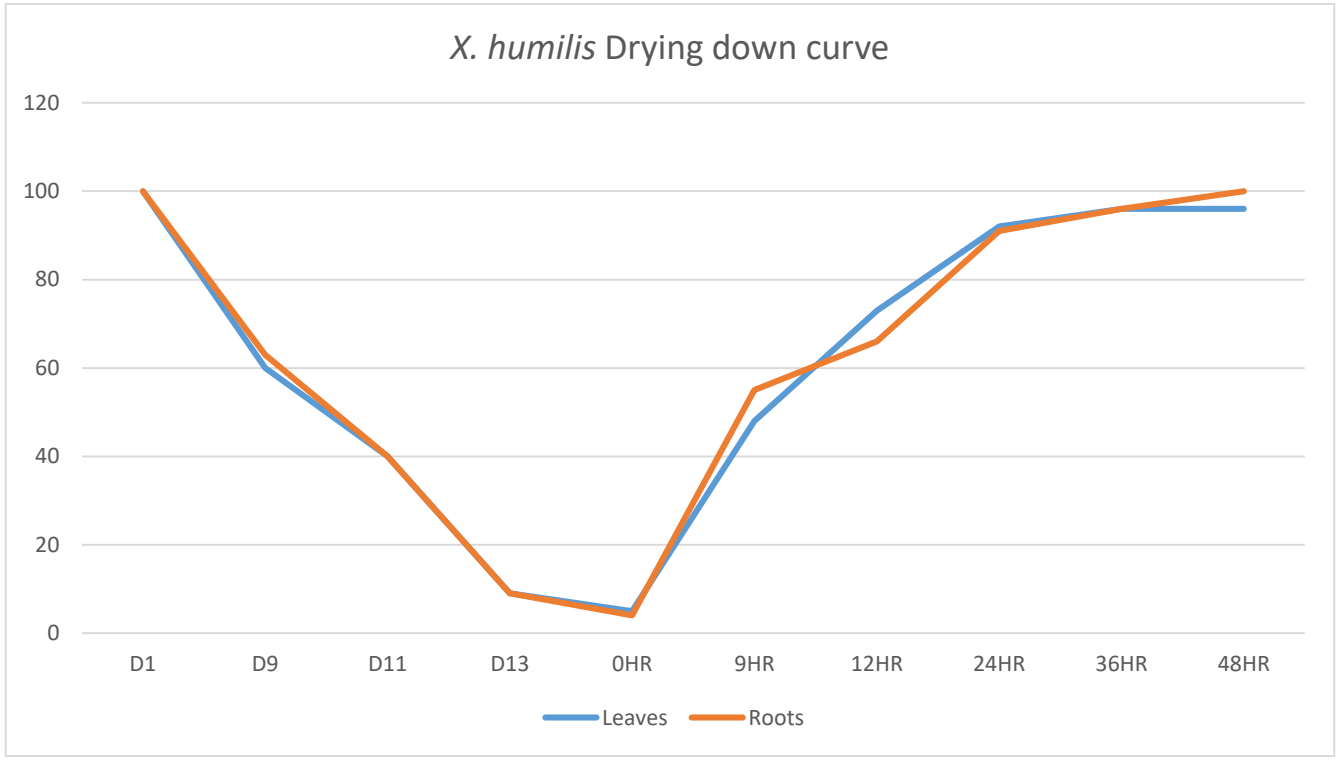

Figure 3.16: Relative water content (RWC in %) of *X. humilis* plants over the course of drought treatment. The blue arrow on D1 indicates the suspension of watering, the red arrow on 0hr corresponds to the rehydration. The dehydration and rehydration experiments were carried out under a 16 hr light, 325 μmol s^{-1} m^{-2}, 25ºC and 8 hr dark, 10ºC regime.

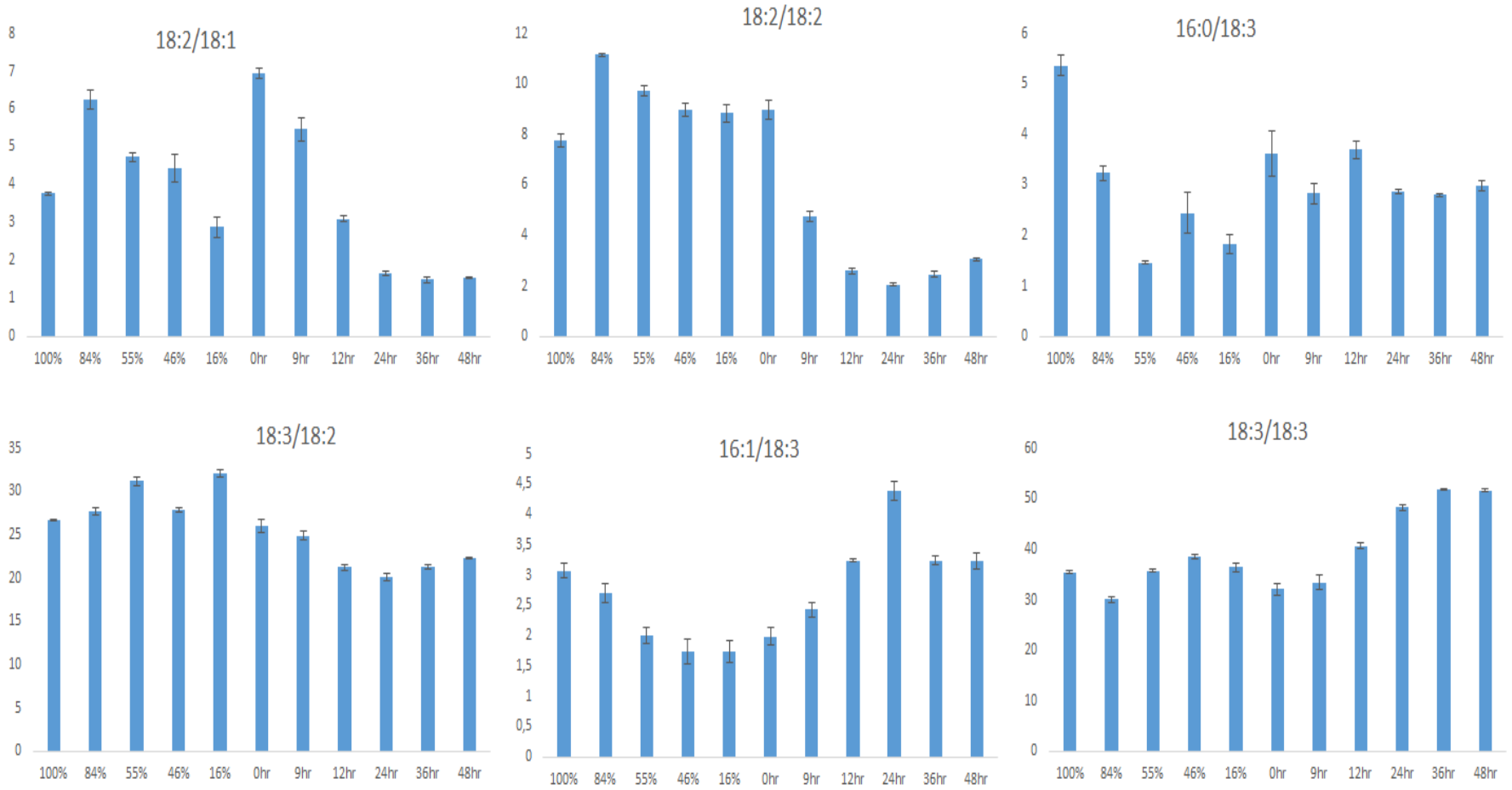

Figure 4.5: Selected lipid molecular species of chloroplastic MGDG (% of total MGDG MRM transitions) of *X. humilis* leaves subjected to gradual dehydration and rehydration treatment. Lipids were analysed searching for the transitions listed in Table 3.1.

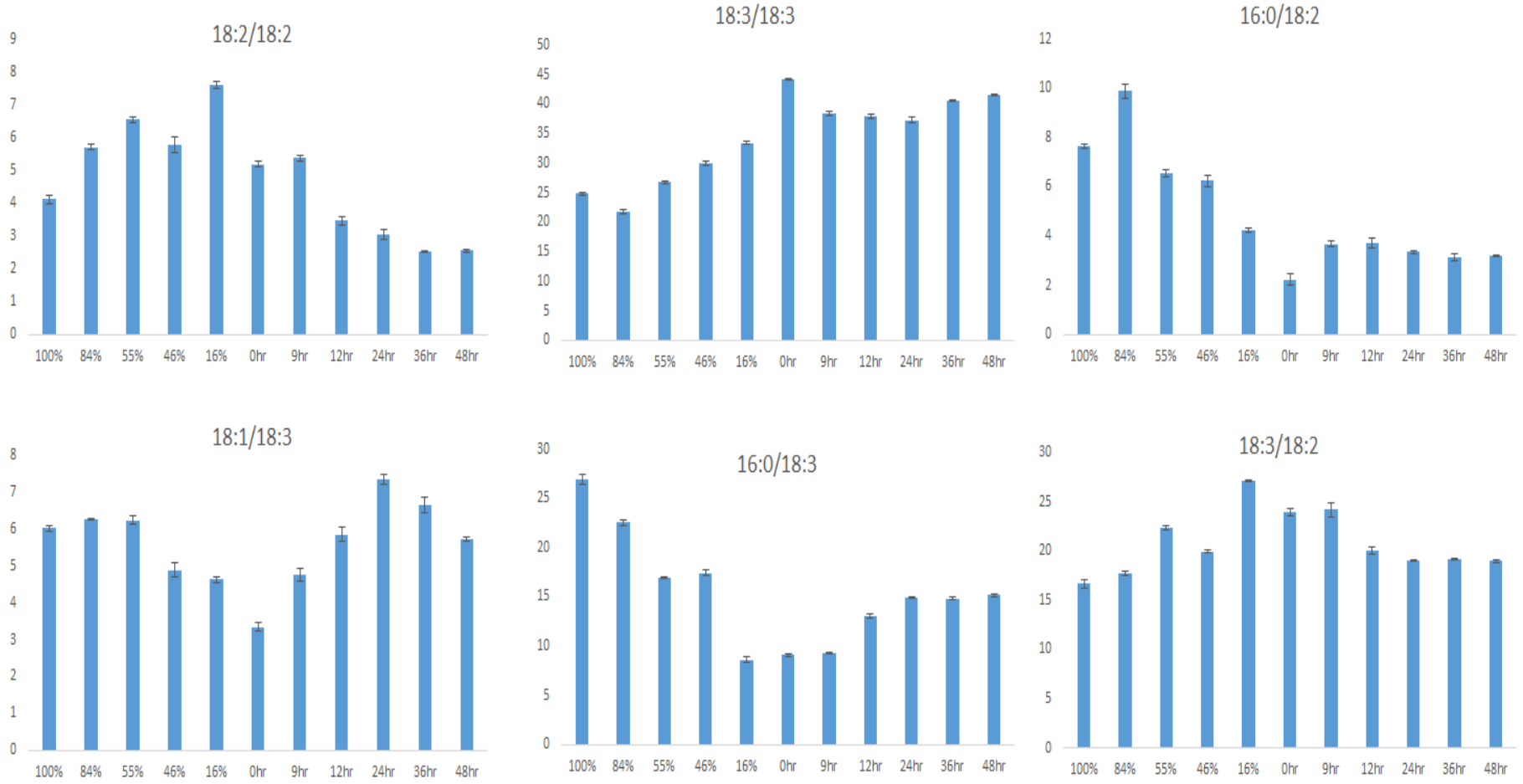

Figure 4.6: Selected lipid molecular species of chloroplastic DGDG (% of total MRM transitions) of *X. humilis* leaves subjected to dehydration and rehydration treatments. Lipids were analysed searching for the transitions listed in Table 3.1.

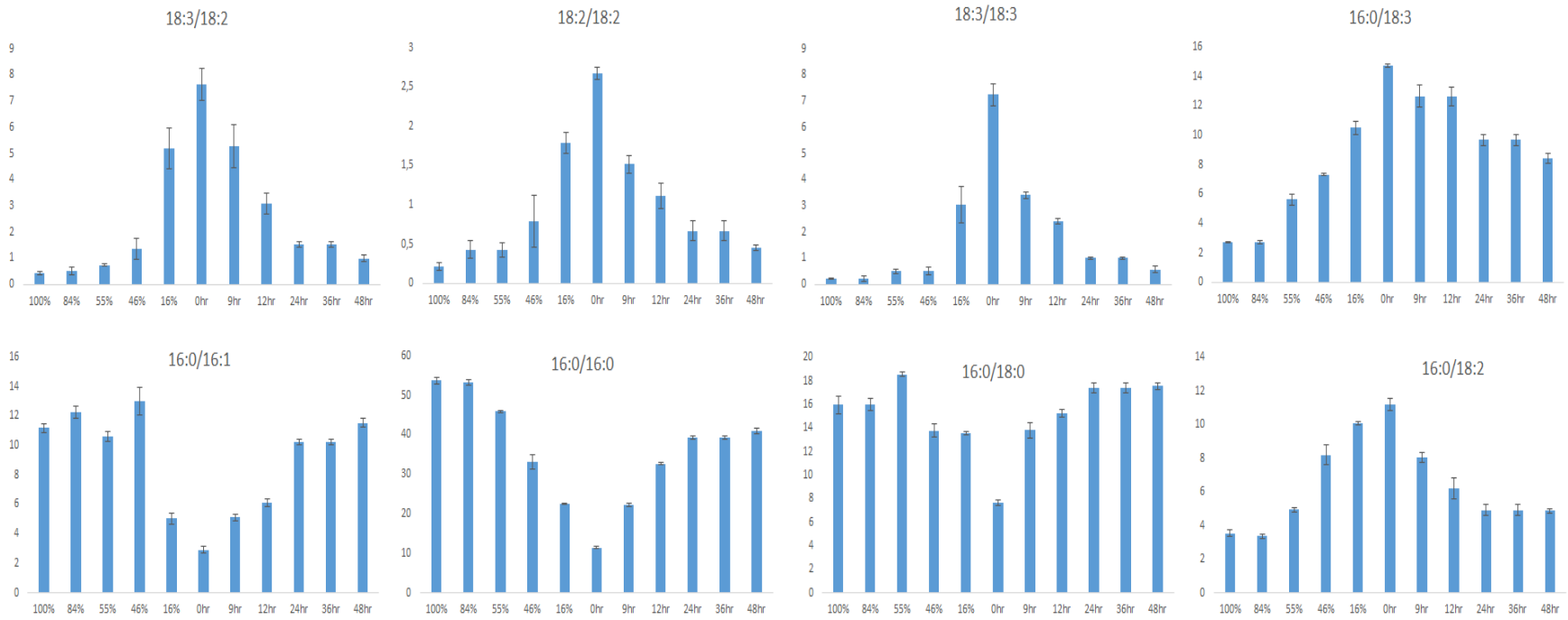

Figure 4.7: Selected lipid molecular species of chloroplastic PG (% of total MRM transition signal) of *X. humilis* leaves subjected to dehydration and rehydration treatments. Lipids were analysed searching for the transitions listed in Table 3.1.

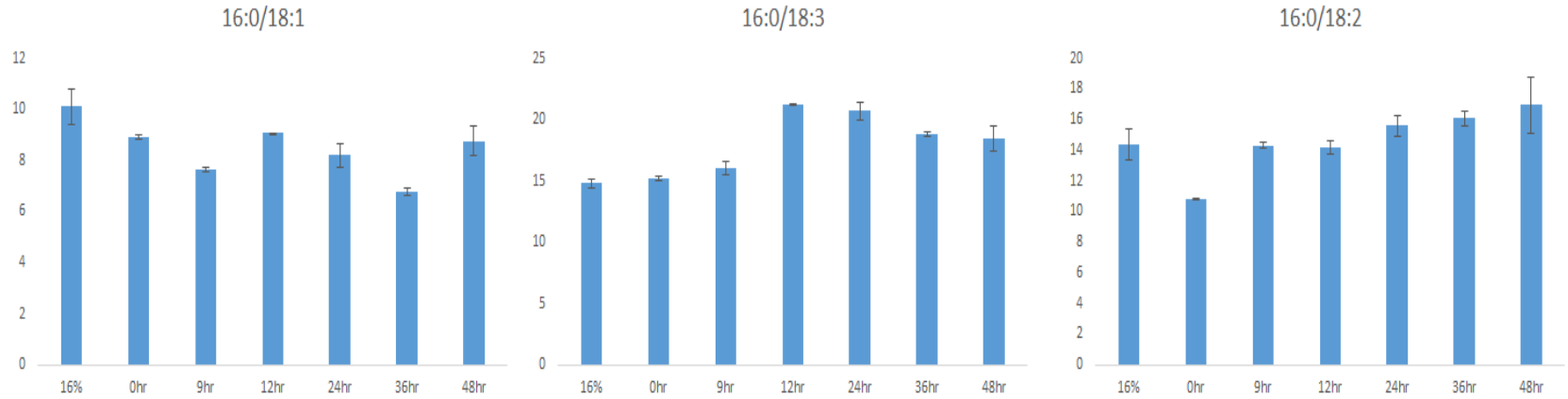

Figure 4.8: Selected lipid molecular species of chloroplastic PE (% of total MRM transition signal) of *X. humilis* leaves subjected to dehydration and rehydration treatments. Lipids were analysed searching for the transitions listed in Table 3.1

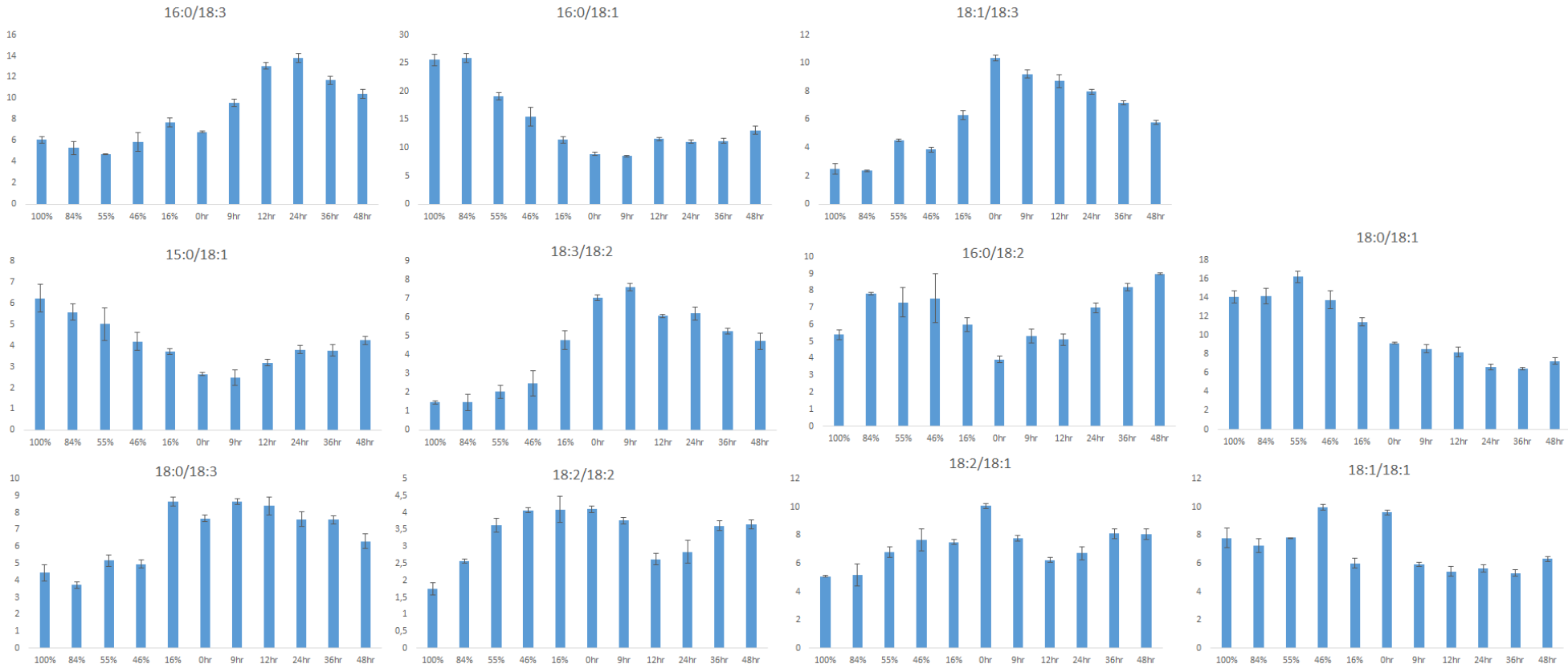

Figure 4.9: Selected lipid molecular species of chloroplastic PC (% of total MRM transition signal) of *X. humilis* leaves subjected to dehydration and rehydration treatments. Lipids were analysed searching for the transitions listed in Table 3.1.

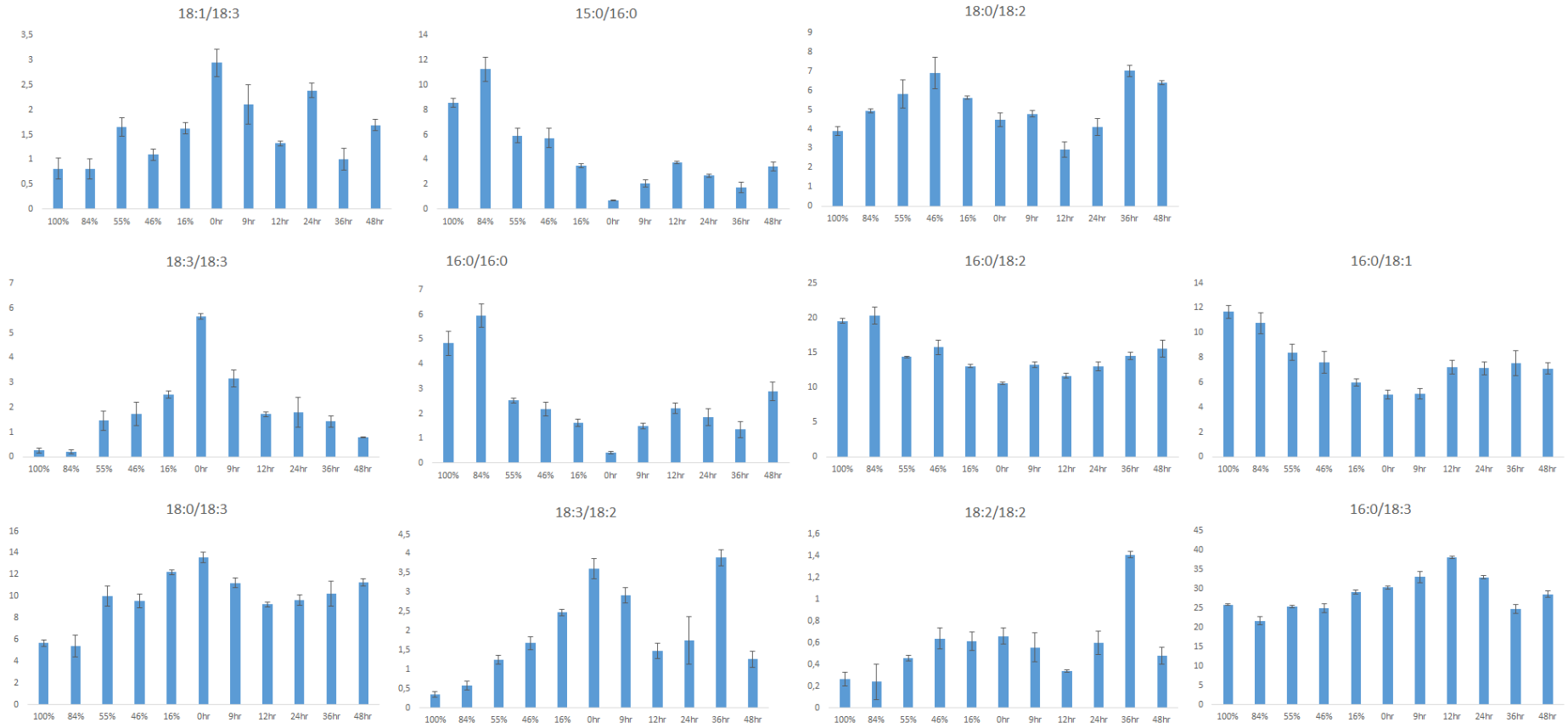

Figure 4.10: Selected lipid molecular species of chloroplastic PI (% of total MRM transition signal) of *X. humilis* leaves subjected to dehydration and rehydration treatments. Lipids were analysed searching for the transitions listed in Table 3.1.